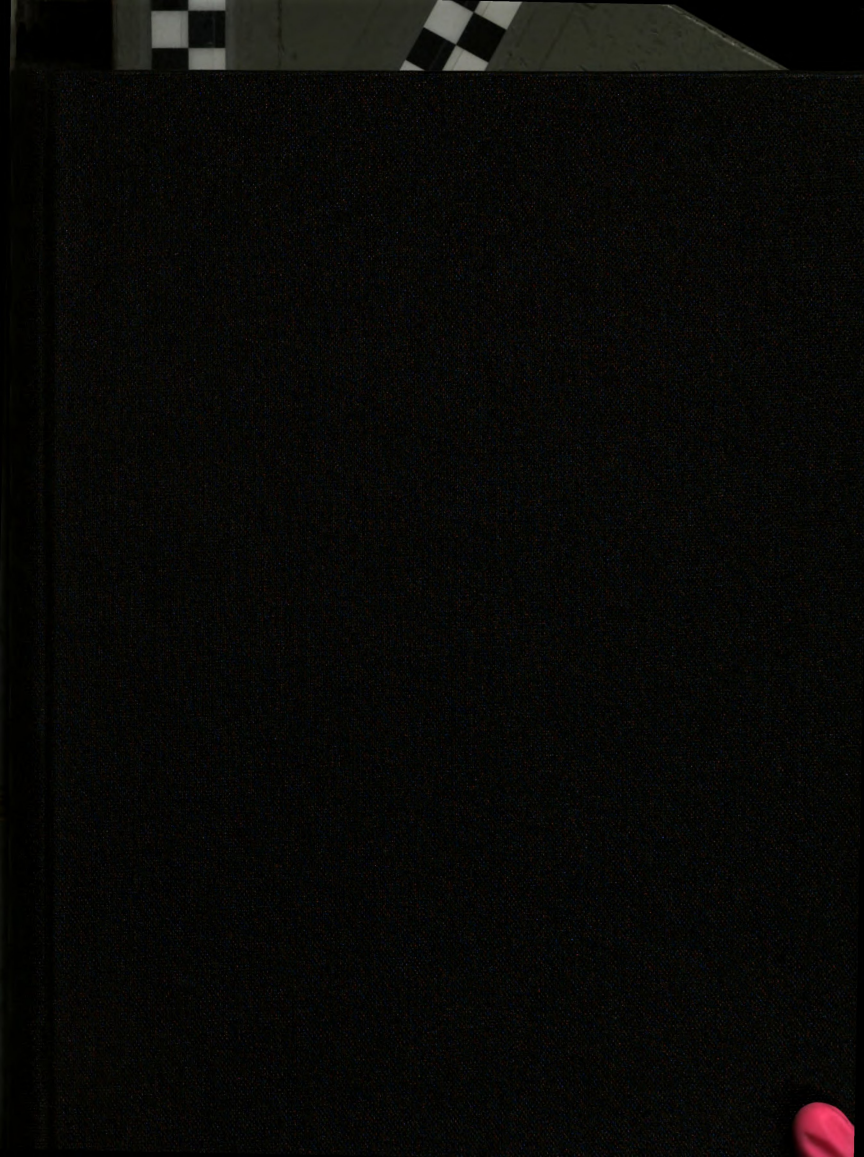

This is to certify that the

dissertation entitled

Buckling of a composite nonlinearly elastic plate under uniaxial loading

presented by

John Z. Song

has been accepted towards fulfillment
of the requirements for

Ph.D degree in Mechanics

Thomas J. Pence
Major professor

Date May 9, 1990

BUCKLING OF A COMPOSITE NONLINEARLY ELASTIC PLATE UNDER UNIAXIAL LOADING

By

John Zhen-hua Song

A DISSERTATION

Submitted to
Michigan State University
in partial fulfillment of the requirements
for the degree of

DOCTOR OF PHILOSOPHY
IN
MECHANICS

Department of Metallurgy, Mechanics and Materials Science

1990

ABSTRACT

BUCKLING OF A COMPOSITE NONLINEARLY ELASTIC PLATE UNDER UNIAXIAL LOADING

By

John Zhen-hua Song

The buckling of a nonlinearly elastic three-ply composite plate is studied in the context of finite deformation incompressible nonlinear elasticity. The buckling of non-composite plates in this context has been studied previously by other authors. Here a general class of incompressible materials is introduced through a material strain energy density dependent variable $A(\lambda)$. Both flexure and barrelling instabilities are examined. The differential equations and boundary conditions for the bifurcation analysis of the composite plate is derived. To simplify the analysis, the neo-Hookean material is the focus of investigation in the latter portion of this investigation. Numerical computer programs are then used to predict the critical loading condition. It is found that the ordering of the failure thrusts for certain composite configurations is more complicated than the ordering that occurs in a non-composite plate. In particular, the thrusts at which barrelling and flexural buckling modes occur can be interlaced. Furthermore, transitions in the ordering of the different failure modes may occur as the aspect ratio of the plate is varied. These results demonstrate the interplay between the properties of the constituent materials and the geometric configuration of the plate. Finally, an optimal design problem for

symmetric three-ply sandwich composite plates is studied. The object is to maximize the resistance to buckling for fixed values of the volume ratio of two different neo-Hookean materials. It is found that there is a single aspect ratio dependent transition in the optimal design.

ACKNOWLEDGEMENT

I would like express my sincere appreciation to my advisor, Professor Thomas J. Pence for his tremendous guidance and support throughout this work. I would also like to thank the other members of the guidance committee, Professor Nicholas Altiero, Professor Yvonne Jasiuk and Professor David Yen.

While preparing this dissertation, I held teaching assistantships awarded by the Department of Metallurgy, Mechanics and Materials Science and a research assistantship from the Composite Materials and Structures Center of Michigan State University under an REF Program Grant. The support of these institutions is gratefully acknowledged.

TABLE OF CONTENTS

LIST OF FIGURES

1. INTRODUCTION

Buckling in plates has been of concern for a long time because of the role it plays in structural failure. Within the theory of finite deformation elasticity theory, buckling has been studied by numerous authors, including for example Green and Spencer [4] for a circular cylinder, Burgess and Levinson [2] for a plate under biaxial load and Wilkes [13] for a circular tube under end thrust. Recently, the buckling of a thick incompressible isotropic elastic plate under thrust has been studied extensively by K.N. Sawyers and R.S. Rivlin [10], [11]. These authors employ the theory of small deformations superposed on finite deformations [9] to determine the critical conditions under which solutions bifurcate from a well known "trivial" solution. Sawyers and Rivlin have shown for the non-composite case that plane-strain buckling can occur involving either flexure or barrelling mode shapes with an arbitrary integer number m of half-wavelengths. In this dissertation a similar problem *for composite constructions* is examined in detail. Specifically, the buckling instability of a thick rectangular three-ply sandwich composite plate is investigated in the context of finite deformation incompressible non-linear elasticity. The buckling behavior of composite plates in the classical theory has been the object of extensive previous study [8]. Here, however, the examination takes place within the fully three-dimensional theory of nonlinear elasticity. This plate, consisting of two different incompressible isotropic nonlinear elastic materials, composed of three stacked rectangular plies with perfect interfacial bonding, is subjected to a deformation by a thrust T

applied to opposite sides. Some striking differences in the buckling behavior from that which would otherwise occur in a non-composite plate are obtained. Drastic changes in stability behavior are not uncommon when one goes from a non-composite construction to a composite construction. This has previously been demonstrated in [5], [6] for the physically different, but mathematically similar, void formation instability mechanism. This dissertation then concludes by using the buckling results obtained here to study a problem in optimal design.

In section 2, the basic boundary value problem is formulated. The composite plate is constructed from 3 plies that are stacked symmetrically in the X_2-direction and the whole assembly is subjected to thrusts applied on the X_1-faces. Thus the boundary and interface conditions are determined. The plies themselves are each assumed to be constructed from a class of nonlinear materials which are studied further in section 3. The boundary value problem is then shown to have a homogeneous deformation solution as given in (2.19). The relation between the thrust and the stretch in the plate is then given by (2.34).

Section 3 presents the mechanical behavior of the class of incompressible non-linear elastic materials that are the focus of this study. These materials are a useful generalization of the neo-Hookean material in that they provide for a wide range of mechanical behavior, while giving rise to buckling equations that have a certain useful analytical form. Finally it is shown that these materials are a special subclass of a more general class of materials introduced by Knowles [7].

In section 4, the bifurcation is fully discussed. Here buckling is defined as the existence of deformed configurations that depart from the homogeneous deformation solutions obtained in section 2. A linearized boundary value problem is formulated governing local bifurcation from these homogeneous deformation solutions. These bifurcations involve plane strain buckled solutions. A general buckling equation (4.53) for determining the thrust associated with these bifurcation modes in the three-ply composite plate is obtained.

Section 5 reveals more detail about the material constant A in the strain energy density (3.1). As shown by Sawyers and Rivlin [10], [11], a nonconstant generalization of A -- $A(\lambda_1, \lambda_2, \lambda_3)$ -- plays an important role in the buckling behavior of a homogeneous plate composed of an *arbitrary* incompressible nonlinearly elasic material. This generaliztion is discussed. It is then shown that the materials used in the present study, and examined in section 3, are the most general class of materials with strain energy density $W=W(I_1)$ for which the value of $A(\lambda_1, \lambda_2, \lambda_3)$ is a constant.

In section 6, and for the remainder of this dissertation, attention is confind to the case in which all plies are composed of a neo-Hookean material. Barrelling and flexure deformation modes are introduced and the bifurcation into each such mode is associated with a "failure" thrust. The buckling equations for each of these modes are obtained. These equations are in fact special cases of equation (4.53) for symmetric and anti-symmetric deformation. Computer programs are developed to solve these two types of problems numerically.

In section 7, these numerical routines are used to study the

flexure and barrelling instabilities in detail. Of particular interest is a wrinkling instability, corresponding to an infinite number of wavelengths in either the flexure or barrelling case. For both flexure and barrelling cases, various different qualitative behaviors in the buckling equations are shown to occur. These different qualitative behaviors effect the failure mode ordering. It is shown that the ordering of the failure thrusts for certain composite configurations is more complicated than the ordering that occurs in the non-composite case. In particular, under suitable conditions, the thrusts at which barrelling and flexure buckling modes occur can be interlaced. Furthermore, transitions in the ordering of the different failure modes may occur as the aspect ratio of the plate is varied. Unlike the non-composite case, the lowest, or critical, thrust need not always correspond to the lowest flexure mode. In fact, for certain constructions, the critical thrust is associated with the wrinkling instability.

The last section focuses on optimal design for three-ply composite plates. A specific design problem is introduced and studied. The problem involves a three-ply composite laminate plate that is to be constructed from fixed amounts of two different neo-Hookean materials. The object is to choose between two competing symmetric three-ply designs: configuration-1 in which the stiffer material is utilized for the construction of the outer plies, and configuration-2 in which the stiffer material is used for the construction of the central ply. The configuration that gives the largest critical thrust is then the optimal design. Cases in which both configurations are ensured to fail in the lowest flexure mode are

considered first. It is shown for these cases that configuration-1 is the optimal design for plates that are sufficiently long in the direction of thrust, while configuration-2 is the optimal design for plates that are sufficient short in the direction of thrust. The transition aspect ratio is also determined. Then the investigation turns to consider the optimal design problem for cases in which either configuration-1 or configuration-2 (or both) may fail in a mode other than the low wavelength flexure mode. It is shown once again that the optimal design switches from configuration-1 to configuration-2 as the aspect ratio of the plate is varied. However now the determination of the transition aspect ratio may be quite subtle. In fact, an example is given in which the failure mode changes from that of low wavelength flexure to that of wrinkling before the transition aspect ratio. Then, at the transition aspect ratio, the failure mode switches back to the low wavelength flexure mode. A unified framework is developed for the systematic determination of the optimal design in this, and similar cases.

2. PROBLEM DESCRIPTION

Consider a thick rectangular composite plate with surfaces perpendicular to the axes of a rectangular cartesian coordinate system $\mathbf{X} = \mathbf{X}(X_1, X_2, X_3)$. This plate occupies the region

$$-l_i \le X_i \le l_i , \qquad i = 1, 2, 3 \tag{2.1}$$

before the application of loads. It is constructed from 3 plies that are stacked symmetrically in the X_2-direction as follows:

$$\begin{aligned} &\text{ply-1: } -l_2 < X_2 < -R, \\ &\text{ply-2: } -R < X_2 < R, \\ &\text{ply-3: } R < X_2 < l_2. \end{aligned} \tag{2.2}$$

The geometry and loading of a particular plate configuration is depicted in Figure 2-1. Plies 1 and 3 are taken to consist of the same incompressible, isotropic, homogeneous elastic material (Material I). Ply 2 is also composed of an incompressible, isotropic, homogeneous elastic material (Material II) which is in general different from Material I.

Within each ply we define a deformation

$$\mathbf{x} = \mathbf{x}(\mathbf{X}). \tag{2.3}$$

The corresponding deformation gradient tensor is then given by

$$\mathbf{F} = \partial \mathbf{x} / \partial \mathbf{X}. \tag{2.4}$$

The requirement of material incompressibility is that

$$\det \mathbf{F} = 1. \tag{2.5}$$

The principal stretches are defined to be the eigenvalues of the tensor $\mathbf{U} = (\mathbf{F}^T\mathbf{F})^{1/2}$ and shall be denoted by λ_1, λ_2 and λ_3. Note that $\lambda_i > 0$, $i = 1, 2, 3$ by virtue of the definition of $\mathbf{U}$ and the nonsingularity of $\mathbf{F}$. The three scalar invariants of the deformation are then given by

$$\begin{aligned} I_1 &= \lambda_1^2 + \lambda_2^2 + \lambda_3^2, \\ I_2 &= \lambda_1^2\lambda_2^2 + \lambda_2^2\lambda_3^2 + \lambda_3^2\lambda_1^2, \\ I_3 &= \lambda_1^2\lambda_2^2\lambda_3^2. \end{aligned} \tag{2.6}$$

The incompressibility constraint (2.5) dictates that $I_3 = (\det\mathbf{F})^2 = 1$, so that

$$\lambda_1\lambda_2\lambda_3 = 1. \tag{2.7}$$

The mechanical response of an incompressible elastic solid is governed by the strain energy density function $W = W(I_1, I_2)$ of the material. In view of (2.6), (2.7) the strain energy density can be regarded as a function of any two of the three principal stretches.

The Cauchy stress tensor for a general imcompressible elastic material is given by

$$\tau = -p\mathbf{I} + 2(\partial W/\partial I_1 + I_1\partial W/\partial I_2)\,\mathbf{B} - 2(\partial W/\partial I_2)\,\mathbf{B}^2, \tag{2.8}$$

where p is hydrostatic pressure, $\mathbf{B} = \mathbf{F}\mathbf{F}^T$ is Green's deformation tensor, I_1, I_2 are the first and second invariants of $\mathbf{B}$, and W is the strain energy density function of the material. Thus in the problem

at hand

$$W = \begin{cases} W^{I}(I_1,I_2), & \text{in plies 1 and 3,} \\ W^{II}(I_1,I_2), & \text{in ply 2.} \end{cases} \tag{2.9}$$

The Piola-Kirchoff stress tensor is then given by

$$S = F^{-1}\tau, \tag{2.10}$$

and the equilibrium equations can be written in the form

$$\text{div } S^{T} = 0. \tag{2.11}$$

The plate is subjected to a thrust on each of the faces initially at $X_1 = \pm l_1$. The surfaces initially at $X_2 = \pm l_2$ are taken to be traction-free. The surfaces initially at $X_3 = \pm l_3$ are held at this location by means of frictionless clamp.

Since this plate is subjected to a thrust on each of the surfaces $X_1 = \pm l_1$, the following boundary conditions will be required to hold:

$$S_{12} = S_{13} = 0, \quad \text{on } X_1 = \pm l_1, \tag{2.12}$$

$$x_1 = \pm \rho\, l_1, \quad \text{on } X_1 = \pm l_1, \tag{2.13}$$

corresponding to a normal thrust, frictionless in the tangential directions, with an overall stretch ratio of ρ. Here $\rho > 0$, rather than the thrust, will temporarily be regarded as a prescribed constant. The physically interesting case of compression corresponds to $0 < \rho < 1$.

Since the surfaces $X_2 = \pm l_2$ are assumed to be traction free, the following boundary conditions are required to hold:

$$S_{21} = S_{22} = S_{23} = 0, \quad \text{on } X_2 = \pm l_2. \tag{2.14}$$

On the surfaces $X_3 = \pm l_3$, the following boundary conditions are now required to hold:

$$S_{31} = S_{32} = 0, \quad \text{on } X_3 = \pm l_3, \tag{2.15}$$

$$x_3 = \pm l_3, \quad \text{on } X_3 = \pm l_3, \tag{2.16}$$

corresponding to a frictionless clamp. Problems of this type for homogeneous (non-composite) plates have been studied by Sawyers and Rivlin [10], [11].

In order to treat the composite three-ply laminate, the additional interface conditions are required to hold:

$$S_{2i}\Big|_{X_2+} = S_{2i}\Big|_{X_2-} \quad (i = 1, 2, 3), \quad X_2 = \pm R \tag{2.17}$$

$$\mathbf{x}\Big|_{X_2+} = \mathbf{x}\Big|_{X_2-} \quad X_2 = \pm R. \tag{2.18}$$

The conditions (2.17) and (2.18) correspond to a case in which the plies are perfectly bonded across the interfaces.

To within an arbitary displacement in the X_2-direction, there is exactly one pure homogeneous deformation solution to the foregoing

boundary value problem. The underlying deformation must be given by

$$x_1 = \rho X_1,$$
$$x_2 = \rho^{-1} X_2, \tag{2.19}$$
$$x_3 = X_3,$$

in order to satisfy (2.13), (2.16) and (2.5). Thus the principal stretches λ_1, λ_2, λ_3 are given by $\lambda_1 = \rho$, $\lambda_2 = \rho^{-1}$, $\lambda_3 = 1$. The material deformation tensor **F**, Green's deformation tensor **B** and the first and second invariants of the deformation are in this case given by

$$\mathbf{F} = \mathrm{diag}(\rho, \rho^{-1}, 1), \quad \mathbf{B} = \mathrm{diag}(\rho^2, \rho^{-2}, 1),$$
$$I_1 = \lambda_1^2 + \lambda_2^2 + \lambda_3^2 = 1 + \rho^2 + \rho^{-2}, \tag{2.20}$$
$$I_2 = \lambda_1^2\lambda_2^2 + \lambda_2^2\lambda_3^2 + \lambda_3^2\lambda_1^2 = 1 + \rho^2 + \rho^{-2}.$$

The equilibrium equations (2.11) require that the hydrostatic pressure p in (2.8) is constant in each ply, say $p^{(1)}$, $p^{(2)}$ and $p^{(3)}$. These values are found from the requirements $(2.14)_2$ and $(2.17)_{i=2}$, from which one obtains with the aid of (2.8), (2.9) and (2.20) that

$$p^{(1)} = p^{(3)} = p^{(I)}, \quad p^{(2)} = p^{(II)}, \tag{2.21}$$

where

$$p^{(k)} = 2\rho^{-2}(W_1^{(k)} + I_1 W_2^{(k)}) - 2\rho^{-4}W_2^{(k)}, \quad k = I, II, \tag{2.22}$$

and $W_i = \dfrac{\partial W}{\partial I_i}$, $i = 1, 2$. This in turn gives

$$\tau = -[\, 2\rho^{-2}(W_1^{(k)} + I_1 W_2^{(k)}) - 2\rho^{-4}W_2^{(k)} \,] I +$$

$$+ 2(W_1^{(k)} + I_1 W_2^{(k)}) B - 2(W_2^{(k)}) B^2, \qquad k = I, II. \tag{2.23}$$

In this work attention will for the most part be restricted to a class of materials for which the strain energy densities (2.9) are of the following form

$$W^{(k)}(I_1, I_2) = W^{(k)}(I_1) = \mu^{(k)} [(1 + I_1)^{1+A_k/2} - 4(2)^{A_k}] /2 ,$$

$$k = I, II. \tag{2.24}$$

here $\mu^{(I)}$, $\mu^{(II)}$, A_I and A_{II} are material constants obeying

$$\mu^{(I)} > 0, \ \mu^{(II)} > 0, \ A_I > -2, \ A_{II} > -2. \tag{2.25}$$

The special choice of $A_I = A_{II} = 0$ gives the case of two neo-Hookean materials. Thus this class of materials generalizes the well known neo-Hookean material in each ply. A thorough discussion of these materials will be given in the next section.

For this class of materials, the pressure (2.22) simplifies to

$$p = \mu^{(k)} \rho^{-2} (1 + A_k/2) (2+\rho^2+\rho^{-2})^{A_k/2} = p^{(k)}. \qquad k=I,II. \quad (2.26)$$

Substituting from (2.24) into (2.23) and using (2.20) now gives the Cauchy stress tensor for the deformation (2.19)

$$\tau = \mu^{(k)} (1 + A_k/2) (2+\rho^2+\rho^{-2})^{A_k/2} \begin{bmatrix} \rho^2-\rho^{-2} & 0 & \\ & 1-\rho^{-2} & \end{bmatrix} = \tau^{(k)},$$

$$k=I,II. \quad (2.27)$$

Finally using (2.10), (2.27) and $(2.20)_1$, the Piola-Kirchoff stress tensor becomes

$$S = \mu^{(k)} (1 + A_k/2) (2+\rho^2+\rho^{-2})^{A_k/2} \begin{bmatrix} \rho-\rho^{-1} & 0 & \\ & 1-\rho^{-2} & \end{bmatrix} = S^{(k)}.$$

$$k=I,II \quad (2.28)$$

Note that the remaining conditions (2.12), (2.14), (2.15) and (2.17) are automatically satisfied.

Let T be the total thrust applied to each of the faces $X_1 = \pm l_1$. Then

$$T = T^{(I)} + T^{(II)}, \quad (2.29)$$

where $T^{(k)}$ (k=I,II) is the thrust applied to material k. Thus for the homogeneous solution, we have

$$r_{11}^{(k)} = T^{(k)}/\text{Area}^{(k)}, \tag{2.30}$$

where $\text{Area}^{(k)}$ (k=I,II) is the current area of the surface to which $T^{(k)}$ is applied,

$$\text{Area}^{(I)} = 4(l_2-R)l_3\rho^{-1}, \quad \text{Area}^{(II)} = 4Rl_3\rho^{-1}. \tag{2.31}$$

Using (2.27) and (2.29)-(2.31), it is found that

$$T^{(I)} = \frac{(l_2-R)\mu^{(I)}(1+A_I/2)(2+\rho^2+\rho^{-2})^{A_I/2}}{\mathfrak{R}(\rho)}\, T, \tag{2.32}$$

$$T^{(II)} = \frac{R\mu^{(II)}(1+A_{II}/2)(2+\rho^2+\rho^{-2})^{A_{II}/2}}{\mathfrak{R}(\rho)}\, T, \tag{2.33}$$

where

$$T = 4l_3\,(\rho-\rho^{-1})\,\mathfrak{R}(\rho)\ , \tag{2.34}$$

and

$$\mathfrak{R}(\rho) = (l_2-R)\mu^{(I)}(1+A_I/2)(2+\rho^2+\rho^{-2})^{A_I/2} + R\mu^{(II)}(1+A_{II}/2)(2+\rho^2+\rho^{-2})^{A_{II}/2}. \tag{2.35}$$

Note for compression ($0 < \rho < 1$) that $T < 0$ with $T \to -\infty$ as $\rho \to 0$ and for elongation ($\rho > 1$) that $T > 0$ with $T \to \infty$ as $\rho \to \infty$. The undeformed state ($\rho = 1$) occurs if $T = 0$. The following argument shows that T is monotonically increasing in ρ if both $A_I \geq 0$ and $A_{II} \geq 0$.

The monotonicity of T depends on the sign of the derivative of T with respect of ρ. Using (2.34) and (2.35)

$$\partial T/\partial \rho = 4l_3(1+\rho^{-2})\mathfrak{R}(\rho) + 8l_3(\rho-\rho^{-1})(\rho-\rho^{-3})Q(\rho) \ , \tag{2.36}$$

where $Q(\rho)$ is given by

$$Q(\rho) = (l_2-R)\mu^{(I)}(1+A_I/2)(A_I/2)(2+\rho^2+\rho^{-2})^{(A_I/2)-1} +$$

$$+ R\mu^{(II)}(1+A_{II}/2)(A_{II}/2)(2+\rho^2+\rho^{-2})^{(A_{II}/2)-1} \ .$$

Note that $(\rho-\rho^{-1})(\rho-\rho^{-3}) \geq 0$ and that $\mathfrak{R}(\rho) > 0$. Thus a sufficient condition for $\partial T/\partial \rho \geq 0$ is that $Q(\rho) \geq 0$. Furthermore $Q(\rho) \geq 0$ if $A_I \geq 0$ and $A_{II} \geq 0$. Thus T is monotonically increasing in ρ if $A_I \geq 0$ and $A_{II} \geq 0$. *Thus if $A_I \geq 0$ and $A_{II} \geq 0$ then each critical stretch $\lambda_1 = \rho > 0$ has associated with it a specific value of thrust, and that larger thrusts (in either tension or compression) give rise to greater length changes.* If $A_I < 0$ or/and $A_{II} < 0$, T may cease to be monotone in ρ. For example let $A_I = A_{II} = -3/2$, $\mu^{(I)} = \mu^{(II)} = \mu$, then

$$\partial T/\partial \rho = l_2 l_3 \mu(\rho+\rho^{-1})^{-3/2}[(1+\rho^{-2})-(3/2)(\rho-\rho^{-1})(\rho+\rho^{-1})^{-2}(\rho-\rho^{-3})] . \tag{2.37}$$

Now under these circumstances T is non-monotone in ρ as can be verified numerically, i.e. although for example

$$\partial T/\partial \rho \Big|_{\rho=2} = 0.1455\ l_2 l_3 \mu > 0, \tag{2.38}$$

one also finds that

$$\partial T/\partial \rho \Big|_{\rho=10} = -0.0139\ l_2 l_3 \mu < 0. \tag{2.39}$$

For cases in which the load deformation relation (2.34), (2.35) is non-monotone, nonuniqueness of the homogeneous solution (2.19) can occur for a given value of ρ. As will be seen in the next section, the case of $A_I = A_{II} = -3/2$ leads to an equally unusual response in simple shear. Consequently this behavior, although of interest in its own right, will not be investigated further here.

This section will now conclude with some general remarks regarding generalization of the boundary value problem (2.5), (2.11)-(2.18) for materials obeying (2.9) and (2.24). This section was devoted solely to obtaining homogeneous solutions (solutions with constant deformation gradiant F). In view of (2.5), (2.13) and (2.16) such solutions must be of the form (2.19). The resulting load-deformation relation is then given by (2.34) and (2.35). Two obvious generalizations immediately come to mind. The first (generalization G-1) involves considering classes of material more general than (2.24). The second (generalization G-2) involves the consideration of

ply lay-ups that generalize (2.2), say an arbitrary number of alternating material plies with no particular thickness symmetry. Obtaining homogeneous solutions for either generalization G-1 or G-2 (or both in concert) presents no great difficulty. In all cases (2.19) must still hold. In fact for the case of G-2 one still obtains the load-deformation relations (2.34), (2.35). In this case (2.28) continues to hold provided k=I and II apply to the associated material ply. Turning now to the case of G-1 (acting either alone or in concert with G-2), one finds that the strategy employed here will again allow one to obtain conditions which ensure that the homogeneous solution (2.19) continues to hold. In this case, however, the pressures $p^{(k)}$ in (2.26) and the load deformation relation (2.34)-(2.35) will be correspondingly altered.

The reason that the generalizations G-1 and G-2 are not developed here is thus not at all related to difficulties in finding homogeneous solutions. Rather, it is related to difficulties which would arise later in connection with obtaining non-homogeneous (buckled) solutions. Put simply, (G-1) leads to buckling equations that are not easily analyzed. Further commentary regarding this will be given in section 5. As shown in the next section, the class of materials (2.24) allows for a wide range of material response, and so the strategy of not pursuing (G-1) does not seem to impose a serious handicap. The consideration of generation G-2 also leads to formidable difficulties. In this case, as additional plies are added, additional boundary conditions corresponding to (2.17) and (2.18) are obtained at each new interface. This brings additional unknowns into the problem for obtaining buckled solutions. The level of difficulty

quickly rises, and one would suspect that "bookkeeping questions" could quickly dominate the analysis. For these reasons, this dissertation will henceforth focus attention on the buckling problem in the absence of generalizations G-1 and G-2.

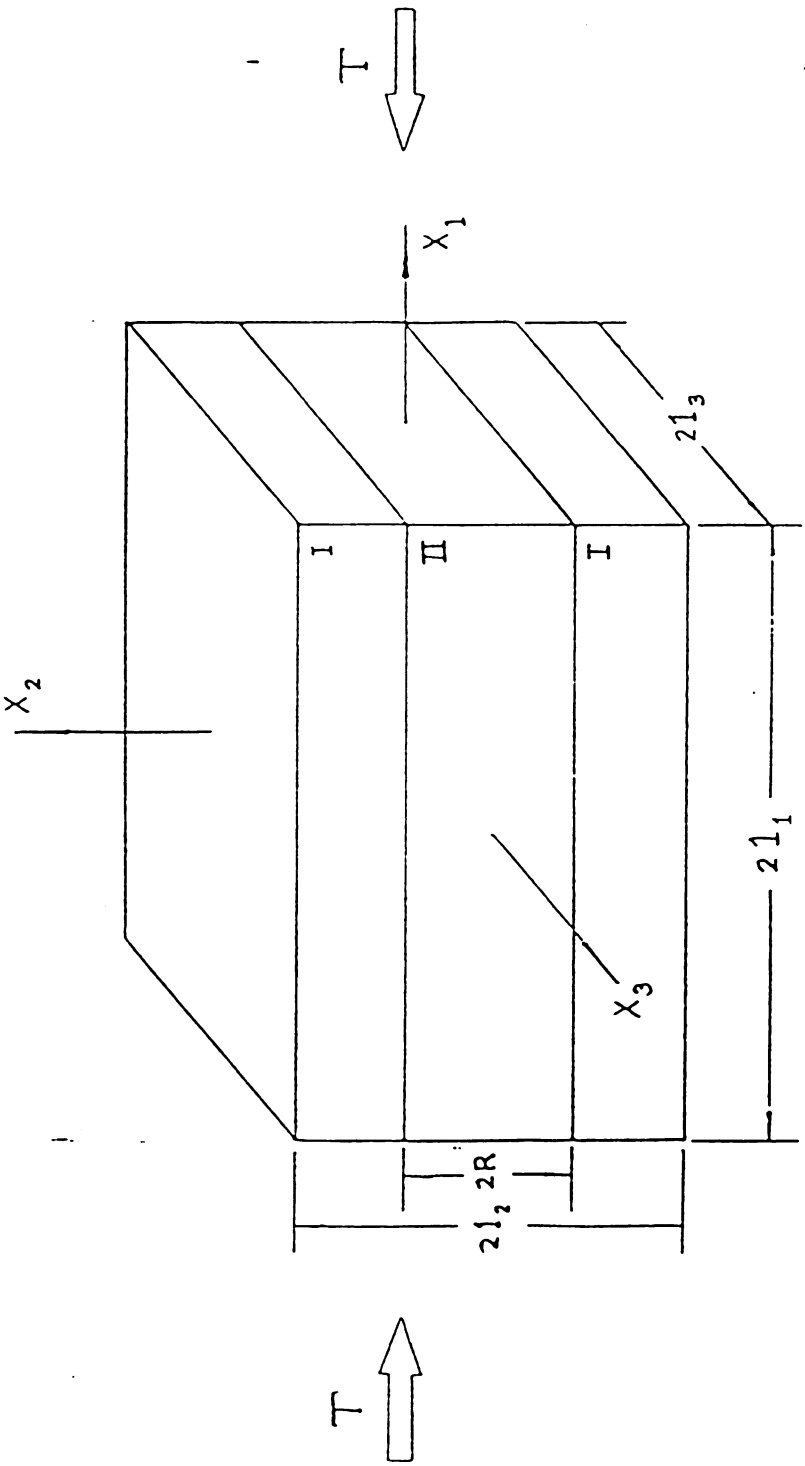

Figure 2-1:

Geometry of the composite plate under consideration. The buckled configurations of interest involve deformations in the (X_1, X_2)-plane.

3. MECHANICAL BEHAVIOR OF THE CLASS OF INCOMPRESSIBLE NONLINEAR ELASTIC MATERIALS UNDER CONSIDERATION

The purpose of this section is to investigate the nature of the elastic response for the class of materials with strain energy density

$$W = \mu\,[(1 + I_1)^{1+A/2} - 4(2^A)]\,/2\ , \tag{3.1}$$

where

$$\mu > 0,\ A > -2\ . \tag{3.2}$$

The subscript k and superscript k used in (2.24) will temporarily be dropped in this section, as attention is here to be focused on the response of a homogeneous material. Substituting from (2.6) it is apparent that this strain energy density is given in terms of principal stretches by

$$W = \mu\,[(1+\lambda_1^2+\lambda_2^2+\lambda_3^2)^{1+A/2} - 4(2^A)]\,/2\ . \tag{3.3}$$

The inessential additive constant term in (3.1) is chosen to ensure that $W = 0$ in an undeformed state, $I_1 = 3$ or $\lambda_1 = \lambda_2 = \lambda_3 = 1$.

The Baker-Ericksen inequality

$$\partial W/\partial I_1 + \lambda_k^2\,\partial W/\partial I_2 > 0\ ,\quad \text{if } \lambda_i \neq \lambda_j,\ k \neq i,\ k \neq j, \tag{3.4}$$

arises from the requirement that if one is given a pair of principal stretches λ_i, λ_j, then the greater of the two corresponding principal

stresses T_i, T_j occurs in the direction associated with the greater principal stretch ($(T_i-T_j)(\lambda_i-\lambda_j)>0$ if $\lambda_i \neq \lambda_j$). Applying (3.4) to (3.3), one obtains the requirement that

$$\mu\ (1+A/2)\ (1+\lambda_1^2+\lambda_2^2+\lambda_3^2)^{A/2} > 0\ . \tag{3.5}$$

Thus (3.5) will hold if and only if $\mu(1 + A/2) > 0$, which is the justification for (3.2). Thus in the composite sandwich construction (2.9), the restrictions (2.25) ensure that the material in each ply is consistent with the Baker-Ericksen inequality.

Since $W = W(I_1)$, we obtain from (2.8) that

$$\tau = -pI + 2\ [\partial W/\partial I_1]\ B\ , \tag{3.6}$$

where (3.1) gives that

$$\partial W/\partial I_1 = (\mu/2)\ (1+A/2)\ (1+I_1)^{A/2}. \tag{3.7}$$

Hence (3.6) can be written as

$$\tau = -pI + \mu(1 + A/2)\ (1+I_1)^{A/2}\ B\ . \tag{3.8}$$

Consider first a state of uniaxial tension/compression:

$$\tau = \begin{bmatrix} \tau_{11} & & \\ & 0 & \\ & & 0 \end{bmatrix}, \tag{3.9}$$

with $\lambda_2 = \lambda_3$. Then (2.7) gives $\lambda_2 = \lambda_3 = \lambda_1^{-1/2}$ so that

$$\mathbf{B} = \begin{bmatrix} \lambda_1^2 & & \\ & \lambda_1^{-1} & \\ & & \lambda_1^{-1} \end{bmatrix} . \tag{3.10}$$

Combining (3.8) and (3.10) yields

$$\begin{aligned} \tau_{11} &= -p + \mu(1+A/2)\ (\lambda_1^2+2\lambda_1^{-1}+1)^{A/2}\ \lambda_1^2 , \\ 0 &= -p + \mu(1+A/2)\ (\lambda_1^2+2\lambda_1^{-1}+1)^{A/2}\ \lambda_1^{-1} , \end{aligned} \tag{3.11}$$

Solving $(3.11)_2$ for the pressure and substituting this value into $(3.11)_1$ gives the uniaxial tension/compression stress-stretch response:

$$\tau_{11} = \mu(1+A/2)\ (1+\lambda_1^2+2\lambda_1^{-1})^{A/2}\ (\lambda_1^2-\lambda_1^{-1}) . \tag{3.12}$$

The stress-stretch relations (3.12) are depicted in Figure 3-1 for different parameters A and μ. In particular it is to be noted that the uniaxial tension/compression response is monotone increasing in λ_1 from $\sigma_{11} = -\infty$ when $\lambda_1 = 0$ to $\sigma_{11} = \infty$ when $\lambda_1 = \infty$ with $\sigma_{11} = 0$ when $\lambda_1 = 1$. It is also to be noted that the slope of these curves indicates that the material is "softening in tension" and "hardening in compression" for all parameter pairs (μ,A) obeying (3.2)

In order to obtain the Young's modulus for the associated linear theory, one may set $\lambda_1 = 1 + \epsilon_{11}$ which upon substitution into

(3.12) gives

$$\tau_{11} = 2^{A-1}\,\mu\,(2+A)\,(3\epsilon_{11} + O(\epsilon_{11}^{2}))\ . \tag{3.13}$$

This provides the Young's modulus of the material in terms of μ and A:

$$E = 3\,(2^{A-1})\,\mu\,(2+A). \tag{3.14}$$

Consider now a state of **simple shear**:

$$\begin{aligned} x_1 &= X_1 + \epsilon_{12}X_2, \\ x_2 &= X_2, \\ x_3 &= X_3, \end{aligned} \tag{3.15}$$

where ϵ_{12} is the amount of simple shear. In this case

$$B = \begin{bmatrix} 1+\epsilon_{12}^{2} & \epsilon_{12} & 0 \\ \epsilon_{12} & 1 & 0 \\ 0 & 0 & 1 \end{bmatrix}, \quad I_1 = 3 + \epsilon_{12}^{2}\ . \tag{3.16}$$

Then (3.6) gives

$$\tau = -pI + 2\partial W/\partial I_1 \begin{bmatrix} 1+\epsilon_{12}^{2} & \epsilon_{12} & 0 \\ \epsilon_{12} & 1 & 0 \\ 0 & 0 & 1 \end{bmatrix}, \tag{3.17}$$

which in view of (3.7) yields

$$\tau_{12} = \mu\ (1+A/2)\ (4+\epsilon_{12}^{2})^{A/2}\ \epsilon_{12}\ . \tag{3.18}$$

The shear stress-simple shear relation (3.18) is depicted in Figure 3-2 for different parameters A and μ obeying (3.2). In particular it is to be noted that the shear stress-simple shear response is linear for the neo-Hookean case $A = 0$. For $A > 0$ the material is hardening in shear and for $-2 < A < 0$ the material is softening in shear. Moreover, only for $A > -1$ is the shear stress-simple shear response monotonically increasing to ∞. For $A = -1$ the shear stress is monotonically increasing to the finite aymptotic value of $\tau_{12} = \mu/2$. For $-2 < A < -1$ the material exhibits a collapse in simple shear whereby it attains its ultimate stress in shear at the value $\tau_{12}=\mu(2+A)(2)^{A}(A/(1+A))^{A/2}(-2/(1+A))^{1/2}$ when $\epsilon_{12}=2(-1-A)^{-1/2}$, before monotonically decreasing towards $\tau_{12} = 0$ as ϵ_{12} tends to ∞. Such a collapse in shear phenomena is associated with loss of ellipticity in the equilibrium equations. Stress response functions exhibiting such a collapse in shear have been used for the continuum mechanical modeling of shear band formation and phase transitions [1].

Linearizing (3.18) gives

$$\tau_{12} = \mu\ (2+A)\ 2^{A-1}\ \epsilon_{12} + O(\epsilon_{12}^{2})\ , \tag{3.19}$$

which provides the infinitesmal shear modulus of the material

$$G = \mu\ 2^{A-1}\ (2+A). \tag{3.20}$$

Note that the neo-Hookean case $A = 0$ implies $G = \mu$. Furthermore, by (3.14) and (3.20), it is seen that $E = 3G$ for all values of the

parameters A and μ obeying (3.2). Thus it is confirmed that the corresponding value of Poission's ratio $\nu = E/(2G) - 1$ takes on the value $\nu = 1/2$, as it must for the corresponding incompressible linear theory.

As the above exposition shows, the class of materials (3.1) can be regarded as a generalization of the neo-Hookean material. Alternatively, it can be shown that the class of materials (3.1) can be regarded as a specialization of a class of *power law materials* utilized by Knowles [7] in the investigation of certain crack problems. These materials are characterized by the strain energy density

$$W = k/(2b)\ [(1 + b(I_1-3)/n)^n - 1], \tag{3.21}$$

where

$$k > 0, \quad b > 0, \quad n > 0. \tag{3.22}$$

It is found that if

$$n = 1+A/2, \ b = (1+A/2)/4 \text{ and } k = 2(1/4)^{-A/2}(1+A/2)\mu, \tag{3.23}$$

then (3.21) reduces to (3.1). Note that the restrictions (3.22) when used in (3.23) ensure (3.1).

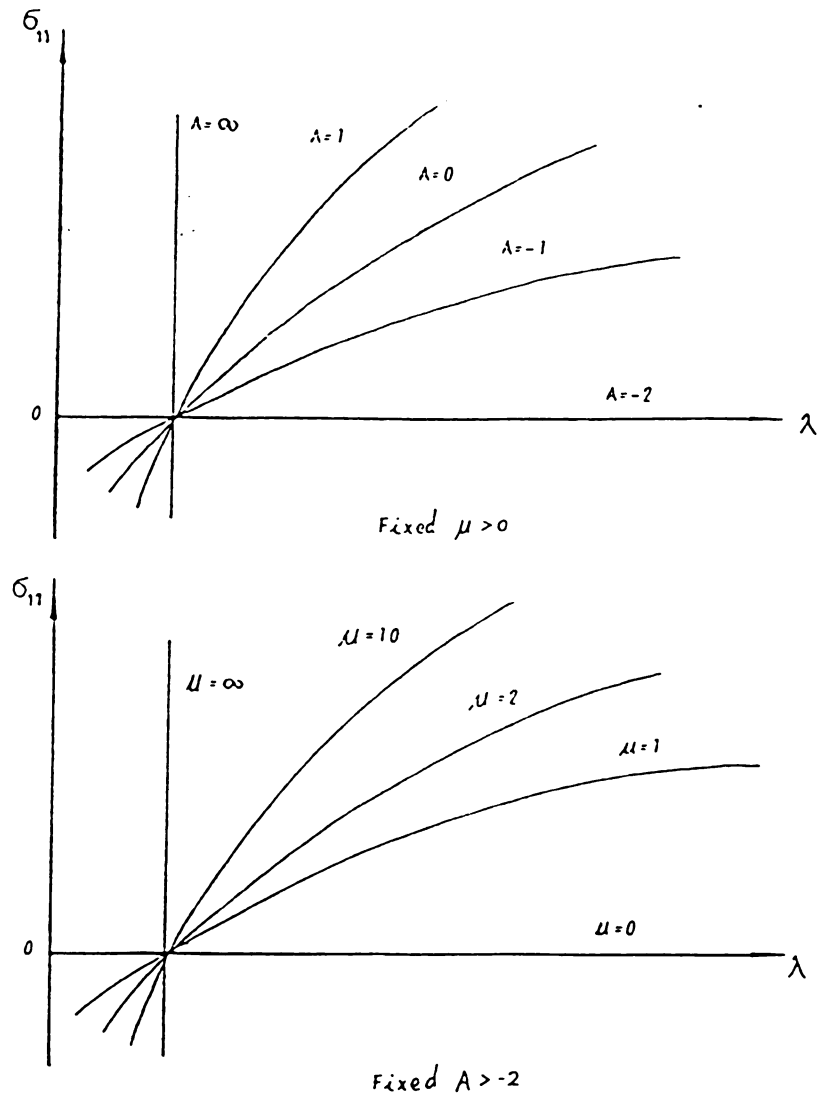

Figure 3-1:

The stress-stretch relation of the materials with strain energy density (3.1) for uniaxial tension/compression for various values of A and μ.

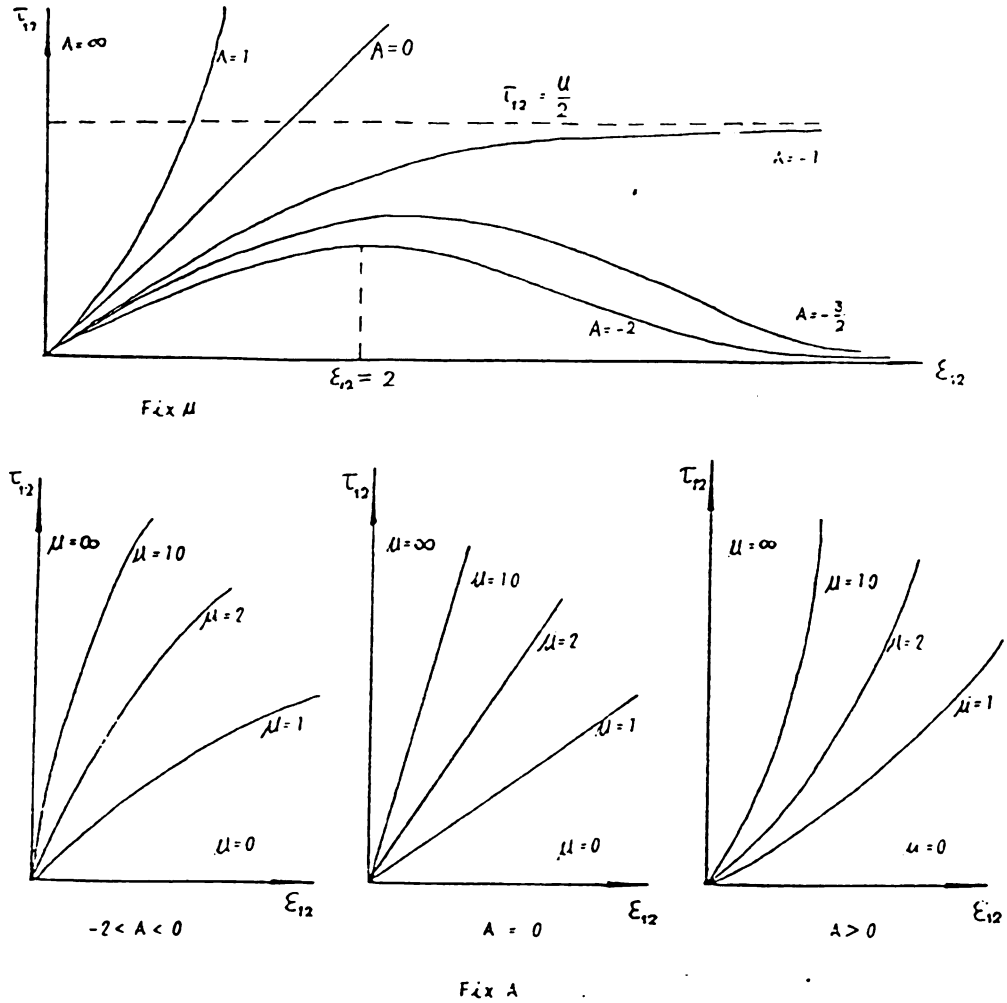

Figure 3-2:

The shear stress-simple shear relation of the materials with strain energy density (3.1) for different values of A and μ.

4. BIFURCATION FROM THE HOMOGENEOUS SOLUTION

Consider now the stability of the homogeneous deformation solution given in (2.19). Attention shall be restricted to the case where buckling takes place in the (X_1,X_2)-plane. To do so, let us consider the fully finite deformation

$$\begin{aligned} \hat{x}_1 &= \rho X_1 + \epsilon \bar{u}_1(X_1,X_2), \\ \hat{x}_2 &= \rho^{-1} X_2 + \epsilon \bar{u}_2(X_1,X_2), \\ \hat{x}_3 &= X_3, \end{aligned} \tag{4.1}$$

where $\bar{u}_1$, $\bar{u}_2$ are unknown functions which are independent of X_3 by assumption. In this section, it will be helpful to use a superposed $\hat{}$ to indicate quantities associated with the finite deformation (4.1). Here ϵ is an order parameter which is introduced for the purposes of obtaining a linearized problem governing bifurcation from the homogeneous deformation solution (2.19). Finally a superposed $\bar{}$ will be used to indicate the $O(\epsilon)$ difference between quantities associated with $\hat{x}$ and quantities associated with this homogeneous deformation solution. Thus, for example, the pressure field corresponding to (4.1) will be given by

$$\hat{p}(\mathbf{X},\epsilon) = p^{(k)} + \epsilon \bar{p}(X_1,X_2,X_3) + O(\epsilon^2), \qquad k = I,II, \tag{4.2}$$

and the Piola-Kirchoff stress tensor is given by

$$\hat{S}(X,\epsilon) = S^{(k)} + \epsilon\bar{S}(X_1,X_2,X_3) + O(\epsilon^2), \qquad k = I,II. \tag{4.3}$$

The material deformation tensor associated with (4.1) is given by

$$\hat{F} = \begin{bmatrix} \rho + \epsilon\bar{u}_{1,1} & \epsilon\bar{u}_{1,2} & 0 \\ \epsilon\bar{u}_{2,1} & \rho^{-1} + \epsilon\bar{u}_{2,2} & 0 \\ 0 & 0 & 0 \end{bmatrix}, \tag{4.4}$$

so that

$$\det \hat{F} = [1 + \epsilon\,(\rho\bar{u}_{2,2} + \rho^{-1}\bar{u}_{1,1}) + \epsilon^2(\bar{u}_{1,1}\bar{u}_{2,2} - \bar{u}_{1,2}\bar{u}_{2,1})]. \tag{4.5}$$

It is well known that the solution to the corresponding linearized boundary value problem locates the failure thrusts at which bifurcation occurs from a homogeneous solution of the type (2.19) (see Davies [3]) for a rigorous discussion in a problem involving a non-composite compressible elastic material). An analysis of the linear problem will not reveal the details of the post buckling and moreover may underestimate the actual thrusts at which instability occurs for the case of snap-buckling. These more difficult issues are not treated in this dissertation. Rather the concern is upon the

determination of the failure thrusts at which bifurcation takes place locally from the homogeneous solution (2.19). Thus it follows from (2.5) and (4.5) that the linearized problem governing local bifurcation obeys

$$\rho^{-2}\bar{u}_{1,1} + \bar{u}_{2,2} = 0. \tag{4.6}$$

One obtains from (4.4), (4.6) that

$$\hat{\mathbf{B}} = \begin{bmatrix} \rho^2+\epsilon(2\rho\bar{u}_{1,1}) & \epsilon(\rho\bar{u}_{2,1}+\rho^{-1}\bar{u}_{1,2}) & 0 \\ \epsilon(\rho\bar{u}_{2,1}+\rho^{-1}\bar{u}_{1,2}) & \rho^{-2}+\epsilon(2\rho^{-1}\bar{u}_{2,2}) & 0 \\ 0 & 0 & 1 \end{bmatrix} + O(\epsilon^2), \tag{4.7}$$

$$\hat{\mathbf{F}}^{-1} = \begin{bmatrix} \rho^{-1} + \epsilon\bar{u}_{2,2} & -\epsilon\bar{u}_{1,2} & 0 \\ -\epsilon\bar{u}_{2,1} & \rho + \epsilon\bar{u}_{1,1} & 0 \\ 0 & 0 & 1 \end{bmatrix} + O(\epsilon^2). \tag{4.8}$$

The corresponding Cauchy stress tensor is by virtue of (2.8) and

(2.24) given by

$$\hat{\tau}^{(k)} = -\hat{p}I + \mu^{(k)} (1 + A_k/2) (1 + I_1)^{A_k/2} \hat{B}, \quad k=I,II. \tag{4.9}$$

Substituting from (4.9) into (2.10) now gives the corresponding Piola-Kirchoff stress tensor

$$\hat{S}^{(k)} = -\hat{p}\hat{F}^{-1} + \mu^{(k)} (1 + A_k/2) (1 + I_1)^{A_k/2} \hat{F}^{-1}\hat{B}, \quad k=I,II. \tag{4.10}$$

To obtain an expansion of this tensor in powers of ϵ, note first of all that

$$I_1 = \text{tr } \hat{B} = 1+\rho^2+\rho^{-2}+\epsilon(2\rho\bar{u}_{1,1}+2\rho^{-1}\bar{u}_{2,2})+O(\epsilon^2), \tag{4.11}$$

which in turn gives

$$\mu^{(k)}(1+A_k/2)(1+I_1)^{A_k/2} = \mu^{(k)}(1+A_k/2)(2+\rho^2+\rho^{-2})^{A_k/2} +$$

$$+ \mu^{(k)}(1+A_k/2)(2+\rho^2+\rho^{-2})^{-1+A_k/2}(\rho\bar{u}_{1,1}+\rho^{-1}\bar{u}_{2,2})\epsilon + O(\epsilon^2),$$

$$k=I,II. \tag{4.12}$$

In addition

$$\hat{p}^{(k)}\hat{F}^{-1} = \begin{bmatrix} \rho^{-1}p^{(k)}+\epsilon(\rho^{-1}\bar{p}+\bar{u}_{2,2}p^{(k)}), & -\epsilon\bar{u}_{1,2}p^{(k)}, & 0 \\ -\epsilon\bar{u}_{2,1}p^{(k)}, & \rho p^{(k)}+\epsilon(\rho\bar{p}+\bar{u}_{1,1}p^{(k)}), & 0 \\ 0, & 0, & p^{(k)}+\epsilon\bar{p} \end{bmatrix} + O(\epsilon^2),$$

$$k=I,II, \qquad (4.13)$$

$$\hat{F}^{-1}\hat{B} = \begin{bmatrix} \rho+\epsilon(2\bar{u}_{1,1}+\rho^2\bar{u}_{2,2}), & \epsilon\bar{u}_{2,1}, & 0 \\ \epsilon\bar{u}_{1,2}, & \rho^{-1}+\epsilon(2\bar{u}_{2,2}+\rho^{-2}\bar{u}_{1,1}), & 0 \\ 0, & 0, & 1 \end{bmatrix} + O(\epsilon^2). \qquad (4.14)$$

Now substitution from (4.12)-(4.14) into (4.10) gives upon comparison with (4.3) that

$$S^{(k)} = \begin{bmatrix} -\rho^{-1}p^{(k)}+\mu^{(k)}(1+A_k/2)(2+\rho^2+\rho^{-2})^{A_k/2}\rho, & 0, & 0 \\ 0, & -\rho p^{(k)}+\mu^{(k)}(1+A_k/2)(2+\rho^2+\rho^{-2})^{A_k/2}\rho^{-1}, & 0 \\ 0, & 0, & -p^{(k)}+\mu^{(k)}(1+A_k/2)(2+\rho^2+\rho^{-2})^{A_k/2} \end{bmatrix},$$

$$k=I,II \qquad (4.15)$$

where $p^{(k)}$ is given by (2.26) and $\bar{S}$ has components as follows:

$$\bar{S}_{11} = -\rho^{-1}\bar{p} - \bar{u}_{2,2}p^{(k)} +$$

$$+ \mu^{(k)}A_k(1+A_k/2)(2+\rho^2+\rho^{-2})^{-1+A_k/2}(\rho\bar{u}_{1,1}+\rho^{-1}\bar{u}_{2,2})\rho +$$

$$+ \mu^{(k)}(1+A_k/2)(2+\rho^2+\rho^{-2})^{A_k/2}(2\bar{u}_{1,1}+\rho^2\bar{u}_{2,2}) ,$$

$$\bar{S}_{12} = \bar{u}_{1,2}p^{(k)}+\mu^{(k)}(1+A_k/2)(2+\rho^2+\rho^{-2})^{A_k/2}\bar{u}_{2,1} ,$$

$$\bar{S}_{21} = \bar{u}_{2,1}p^{(k)}+\mu^{(k)}(1+A_k/2)(2+\rho^2+\rho^{-2})^{A_k/2}\bar{u}_{1,2} ,$$

$$\bar{S}_{22} = -\rho\bar{p} - \bar{u}_{1,1}p^{(k)} +$$

$$+ \mu^{(k)}A_k(1+A_k/2)(2+\rho^2+\rho^{-2})^{-1+A_k/2}(\rho\bar{u}_{1,1}+\rho^{-1}\bar{u}_{2,2})\rho^{-1} +$$

$$+\mu^{(k)}(1+A_k/2)(2+\rho^2+\rho^{-2})^{A_k/2}(2\bar{u}_{2,2}+\rho^{-2}\bar{u}_{1,1}) ,$$

$$\bar{S}_{33} = -\bar{p}+\mu^{(k)}A_k(1+A_k/2)(2+\rho^2+\rho^{-2})^{-1+A_k/2}(\rho\bar{u}_{1,1}+\rho^{-1}\bar{u}_{2,2}) ,$$

$$\bar{S}_{13} = \bar{S}_{23} = \bar{S}_{31} = \bar{S}_{32} = 0 ,$$

$$k=I,II. \qquad (4.16)$$

The equilibrium equation (2.11) in conjunction with (4.16) then yields the following system of linear partial differential equations for the $O(\epsilon)$ problem:

$$\mu^{(k)}A_k(1+A_k/2)(2+\rho^2+\rho^{-2})^{-1+A_k/2}(\rho\bar{u}_{1,11}+\rho^{-1}\bar{u}_{2,21})\rho +$$

$$+ \mu^{(k)}(1+A_k/2)(2+\rho^2+\rho^{-2})^{A_k/2}(2\bar{u}_{1,11}+\rho^2\bar{u}_{2,21}+\bar{u}_{1,22}) -$$

$$-\rho^{-1}\bar{p}_{,1} = 0 ,$$

$$\mu^{(k)}A_k(1+A_k/2)(2+\rho^2+\rho^{-2})^{-1+A_k/2}(\rho\bar{u}_{1,12}+\rho^{-1}\bar{u}_{2,22})\rho^{-1} +$$

$$+\mu^{(k)}(1+A_k/2)(2+\rho^2+\rho^{-2})^{A_k/2}(2\bar{u}_{2,22}+\rho^{-2}\bar{u}_{1,12}+\bar{u}_{2,11}) -$$

$$-\rho\bar{p}_{,2} = 0 ,$$

$$\bar{p}_{,3} = 0 ,$$

$$k=I,II. \qquad (4.17)$$

Differentiation of (4.6) yields

$$\bar{u}_{2,21} = -\rho^{-2}\,\bar{u}_{1,11} , \qquad \bar{u}_{1,12} = -\rho^2\,\bar{u}_{2,22} . \qquad (4.18)$$

Substituting from (4.18) into (4.17) gives rise to the following, more convenient, form

$$\mu^{(k)}A_k(1+A_k/2)(2+\rho^2+\rho^{-2})^{-1+A_k/2}(\rho^2-\rho^{-2})\bar{u}_{1,11} +$$

$$+ \mu^{(k)}(1+A_k/2)(2+\rho^2+\rho^{-2})^{A_k/2}(\bar{u}_{1,11}+\bar{u}_{1,22}) - \rho^{-1}\bar{p}_{,1} = 0 ,$$

$$\mu^{(k)}A_k(1+A_k/2)(2+\rho^2+\rho^{-2})^{-1+A_k/2}(\rho^{-2}-\rho^2)\bar{u}_{2,22} +$$

$$+\mu^{(k)}(1+A_k/2)(2+\rho^2+\rho^{-2})^{A_k/2}(\bar{u}_{2,22}+\bar{u}_{2,11}) - \rho\bar{p}_{,2} = 0 ,$$

$$\bar{p}_{,3} = 0 .$$

$$k=I,II \qquad (4.19)$$

Note that $(4.19)_3$ is satisfied if and only if

$$\bar{p}(X_1,X_2,X_3) = \bar{p}(X_1,X_2) . \qquad (4.20)$$

In addition, boundary conditions (2.15) and (2.16) are satisfied automatically. Thus the linearized problem for local bifurcation from the homogeneous solution (2.19) is governed by field equations $(4.19)_{1,2}$ and (4.6) for functions $\bar{u}_1(X_1,X_2)$, $\bar{u}_2(X_1,X_2)$, $\bar{p}(X_1,X_2)$ subjected to boundary conditions that follow from (2.12)-(2.14), (2.17), (2.18). In fact the boundary conditions (2.14), (2.17) and (2.18) give rise to:

$$\left.\begin{aligned} &\rho^{-2}\bar{u}_{2,1}(X_2) + \bar{u}_{1,2}(X_2) = 0 \ , \\ &(1 + C_2^{(I)})\, \bar{u}_{2,2}(X_2) - D^{(I)}\rho\bar{p}^{(I)}(X_2) = 0 \ , \end{aligned}\right\} \quad \text{on } X_2 = \pm\, l_2,$$

$$\left.\begin{aligned} &\bar{u}_2(X_2+) = \bar{u}_2(X_2-) \ , \\ &\bar{u}_1(X_2+) = \bar{u}_1(X_2-) \ , \end{aligned}\right\} \quad \text{on } X_2 = \pm\, R,$$

$$\left.\begin{aligned} &(D^{(k)})^{-1}\,[\rho^{-2}\bar{u}_{2,1}(X_2+) + \bar{u}_{1,2}(X_2+)] - \\ &- (D^{(\hat{k})})^{-1}\,[\rho^{-2}\bar{u}_{2,1}(X_2-) + \bar{u}_{1,2}(X_2-)] \ , \\ &-\rho\bar{p}^{(k)}(X_2+) + (D^{(k)})^{-1}(1+C_2^{(k)})\bar{u}_{2,2}(X_2+) - \\ &- -\rho\bar{p}^{(\hat{k})}(X_2-) + (D^{(\hat{k})})^{-1}(1+C_2^{(\hat{k})})\bar{u}_{2,2}(X_2-) \ , \end{aligned}\right\} \quad \text{on } X_2 = \pm R. \tag{4.21}$$

where, $X_2 = -R$ implies $k = II$, $\hat{k} = I$ and $X_2 = R$ implies $k = I$, $\hat{k} = II$. In addition the following "constants", parameterized by ρ, have been introduced:

$$C_1^{(k)} = \frac{(\rho^2 - \rho^{-2})A_k}{2+\rho^2+\rho^{-2}} + 1 \ , \tag{4.22}$$

$$C_2^{(k)} = -\frac{(\rho^{-2}-\rho^2)A_k}{2+\rho^2+\rho^{-2}} + 1 \quad , \tag{4.23}$$

$$D^{(k)} = [\ \mu^{(k)}(1+A_k/2)(2+\rho^2+\rho^{-2})^{A_k/2}\ ]^{-1}$$

$$= [\ \mu^{(k)}(1+A_k/2)(\rho+\rho^{-1})^{A_k}\ ]^{-1} \quad , \qquad k=I,II. \tag{4.24}$$

We may obtain the solution for the problem at hand by assumming

$$\bar{u}_1 = \left.\begin{matrix} -\sin(\Phi X_1) \\ \cos(\Psi X_1) \end{matrix}\right\} U_1(X_2), \quad \bar{u}_2 = \left.\begin{matrix} \cos(\Phi X_1) \\ \sin(\Psi X_1) \end{matrix}\right\} U_2(X_2), \quad \bar{p} = \left.\begin{matrix} \cos(\Phi X_1) \\ \sin(\Psi X_1) \end{matrix}\right\} P(X_2), \tag{4.25}$$

where the choices of $\Phi = k\pi/l_1$ ($k = 1,2,3\ldots$) and $\Psi = (j - 1/2)\pi/l_1$ ($j = 1,2,3\ldots$) results in the satisfaction of boundary conditions obtained from linearizing (2.12), (2.13). Let $\Omega = \Phi$ or Ψ accordingly as one considers either the upper or lower terms in (4.25). Thus $\Omega = m\pi/2l_1$ where $m = 2k$ for the upper terms and $m = 2j - 1$ for the lower terms. The integer m shall be refered to as the *mode number*, since it determines the number of repeating half-wavelengths in the X_1-direction of a basic deformation mode.

For both the upper and lower terms in (4.25) the field equations $(4.19)_{1,2}$ and (4.6) then become ordinary differential equations:

$$U_1'' - C_1^{(k)}\Omega^2 U_1 - D^{(k)}\rho^{-1}\Omega P = 0 ,$$

$$C_2^{(k)}U_2'' - \Omega^2 U_2 - D^{(k)}\rho P' = 0 , \tag{4.26}$$

$$U_2' - \rho^{-2}\Omega U_1 = 0 .$$

Here the superscript $'$ denotes differentiation with respect to X_2. The boundary and interface conditions (4.21) will presently be written in terms of $P(X_2)$, $U_1(X_2)$, $U_2(X_2)$ as well.

Define the stretch ratio λ

$$\lambda = \lambda_2/\lambda_1 = \rho^{-2}. \tag{4.27}$$

Note that $\lambda > 1$ when the ends are compressed ($0 < \rho < 1$), and $\lambda < 1$ when the ends are extended ($\rho > 1$). One method to solve (4.26) is to reduce this set of equations into a single ordinary differential equation for U_2 alone. From $(4.26)_3$ one may solve for U_1 in terms of the derivative of the function U_2:

$$U_1 = (\lambda\Omega)^{-1} U_2' . \tag{4.28}$$

Furthermore, from $(4.26)_1$, one may solve for P in terms of the function U_1 and it's derivitives, and hence, by virtue of (4.28), in terms of the derivatives of U_2:

$$P = (D^{(k)})^{-1}\lambda^{-1/2}\Omega^{-1} (U_1'' - C_1^{(k)}\Omega^2 U_1)$$

$$= (D^{(k)})^{-1}\lambda^{-3/2}\Omega^{-2} (U_2''' - C_1^{(k)}\Omega^2 U_2') . \tag{4.29}$$

Upon using these results in $(4.26)_2$ one obtains a single 4-th order ordinary differential equation for U_2,

$$C_2^{(k)} U_2'' - \Omega^2 U_2 - \lambda^{-2}\Omega^{-2} (U_2'''' - C_1^{(k)} \Omega^2 U_2'') = 0 , \tag{4.30}$$

which is the same as

$$U_2'''' - (C_1^{(k)} + C_2^{(k)} \lambda^2) \Omega^2 U_2'' + \lambda^2 \Omega^4 U_2 = 0 . \tag{4.31}$$

The constant coefficient of the middle term is, by virtue of (4.22) and (4.23), given by

$$C_1^{(k)} + C_2^{(k)} \lambda^2 = 1 + \lambda^2 + (1 - \lambda)^2 A_k , \quad k = I, II. \tag{4.32}$$

Note that the solution of (4.26) is thus reduced to the solution of (4.31) for U_2, after which U_1 and P are obtained directly from (4.28) and (4.29).

In a similar fashion the boundary and interface conditions (4.21) together with (4.25), (4.28) and (4.29) now become:

$$\left.\begin{aligned} &(\lambda\Omega)^2\, U_2(X_2) + U_2''(X_2) = 0\ , \\ &(\lambda\Omega)^2\, [2+\lambda^{-2}+(1-\lambda^{-1})^2 A_I]\, U_2'(X_2) - U_2'''(X_2) = 0\ , \end{aligned}\right\} \text{ on } X_2 = \pm l_2,$$

$$\left.\begin{aligned} &U_2(X_2+) = U_2(X_2-)\ , \\ &U_2'(X_2+) = U_2'(X_2-)\ , \end{aligned}\right\} \text{ on } X_2 = \pm R,$$

$$\left.\begin{aligned} &(D^{(k)})^{-1}\, [(\lambda\Omega)^2 U_2(X_2+) + U_2''(X_2+)] - \\ &- (D^{(\hat{k})})^{-1}\, [(\lambda\Omega)^2 U_2(X_2-) + U_2''(X_2-)]\ , \\ &(D^{(k)})^{-1}\, \{(\lambda\Omega)^2 [2+\lambda^{-2}+(1-\lambda^{-1})^2 A_k] U_2'(X_2+) - U_2'''(X_2+)\} - \\ &- (D^{(\hat{k})})^{-1}\, \{(\lambda\Omega)^2 [2+\lambda^{-2}+(1-\lambda^{-1})^2 A_{\hat{k}}] U_2'(X_2-) - U_2'''(X_2-)\}\ , \end{aligned}\right\}$$

(4.33)

where, $X_2 = -R$ implies $k = II$, $\hat{k} = I$ and $X_2 = R$ implies $k = I$, $\hat{k} = II$.

The general solution of (4.31) is

$$\begin{aligned} U_2 = {} & L_1(X_2)\cosh(\Omega_1^{(k)} X_2) + L_2(X_2)\sinh(\Omega_1^{(k)} X_2) + \\ & + M_1(X_2)\cosh(\Omega_2^{(k)} X_2) + M_2(X_2)\sinh(\Omega_2^{(k)} X_2), \quad k = I, II \end{aligned}$$

(4.34)

where four step functions $L_n(X_2)$, $M_n(X_2)$ for n=1 or n=2 have been

introduced

$$L_n(X_2)\begin{cases} L_n^{(1)}, \\ L_n^{(2)}, \\ L_n^{(3)}, \end{cases} \qquad M_n(X_2)\begin{cases} M_n^{(1)}, & X_2\in(-l_2, -R), \\ M_n^{(2)}, & X_2\in(-R, R), \\ M_n^{(3)}, & X_2\in(R, l_2), \end{cases}$$

$$(n=1,2). \tag{4.35}$$

In addition the values for $\Omega_1^{(k)}$ and $\Omega_2^{(k)}$, k = I or II, are given as follows

$$\left.\begin{matrix}\Omega_1^{(k)} \\ \Omega_2^{(k)}\end{matrix}\right\} = \{\Omega^2\ \{[1+\lambda^2+(1-\lambda)^2A_k] \pm [(1+\lambda^2+(1-\lambda)^2A_k)^2-4\lambda^2]^{1/2}\}/2\}^{1/2}, \tag{4.36}$$

and it is assumed that

$$\Omega_1^{(I)} \neq \Omega_2^{(I)}, \quad \Omega_1^{(II)} \neq \Omega_2^{(II)}, \quad \text{whenever } \lambda \neq 1. \tag{4.37}$$

The relation $(4.37)_1$ will hold if and only if

$$A_I \neq -1 \text{ and } A_I \neq -\frac{(\lambda+1)^2}{(\lambda-1)^2}, \tag{4.38}$$

and relation $(4.37)_2$ will hold if and only if

$$A_{II} \neq -1 \text{ and } A_{II} \neq -\frac{(\lambda+1)^2}{(\lambda-1)^2}. \tag{4.39}$$

In the event that either (4.38) or (4.39) (or perhaps both) are not true, then additional terms of the form $X_2\cosh(\Omega^{(k)}X_2)$ and $X_2\sinh(\Omega^{(k)}X_2)$ make up for the coalescence of terms that takes place in (4.34).

Note in general that

$$-\frac{(\lambda+1)^2}{(\lambda-1)^2} < -1\ , \tag{4.40}$$

since $\lambda > 0$. In particular one finds from (4.36) that the values for both $(\Omega_1^{(I)})^2$ and $(\Omega_2^{(I)})^2$ are distinct, real and negative if

$$A_I < -\frac{(\lambda+1)^2}{(\lambda-1)^2}\ , \tag{4.41}$$

and are distinct, real and positive if

$$A_I > -1. \tag{4.42}$$

However the pair $\Omega_1^{(I)}$ and $\Omega_2^{(I)}$ are complex conjugates if

$$-\frac{(\lambda+1)^2}{(\lambda-1)^2} < A_I < -1\ . \tag{4.43}$$

Corresponding results hold for $\Omega_1^{(II)}$ and $\Omega_2^{(II)}$ when A_I is replaced

by A_{II} in (4.41)-(4.43). Thus if

$$A_I > -1, \quad A_{II} > -1, \tag{4.44}$$

the hyperbolic exponential functions in (4.34) have their standard meaning, while if either member of (4.44) is not true, then standard trigonometric functions enter into (4.34). The form (4.34) has been chosen for convenience of study in the case in which (4.44) holds. As shown in section 3, the case in which (4.44) holds corresponds to materials with more or less "usual" engineering behavior. In addition it is to be noted that in APPENDIX A a fairly elaborate argument is given establishing that the following relations always hold:

$$\Omega_2^{(I)} < \Omega_2^{(II)} < \Omega_1^{(II)} < \Omega_1^{(I)}, \quad \text{if} \quad 0 < A_{II} < A_I, \quad \lambda > 0, \ \lambda \neq 1. \tag{4.45}$$

Substituting from (4.34) into boundary conditions (4.33) now gives rise to a 12×12 linear system for the 12 unknown constants denoted by the L's and M's. This system will be written as the form

$$J_{12\times12}\, L_{12\times1} = 0_{12\times1}\,, \tag{4.46}$$

where

$$L=(L_1^{(1)},L_2^{(1)},M_1^{(1)},M_2^{(1)},L_1^{(2)},L_2^{(2)},M_1^{(2)},M_2^{(2)},L_1^{(3)},L_2^{(3)},M_1^{(3)},M_2^{(3)})^T, \tag{4.47}$$

and J is a 12×12 matrix which will be described in (4.50) and (4.51)

in detail. Bifurcation takes place provided that a nontrivial solution exists for (4.46). This in turn requires that

$$\det J = 0. \tag{4.48}$$

Equation (4.48) can now be regarded as an equation for those λ's at which buckling can occur for a given value of the mode variable $\Omega = m\pi/(2l_1)$.

It is convinient to study (4.48) by introducing additional dimensionless parameters as follows

$$\eta = \Omega l_2 = m\pi l_2/l_1, \quad \beta = \mu^{(II)}/\mu^{(I)}, \quad \alpha = R/l_2. \tag{4.49}$$

Here η is the mode number of the buckled configuration scaled with respect to the aspect ratio l_2/l_1; β plays a role similar to that of a stiffness ratio of the two composite materials comprising the construction; and α is the volume fraction of the central ply within the complete construction.

It will be convenient to write J as follows

$$J = \begin{bmatrix} J_{11} & J_{12} & J_{13} \\ J_{21} & J_{22} & J_{23} \\ J_{31} & J_{32} & J_{33} \end{bmatrix}, \tag{4.50}$$

with J_{mn} (m,n=1,2,3) are 4x4 submatrices whose entries are functions of the parameters η, β, α, λ, A_I and A_{II}. These submatrices are found to be

$$J_{12} = J_{23} = J_{31} = 0_{4\times4} ,$$

$$J_{11} =$$

$$\begin{bmatrix} B_1^I\cosh(\Omega_1^{(I)}l_2), & -B_1^I\sinh(\Omega_1^{(I)}l_2), & B_2^I\cosh(\Omega_2^{(II)}l_2), & -B_2^I\sinh(\Omega_2^{(II)}l_2) \\ -E_1^I\sinh(\Omega_1^{(I)}l_2), & E_1^I\cosh(\Omega_1^{(I)}l_2), & -E_2^I\sinh(\Omega_2^{(I)}l_2), & E_2^I\cosh(\Omega_2^{(I)}l_2) \\ 0, & 0, & 0, & 0, \\ 0, & 0, & 0, & 0, \end{bmatrix}$$

$$J_{13} =$$

$$\begin{bmatrix} 0, & 0, & 0, & 0, \\ 0, & 0, & 0, & 0, \\ B_1^I\cosh(\Omega_1^{(I)}l_2), & B_1^I\sinh(\Omega_1^{(I)}l_2), & B_2^I\cosh(\Omega_2^{(I)}l_2), & B_2^I\sinh(\Omega_2^{(I)}l_2), \\ E_1^I\sinh(\Omega_1^{(I)}l_2), & E_1^I\cosh(\Omega_1^{(I)}l_2), & E_2^I\sinh(\Omega_2^{(I)}l_2), & E_2^I\cosh(\Omega_2^{(I)}l_2), \end{bmatrix}$$

$$J_{21} =$$

$$\begin{bmatrix} -\cosh(\Omega_1^{(I)}R), & \sinh(\Omega_1^{(I)}R), & -\cosh(\Omega_2^{(I)}R), & \sinh(\Omega_2^{(I)}R), \\ \Omega_1^{(I)}s(I\sinh(\Omega_1^{(I)}R), & -\Omega_1^{(I)}\cosh(\Omega_1^{(I)}R), & \Omega_2^{(I)}\sinh(\Omega_2^{(I)}R), & -\Omega_2\cosh(\Omega_2^{(I)}R), \\ -B_1^I\cosh(\Omega_1^{(I)}R), & B_1^I\sinh(\Omega_1^{(I)}R), & -B_2^I\cosh(\Omega_2^{(I)}R), & B_2^I\sinh(\Omega_2^{(I)}R), \\ E_1^I\sinh(\Omega_1^{(I)}R), & -E_1^I\cosh(\Omega_1^{(I)}R), & E_2^I\sinh(\Omega_2^{(I)}R), & -E_2^I\cosh(\Omega_2^{(I)}R), \end{bmatrix}$$

$$J_{22}=$$

$$\begin{bmatrix}
\cosh(\Omega_1^{(II)}R), & -\sinh(\Omega_1^{(II)}R), & \cosh(\Omega_2^{(II)}R), \\
-\Omega_1^{(II)}\sinh(\Omega_1^{(II)}R), & \Omega_1^{(II)}\cosh(\Omega_1^{(II)}R), & -\Omega_2^{(II)}\sinh(\Omega_2^{(II)}R), \\
\xi B_1^{II}\cosh(\Omega_1^{(II)}R), & -\xi B_1^{II}\sinh(\Omega_1^{(II)}R), & \xi B_2^{II}\cosh(\Omega_2^{(II)}R), \\
-\xi E_1^{II}\sinh(\Omega_1^{(II)}R), & \xi E_1^{II}\cosh(\Omega_1^{(II)}R), & -\xi E_2^{II}\sinh(\Omega_2^{(II)}R),
\end{bmatrix}$$

$$\begin{bmatrix}
-\sinh(\Omega_2^{(II)}R), \\
\Omega_2^{(II)}\cosh(\Omega_2^{(II)}R), \\
-\xi B_2^{II}\sinh(\Omega_2^{(II)}R), \\
\xi E_2^{II}\cosh(\Omega_2^{(II)}R),
\end{bmatrix}$$

$$J_{32}=$$

$$\begin{bmatrix}
-\cosh(\Omega_1^{(II)}R), & -\sinh(\Omega_1^{(II)}R), & -\cosh(\Omega_2^{(II)}R), \\
-\Omega_1^{(II)}\sinh(\Omega_1^{(II)}R), & -\Omega_1^{(II)}\cosh(\Omega_1^{(II)}R), & -\Omega_2^{(II)}\sinh(\Omega_2^{(II)}R), \\
-\xi B_1^{II}\cosh(\Omega_1^{(II)}R), & -\xi B_1^{II}\sinh(\Omega_1^{(II)}R), & -\xi B_2^{II}\cosh(\Omega_2^{(II)}R), \\
-\xi E_1^{II}\sinh(\Omega_1^{(II)}R), & -\xi E_1^{II}\cosh(\Omega_1^{(II)}R), & -\xi E_2^{II}\sinh(\Omega_2^{(II)}R),
\end{bmatrix}$$

$$\begin{bmatrix}
-\sinh(\Omega_2^{(II)}R), \\
-\Omega_2^{(II)}\cosh(\Omega_2^{(II)}R), \\
-\xi B_2^{II}\sinh(\Omega_2^{(II)}R), \\
-\xi E_2^{II}\cosh(\Omega_2^{(II)}R),
\end{bmatrix}$$

$$J_{33}=$$

$$\begin{bmatrix} \cosh(\Omega_1^{(I)}R), & \sinh(\Omega_1^{(I)}R), & \cosh(\Omega_2^{(I)}R), \\ \Omega_1^{(I)}\sinh(\Omega_1^{(I)}R), & \Omega_1^{(I)}\cosh(\Omega_1^{(I)}R), & \Omega_2^{(I)}\sinh(\Omega_2^{(I)}R), \\ B_1^{I}\cosh(\Omega_1^{(I)}R), & B_1^{I}\sinh(\Omega_1^{(I)}R), & B_2^{I}\cosh(\Omega_2^{(I)}R), \\ E_1^{I}\sinh(\Omega_1^{(I)}R), & E_1^{I}\cosh(\Omega_1^{(I)}R), & E_2^{I}\sinh(\Omega_2^{(I)}R), \end{bmatrix}$$

$$\begin{bmatrix} \sinh(\Omega_2^{(I)}R), \\ \Omega_2\cosh(\Omega_2^{(I)}R), \\ B_2^{I}\sinh(\Omega_2^{(I)}R), \\ E_2^{I}\cosh(\Omega_2^{(I)}R), \end{bmatrix}$$

where

$$B_j^{k} = \lambda\Omega + (\lambda\Omega)^{-1}\,\Omega_j^{(k)2}, \qquad j=1,2,\ k=I,II,$$

$$E_j^{k} = \{\,[2+\lambda^{-2}+(1-\lambda^{-1})^2 A_k]\Omega_j^{(k)} - (\lambda\Omega)^{-2}\Omega_j^{(k)3}\,\}, \qquad j=1,2,\ k=I,II,$$

$$\xi = D^{(I)}/D^{(II)} = \beta\,(\lambda^{-1/2}+\lambda^{1/2})^{(A_{II}-A_I)}\,(1+A_{II}/2)/(1+A_I/2). \tag{4.51}$$

It is to be noted that (4.48) constitutes a relation for the ordered variable set $(\lambda,\eta,\beta,\alpha,A_I,A_{II})$. Thus if one defines

$$\Psi(\lambda,\eta,\beta,\alpha,A_I,A_{II}) = \det J, \tag{4.52}$$

then (4.48) gives rise to

$$\Psi(\lambda,\eta,\beta,\alpha,A_I,A_{II}) = 0 \tag{4.53}$$

as a condition for bifurcations of the type (4.1) away from the homogeneous solution (2.19). In addition to the conditions (4.44) it may be concluded from (4.27) and (4.49) that λ, η, β, α are restricted to the following intervals

$$\lambda > 0; \quad \eta > 0; \quad \beta > 0; \quad 0 \le \alpha \le 1. \tag{4.54}$$

Although η must take on discrete values determined by the aspect ratio l_2/l_1, it can be treated as a continuous variable for the purpose of analysis. Equation (4.53) shall be called the **general buckling equation.**

Note that this problem ought to reduce to the non-composite case for the following two special cases:

(i) β=1 and A_I=A_{II},
since then material I is identical to material II,

(ii) either α=0 or α=1,
since then only one phase is present.

(4.55)

5. GENERALIZATION OF THE MATERIAL CONSTANT A

The purpose of this section is to provide additional detail of the logic which led to the choice of (2.9) as the class of strain energy densities to consider. The reader will lose no continuity to the rest of this dissertation if one proceeds directly to section 6.

As already mentioned, Sawyers and Rivlin [10] have already examined, in great deal, the problem corresponding to that under study here, for the case in which the body is composed of a single material (the non-composite case). In fact Sawyers and Rivlin [10] accomplish the reduction to the problem of a single ordinary differential equation (corresponding to (4.31) here) for the case of an arbitrary strain energy density $W(I_1,I_2)$. As might be expected, the associated linearization, although not difficult in principle, requires very careful Taylor expansions of the associated stress and deformation measures, and hence an extraordinary attention to detail. Sawyers and Rivlin [10] then show that the results so obtained depend heavily on the expression.

$$A(\lambda_1,\lambda_2,\lambda_3) = \frac{2(\lambda_1 + \lambda_2)^2}{W_1 + \lambda_3^2 W_2}\,(W_{11} + 2\lambda_3^2 W_{12} + \lambda_3^4 W_{22}). \qquad (5.1)$$

Here λ_1, λ_2, λ_3 are principal stretches associated with the homogeneous solution (2.19) so that $\lambda_1 = \rho$, $\lambda_2 = \rho^{-1}$ and $\lambda_3 = 1$. In (5.1) the derivatives of $W(I_1,I_2)$ are with respect to the principal invariants

$$W_i(I_1,I_2) = \frac{\partial W}{\partial I_i}, \quad W_{ij} = \frac{\partial^2 W}{\partial I_i \partial I_j}. \quad i,j = 1,2. \tag{5.2}$$

Thus, in view of (2.20), all of the derivatives appearing in the right hand side of (5.1) can be regarded as a function of ρ. Furthermore, since $\lambda = \lambda_2/\lambda_1 = \rho^{-2}$, (5.1) gives

$$A(\lambda_1,\lambda_2,\lambda_3) = A(\rho,\rho^{-1},1) = \tilde{A}(\rho) = \tilde{A}(\lambda^{-1/2}) = \bar{A}(\lambda). \tag{5.3}$$

Sawyers and Rivlin [10] show that a great deal of simplification to the ensueing analysis results for the case in which $\bar{A}(\lambda)$ is constant, and, in fact they, for the most part restrict their treatment to this particular circumstance. The reason for this simplification will be discussed at the end of this section. Now, as noted in [10], it is easily verified that $\bar{A}(\lambda)$ is constant for the case of a neo-Hookean material. The answer to the following question, however, is not immediately clear:

What strain energies $W(I_1,I_2)$ give rise to a function $\bar{A}(\lambda)$ that is constant?

(Q_1)

In view of the anticipated complications that the study of composite construction would introduce, it was decided to investigate (Q_1) with a view towards using such strain energies for the individual materials in the problem under consideration here. In fact, there is apparently no increase in difficulty in investigating the following

obvious generalization of (Q_1):

For a given function $A(\lambda_1,\lambda_2,\lambda_3)$, and hence a given $\tilde{A}(\lambda)$, what strain energies $W(I_1,I_2)$ ensure that (5.1) is obtained?

(Q_2)

An examination of (5.1) indicates that for a given $\tilde{A}(\lambda)$, the equation (5.1) can be viewed as a single linear partial differential equation for $W(I_1,I_2)$. Since there are no associated boundary conditions, one would suspect that it might be a relatively simple matter to "solve" (5.1) for $W(I_1,I_2)$ and, moreover, that numerous solutions $W(I_1,I_2)$ ought to exist. Indeed, this is apparently the case.

For simplicity, attention will be restricted to the class of materials that are independent of the second strain invariant I_2:

$$W = W(I_1) \tag{5.4}$$

so that (5.1) and (5.3) gives

$$\tilde{A}(\rho) = 2(\rho+\rho^{-1})^2 W_{11}(1+\rho^2+\rho^{-2})/W_1(1+\rho^2+\rho^{-2}), \tag{5.5}$$

and

$$\tilde{A}(\lambda) = \tilde{A}(\lambda^{-1/2}). \tag{5.6}$$

It is to be noted that both the power law material (3.21) and (it's specialization) the material (3.1) utilized in the present study, are special cases of (5.4). In fact for the power law material (3.21), one obtains from (5.5) and (5.6) that

$$\tilde{A}(\lambda) = \frac{2(n-1)(\lambda+1)^2}{\lambda^2 + [(n/b)-2]\lambda + 1} \tag{5.7}$$

while for the material (3.1) one similarly obtains

$$\tilde{A}(\lambda) = A \tag{5.8}$$

Thus the class of materials (3.1) meets the objective of ensuring that $\tilde{A}(\lambda)$ is constant. Moreover, in view of (5.7), the material (3.21) does not meet this objetive unless the denominater in (5.7) is equal to $(\lambda+1)^2$, which in turn will be true if and only if

$$(n/b) - 2 = 2 \quad \text{or} \quad n = 4b. \tag{5.9}$$

Thus the number of free constants reduces from three to two for the material (3.21) under the requirement that $\tilde{A}(\lambda)$ is constant. In fact, in view of (3.23), the material (3.1) is the most general case of a material (3.21) that in addition gives a constant value for $\tilde{A}(\lambda)$.

With this background, the question (Q_2) will now be investigated in general for the class of materials (5.4). Let

$$W_1(1+\rho^2+\rho^{-2}) = F(\rho). \tag{5.10}$$

Then

$$W_{11}(1+\rho^2+\rho^{-2}) = \frac{dF(\rho)}{d\rho} \Big/ \frac{dI_1}{d\rho}, \tag{5.11}$$

where

$$dI_1/d\rho = 2\rho - 2\rho^{-3}. \tag{5.12}$$

Thus (5.5) is equivalent to

$$\frac{dF}{d\rho} - \frac{(\rho-\rho^{-3})\tilde{A}(\rho)}{2(\rho+\rho^{-1})^2} F = 0 \quad , \tag{5.13}$$

which in turn will be true if and only if

$$\ln F(\rho) = \int^{\rho} \frac{\tilde{A}(s)\ (s^2-1)}{s\ (s^2+1)}\, ds \quad . \tag{5.14}$$

The equation (5.14) provides an explicit formula for the determination of $F(\rho)$ and hence $W(I_1)$. Returning to the case of $\tilde{A}(\rho) = A$, a constant, one obtains from (5.14) that

$$\ln F(\rho) = \int^{\rho} \frac{\tilde{A}(s)\ (s^2-1)}{s\ (s^2+1)}\, ds = -\frac{A}{2} \ln(2+\rho^2+\rho^{-2}) + \ln(c_1), \tag{5.15}$$

where c_1 is an arbitrary constant. This in turn gives

$$F(\rho) = c_1(2+\rho^2+\rho^{-2})^{A/2}, \tag{5.16}$$

which in view of (5.10) gives

$$\frac{dW(I_1)}{dI_1} = c_1(1+I_1)^{A/2}. \tag{5.17}$$

Simple integration now yields

$$W(I_1) = (2c_1/A)\{(1+I_1)^{1+A/2} + c_2\}, \tag{5.18}$$

where c_1 and c_2 are as yet undetermined constants. Thus (5.18) is the most general form of a strain energy density (5.4) that in addition gives a constant value of $\bar{A}(\lambda)$. As is standard, the inessential additive constant in the strain energy density (5.18) is chosen so that $W = 0$ in the undeformed state ($I_1=3$). This gives

$$c_2 = -4(2)^A. \tag{5.19}$$

Finally, by choosing

$$c_1 = \mu A/4, \tag{5.20}$$

one obtains (3.1). Thus it may be concluded that (3.1) is the most general class of strain energy densities that obey (5.4) and in addition give rise to a constant value for $\bar{A}(\lambda)$.

As the above procedure indicates, the particular requirement that $\bar{A}(\lambda)$ must be a constant did *not* provide an essential simplification to obtaining a strain energy density obeying (5.4).

Thus the above procedure could be utilized to determine classes of materials obeying (5.4), and hence (5.1), that give rise to any given function $\tilde{A}(\lambda)$.

If $\tilde{A}(\lambda)$ is *not* constant, the work of Sawyers and Rivlin [10] for the non-composite case would seem to indicate that an equation analogous to (4.53) would continue to govern buckling provided that A_I and A_{II} were replaced by the associated functions $\tilde{A}_I(\lambda)$ and $\tilde{A}_{II}(\lambda)$. Since complicated expressions are then compounded inside the hyperbolic functions that comprise the entries of J in (4.50), a treatment of (4.53) would seemingly present a great deal of complication. This is the essential reason why attention in this dissertation has focussed on the class of materials (2.24).

6. TWO SPECIAL DEFORMATION TYPES FOR THE NEO-HOOKEAN COMPOSITE PLATE: FLEXURE AND BARRELLING

The analysis of the problem at hand is quite complicated even if the material constant A is non-zero. Thus for the rest of this dissertation, attention shall be restricted to the case in which both materials are neo-Hookean:

$$A_k = 0, \qquad k=(I,II). \tag{6.1}$$

This gives the following simplifications

$$W^{(k)}(I_1) = \mu^{(k)} (I_1 - 3)/2 , \qquad k=I,II \tag{6.2}$$

$$C_j^{(k)} = 1, \quad D^{(k)} = (\mu^{(k)})^{-1}, \qquad j=1,2; \quad k=I,II \tag{6.3}$$

$$\left.\begin{matrix}\Omega_1 \\ \Omega_2\end{matrix}\right\} = \begin{cases}\lambda\Omega , \\ \Omega , \end{cases} \tag{6.4}$$

$$\left.\begin{matrix}B_1^k \\ B_2^k\end{matrix}\right\} = \begin{cases}2\lambda\Omega , \\ (\lambda+\lambda^{-1})\ \Omega , \end{cases} \qquad k=I,II \tag{6.5}$$

$$\left.\begin{matrix}E_1^k \\ E_2^k\end{matrix}\right\} = \begin{cases}(2+\lambda^{-2})\ \lambda\Omega , \\ 2\Omega , \end{cases} \qquad k=I,II \tag{6.6}$$

$$\xi = \beta , \tag{6.7}$$

$$J_{12} = J_{23} = J_{31} = 0_{4\times 4} ,$$

$$J_{11} = \begin{bmatrix} 2\lambda c_2 & -2\lambda s_2 & \Lambda c_1 & -\Lambda s_1 \\ -\Lambda s_2 & \Lambda c_2 & -2s_1 & 2c_1 \\ 0 & 0 & 0 & 0 \\ 0 & 0 & 0 & 0 \end{bmatrix} ,$$

$$J_{13} = \begin{bmatrix} 0 & 0 & 0 & 0 \\ 0 & 0 & 0 & 0 \\ 2\lambda c_2 & 2\lambda s_2 & \Lambda c_1 & \Lambda s_1 \\ \Lambda s_2 & \Lambda c_2 & 2s_1 & 2c_1 \end{bmatrix} ,$$

$$J_{21} = \begin{bmatrix} -c_4 & s_4 & -c_3 & s_3 \\ \lambda s_4 & -\lambda c_4 & s_3 & -c_3 \\ -2\lambda c_4 & 2\lambda s_4 & -\Lambda c_3 & \Lambda s_3 \\ \Lambda s_4 & -\Lambda c_4 & 2s_3 & -2c_3 \end{bmatrix} ,$$

$$J_{22} = \begin{bmatrix} c_4 & -s_4 & c_3 & -s_3 \\ -\lambda s_4 & \lambda c_3 & -s_3 & c_3 \\ 2\beta\lambda c_4 & -2\beta\lambda s_4 & \beta\Lambda c_3 & -\beta\Lambda s_3 \\ -\beta\Lambda s_4 & \beta\Lambda c_4 & -2\beta s_3 & 2\beta c_3 \end{bmatrix} ,$$

$$J_{32} = \begin{bmatrix} -c_4 & -s_4 & -c_3 & -s_3 \\ -\lambda s_4 & -\lambda c_3 & -s_3 & -c_3 \\ -2\beta\lambda c_4 & -2\beta\lambda s_4 & -\beta\Lambda c_3 & -\beta\Lambda s_3 \\ -\beta\Lambda s_4 & -\beta\Lambda c_4 & -2\beta s_3 & -2\beta c_3 \end{bmatrix} ,$$

$$J_{33} = \begin{bmatrix} c_4 & s_4 & c_3 & s_3 \\ \lambda s_4 & \lambda c_4 & s_3 & c_3 \\ 2\lambda c_4 & 2\lambda s_4 & \Lambda c_3 & \Lambda s_3 \\ \Lambda s_4 & \Lambda c_4 & 2s_3 & 2c_3 \end{bmatrix}, \tag{6.8}$$

where

$$c_1=\cosh(\eta),\ c_2=\cosh(\lambda\eta),\ c_3=\cosh(\eta\alpha),\ c_4=\cosh(\lambda\eta\alpha),$$

$$s_1=\sinh(\eta),\ s_2=\sinh(\lambda\eta),\ s_3=\sinh(\eta\alpha),\ s_4=\sinh(\lambda\eta\alpha),$$

$$\Lambda=(\lambda+1/\lambda). \tag{6.9}$$

Furthermore, the load-deformation relation (2.34) becomes

$$T = 4l_3\ (\rho-\rho^{-3})\ [R\mu^{(II)} + (l_2-R)\mu^{(I)}]. \tag{6.10}$$

For the non-composite case, it is shown in [10], [11] that two deformation types are possible. The first of which is a flexural deformation and the second of which is a barrelling deformation. Moreover it is also shown that these two types exhaust all possible solutions. For the composite case, both of these deformation types remain possible. However, analytical difficulties have so far prevented this investigation from showing that these two types exhaust all of the possible solutions.

Nevertheless, in what follows, attention is limited to these two deformation types.

A Flexural deformation is one in which the corresponding

solution U_2 is an even function of X_2 so that U_1 is an odd function of X_2 by virtue of (4.28). Considering (4.34) and (4.35), this requires that

$$(L_1^{(1)}, L_2^{(1)}, M_1^{(1)}, M_2^{(1)}) = (L_1^{(3)}, -L_2^{(3)}, M_1^{(3)}, -M_2^{(3)}),$$

$$L_2^{(2)} = M_2^{(2)} = 0, \tag{6.11}$$

so that system (4.46) reduces from the 12 × 12 system to the following 6 × 6 system:

$$\begin{bmatrix} 2\lambda c_2 & -2\lambda s_2 & \Lambda c_1 & -\Lambda s_1 & 0 & 0 \\ -\Lambda s_2 & \Lambda c_2 & -2s_1 & 2c_1 & 0 & 0 \\ -c_4 & s_4 & -c_3 & s_3 & c_4 & c_3 \\ \lambda s_4 & -\lambda c_4 & s_3 & -c_3 & -\lambda s_4 & -s_3 \\ -2\lambda c_4 & 2\lambda s_4 & -\Lambda c_3 & \Lambda s_3 & 2\lambda\beta c_4 & \Lambda\beta c_3 \\ \Lambda s_4 & -\Lambda c_4 & 2s_3 & -2c_3 & -\Lambda\beta s_4 & -2\beta s_3 \end{bmatrix} \begin{bmatrix} L_1^{(1)} \\ L_2^{(1)} \\ M_1^{(1)} \\ M_2^{(1)} \\ L_1^{(2)} \\ M_1^{(2)} \end{bmatrix} = 0_{6\times 1} . \tag{6.12}$$

In place of equation (4.53) one then obtains a simpler **flexural buckling equation** found by setting the determinant of the matrix in (6.12) equal to zero. Denote this relation as:

$$\Psi_F(\lambda, \eta, \beta, \alpha) = 0 . \tag{6.13}$$

A **barrelling deformation** is one in which the corresponding

solution U_2 is an odd function of X_2 and U_1 is an even function of X_2. This requires that

$$(L_1^{(1)}, L_2^{(1)}, M_1^{(1)}, M_2^{(1)}) = (-L_1^{(3)}, L_2^{(3)}, -M_1^{(3)}, M_2^{(3)}),$$

$$L_1^{(2)} = M_1^{(2)} = 0, \tag{6.14}$$

which in turn gives that system (4.46) also reduces from a 12 × 12 system to a 6 × 6 system,

$$\begin{bmatrix} 2\lambda c_2 & -2\lambda s_2 & \Lambda c_1 & -\Lambda s_1 & 0 & 0 \\ -\Lambda s_2 & \Lambda c_2 & -2s_1 & 2c_1 & 0 & 0 \\ -c_4 & s_4 & -c_3 & s_3 & -s_4 & -s_3 \\ \lambda s_4 & -\lambda c_4 & s_3 & -c_3 & \lambda c_4 & c_3 \\ -2\lambda c_4 & 2\lambda s_4 & -\Lambda c_3 & \Lambda s_3 & -2\lambda\beta s_4 & -\Lambda\beta s_3 \\ \Lambda s_4 & -\Lambda c_4 & 2s_3 & -2c_3 & \Lambda\beta c_4 & 2\beta c_3 \end{bmatrix} \begin{bmatrix} L_1^{(1)} \\ L_2^{(1)} \\ M_1^{(1)} \\ M_2^{(1)} \\ L_2^{(2)} \\ M_2^{(2)} \end{bmatrix} = 0_{6\times 1} . \tag{6.15}$$

In this case the associated barrelling buckling equation, found by setting the determinant of the matrix in (6.15) equal to zero, will be written as:

$$\Psi_B(\lambda, \eta, \beta, \alpha) = 0 . \tag{6.16}$$

Both Ψ_F and Ψ_B are smooth functions of λ, η, β and α. For a given composite construction, both β and α are fixed. Then flexural and barrelling bifurcations are governed by the η-λ relation that follow from (6.13) and (6.16) respectively.

Consider the flexural case, for a given triple (η,β,α), one seeks roots λ to (6.13). It is easily seen that

$$\Psi_F(1,\eta,\beta,\alpha) = 0,$$

since the final two columns in the coefficent matrix of (6.12) are then identical. Thus $\lambda = 1$ is always a solution to (6.13). However since this corresponds to no end displacement and hence no thrust, it is not of interest and so will not be considered further.

The complicated nature of (6.13) gives rise to formidable analytical difficulties. Consequently a numerical investigation of this equation has been pursued. Such an investigation indicates for fixed η, β, α that Ψ_F monotonically increases from $\Psi_F = -\infty$ at $\lambda = 0$ through $\Psi_F = 0$ at $\lambda = 1$ to some maximum value. Then Ψ_F subsequently is found to monotonically decreases as $\lambda \to \infty$, again passing through $\Psi_F = 0$. Thus in addition to the root $\lambda = 1$, a second root $\lambda > 1$ exists for equation (6.13). Moreover since $\lambda > 1$, these solutions only exist for compressive loads. That is, bifurcation instability only occurs upon thrust. Henceforth denote this nontrivial root by

$$\lambda = \Phi_F(\eta,\beta,\alpha) \quad . \tag{6.17}$$

The barrelling case is similar, namely for all triples (η,β,α), $\lambda = 1$ is always a root of (6.16). In addition one finds that there always exists exactly one other root $\lambda > 1$ to the barrelling equation (6.16).

Likewise denote this nontrivial root by

$$\lambda = \Phi_B(\eta,\beta,\alpha) \quad . \tag{6.18}$$

Numerical routines were developed, based on simple bisection, to determine the functions $\Phi_F(\eta,\beta,\alpha)$ and $\Phi_B(\eta,\beta,\alpha)$. The corresponding computer programs FLEXURE1 and BARRELLING1 can be found in (I) and (VI) respectively of APPENDIX C. Specifically (I) calculates $\Phi_F(\eta,\beta,\alpha)$ and (VI) calculates $\Phi_B(\eta,\beta,\alpha)$.

Although it would be interesting to develop a completely analytical, as opposed to numerical, treatment of the bifurcation equations, the size of the matrices involved makes this a very difficult prospect. That is the general buckling equation (4.53) stems from a 12 × 12 matrix. In general the size of the matrix for an arbitrary number of plies N will be 4N × 4N, where, in the problem at hand N = 3. Sawyers and Rivlin [10] for the non-composite case N = 1, are succesful in developing their analysis to a point much further than that attained here, before turning to a numerical procedure. In APPENDIX B, it is shown that the results attained here for the composite case can, by purely analytical means, be made to yield the results obtained in [10], for the special case in which the construction is in fact not a true composite (i.e. if (4.55) holds).

7. BUCKLING AND WRINKLING FAILURE MODES FOR THE COMPOSITE CONSTRUCTION

The purpose of this section is to determine the critical instability, and more generally the ordering of the stability modes, for the problem under consideration. As mentioned in the previous section, Sawyers and Rivlin [10], [11] have shown for the non-composite case that buckling can occur involving either flexural or barrelled mode shapes with an arbitrary integer number m of half-wavelengths. A diagram of these failure modes, as they would occur in the composite consturction under consideration here, is presented in Figure 7-1, where T_m^F and T_m^B (m = 1,2,3...) denote the corresponding failure thrusts. A central issue is to determine the ordering of these failure thrusts. For the non-composite plate, Sawyers and Rivlin [10] have obtained the following result

$$0<T_1^F<T_2^F<\ldots<T_m^F<T_{m+1}^F<\ldots\rightarrow T_\infty \leftarrow \ldots<T_{m+1}^B<T_m^B<\ldots<T_2^B<T_1^B \quad . \tag{7.1}$$

Here T_∞ is the value associated with an infinite number of wave lengths and can be identified with a wrinkling instability. For the composite case some striking differences are obtained, most notable is a possible change in ordering of the failure thrusts. These results will be demonstrated in this section and some of their practical consequences will be discussed.

The failure stretch ratios are now defined as follows:

$$\left.\begin{aligned} \lambda_m^F &= \Phi_F(m\pi l_2/2l_1,\beta,\alpha) \\ \lambda_m^B &= \Phi_B(m\pi l_2/2l_1,\beta,\alpha) \end{aligned}\right\}, \quad m = 1,2,3... \tag{7.2}$$

once these failure stretch ratios are found, the corresponding failure thrusts are found from (6.10). In particular it is to be noted that the failure thrusts are ordered the same as the failure stretch ratios.

To find the ordering of the flexure failure stretch ratios for fixed values of β and α, one plots the points $(m\pi l_2/2l_1, \lambda_m^F)$ using (7.2). Programs FLEXURE2 and BARRELLING2, found in (II) and (VII) of APPENDIX C, can be used for this purpose. The lowest value of λ_m^F determines the critical mode number m for flexure as well as the critical flexure failure stretch ratio and hence the critical flexure failure thrust. The critical mode number m for barrelling as well as the critical barrelling failure stretch ratio and the critical barrelling failure thrust are found similarly.

For all of the non-composite cases (4.55), the numerical method embodied in those programs consistently gives the (η,λ)-relation as found by Sawyers and Rivlin (10) and displayed in Figure 7-2. Notice in this case that Φ_F as a function of η is monotonically increasing from $\lambda = 1$ at $\eta = 0$ to $\lambda = 3.3833...$ as $\eta \to \infty$. Hence according to $(7.2)_1$ the flexural failure thrusts are ordered as follows:

$$T_1^F < T_2^F < \ldots < T_m^F < T_{m+1}^F < \ldots \to T_\infty^F , \tag{7.3}$$

where T_∞^F is found from (6.10) using the asymptotic value $\lambda = 3.383...$

Similarly for the non-composite case, Φ_B as a function of η is monotonically decreasing from $\lambda = \infty$ at $\eta = 0$ to $\lambda = 3.383...$ as $\eta \to \infty$. Hence according to $(7.2)_2$:

$$T_1^B > T_2^B > \ldots > T_m^B > T_{m+1}^B > \ldots \to T_\infty^B \ . \tag{7.4}$$

Finally since both Φ_F and Φ_B have the same asymptote as $\eta \to \infty$, it follows that

$$T_\infty^F = T_\infty^B = T_\infty \ . \tag{7.5}$$

Physically T_∞ gives rise to an instability which corresponds to a wrinkling failure. Combining (7.3)-(7.5) gives (7.1).

It is found that the orderings (7.3), (7.4) and (7.1) given by Sawyers and Rivlin (1974,1982), and confirmed by the programs FLEXURE2 and BARRELLING2 for non-composite constructions, will, for certain composite constructions, cease to hold. The ordering of the failure thrusts is determined by two factors: (i) the qualitative behavior of the functions $\Phi_F(\eta,\beta,\alpha)$ and $\Phi_B(\eta,\beta,\alpha)$ for fixed (β,α) as the mode parameter η is allowed to vary, and (ii) the spacing of the sequence of η values.

The qualitative behavior of the η-dependence can be characterized with respect to the parameter pair (β,α). The spacing of η-values is then determined by the aspect ratio l_2/l_1. Thus the three parameters: ply stiffness ratio β, central ply volume fraction α, and aspect ratio l_2/l_1, completely determine the ordering of the failure thrusts for the problem at hand. Within this framework the present section is organized as follows. Begining with the function $\Phi_F(\eta,\beta,\alpha)$ the possibilities for the qualitative behavior of the η dependence is

documented. Then for each distinct qualitative behavior so obtained the consequence of different possible η-spacings is examined. A similar program is followed for the function $\Phi_B(\eta,\beta,\alpha)$. In this fashion the possible new ordering for the failure thrusts are uncovered and these new orderings are correlated with the associated composite constructions by means of the parameter pairs (β,α) and the aspect ratio l_2/l_1.

First of all, however, it will be expedient to demonstrate those qualitative behaviors that hold regardless of the pair (β,α). For all values of (β,α) one finds that $\Phi_F(\eta,\beta,\alpha)$ is initially monotonically increasing from the value 1 at $\eta = 0$ and tends to an asymptotic value as $\eta \to \infty$. Similarly for all values of (β,α) one finds that $\Phi_B(\eta,\beta,\alpha)$ is initially monotonically decreasing from ∞ at $\eta = 0$ and tends to the same asymptotic value as $\eta \to \infty$. This common asymptotic value shall be denoted as:

$$\lambda_\infty(\beta,\alpha) = \lim_{\eta\to\infty} \Phi_F(\eta,\beta,\alpha) = \lim_{\eta\to\infty} \Phi_B(\eta,\beta,\alpha) \ . \tag{7.6}$$

Moreover it is found that

$$\Phi_F(\eta,\beta,\alpha) < \Phi_B(\eta,\beta,\alpha) \tag{7.7}$$

for all finite $\eta > 0$. Thus (7.5) holds for all composite configurations where now $T_\infty = T_\infty(\beta,\alpha)$. In addition (7.7) yieids

$$T_m^F < T_m^B \ , \quad m = 1,2,3... \tag{7.8}$$

In particular (7.8) indicates that the critical flexure failure thrust is always less than the critical barrelling failure thrust. Thus the critical flexure failure thrust gives the first bifurcation for all

pair (β,α) and all aspect ratio l_2/l_1 within the class of bifurcations under consideration.

At this point the investigation shall consider those qualitative behaviors for the η-dependence of the functions $\Phi_F(\eta,\beta,\alpha)$ and $\Phi_B(\eta,\beta,\alpha)$ which result in new orderings of the failure thrusts. The ordering (7.3) of flexure failure thrusts will continue to hold if $\Phi_F(\eta,\beta,\alpha)$ is monotonically increasing for all $\eta \geq 0$. Pairs (β,α) which give rise to $\Phi_F(\eta,\beta,\alpha)$ having this property will be said to belong to the set Γ_i^F. For example, one finds that $(\beta,\alpha) = (0.5,0.5) \in \Gamma_i^F$ (Figure 7-3). Note in this case that $\lambda_\infty = 3.271...$

However one finds for certain pairs (β,α) that $\Phi_F(*,\beta,\alpha)$ is no longer monotonically increasing over the whole domain $\eta \geq 0$. In particular it is sometimes found that $\Phi_F(\eta,\beta,\alpha)$ is monotonically increasing over a finite domain $0 \leq \eta < \eta_{max} = \eta_{max}(\beta,\alpha)$ but is subsequently monotonically decreasing to $\lambda_\infty(\beta,\alpha)$ for $\eta > \eta_{max}(\beta,\alpha)$. Pairs (β,α) which give rise to this behavior will be said to belong to the set Γ_{ii}^F. For example one finds that $(2,0.5) \in \Gamma_{ii}^F$, in which case $\eta_{max} = 1.977...$ and $\lambda_\infty = 3.439...$ (Figure 7-4).

Composite configurations for which $(\beta,\alpha) \in \Gamma_{ii}^F$ give rise to flexure failure thrusts that no longer obey (7.3). To determine the ordering in such a case one should note for $(\beta,\alpha) \in \Gamma_{ii}^F$ that the equation

$$\Phi_F(\eta,\beta,\alpha) = \lambda_\infty(\beta,\alpha) \ , \tag{7.9}$$

will have a unique finite root, which shall be denoted by $\eta_T(\beta,\alpha)$, and that this root will obey

$$\eta_T(\beta,\alpha) < \eta_{max}(\beta,\alpha) \ . \tag{7.10}$$

The program PROJ1 in (XI) of APPENDIX C can be used to find this root. For example, refering to Figure 7-4, note that $\eta_T(2,0.5) = 1.392... < 1.977... = \eta_{max}(2,0.5)$. Recalling that the discrete values of the sequence of η-values is determined by l_2/l_1, it follows that, for a given aspect ratio l_2/l_1, one can then determine integers p, q such that

$$p\pi l_2/2l_1 < \eta_T \leq (p + 1)\ \pi l_2/2l_1 ,$$

$$q\pi l_2/2l_1 \leq \eta_{max} < (q + 1)\ \pi l_2/2l_1 . \qquad (7.11)$$

It is clear that $0 \leq p \leq q$.

If $p > 0$ it follows that $\pi l_2/2l_1 < \eta_T$ so that T_1^F is the critical flexure failure thrust. In this event one may define the flexure failure thrust sequences

$$\mathfrak{S}_1 = \{ T_1^F, \ldots, T_p^F \} ,$$

$$\mathfrak{S}_2 = \{ T_{p+1}^F, \ldots, T_q^F \} ,$$

$$\mathfrak{S}_3 = \{ T_{q+1}^F, \ldots \rightarrow T_\infty^F \} , \qquad \text{(provided } p<q\text{)}. \qquad (7.12)$$

The ordering of the flexure failure thrusts will now consist of $\mathfrak{S}_1$ followed by an interspersing of $\mathfrak{S}_2$ with a reverse ordering of the sequence $\mathfrak{S}_3$.

On the other hand if $p = 0$, then $\pi l_2/2l_1 \geq \eta_T$. Assume for the moment that the inequality is strict. It then follows that T_∞^F is the critical flexure failure thrust. In this event the sequence $\mathfrak{S}_1$ is empty and the ordering of the flexure failure thrusts will consist of an interspersing of $\mathfrak{S}_2$ with the reverse ordering of the sequence $\mathfrak{S}_3$. It is to be emphasized in this interspersing that T_∞^F will in this

case lead the sequence of flexure failure thrusts.

In both cases $p = 0$ and $p > 0$ the thrust T_∞ is not an upper bound for the set of values T_m^F. Recall now that both the flexure failure thrusts and the barrelling failure thrusts cluster around T_∞. Hence it may be concluded that some of the barrelling failure thrusts will be interlaced with some of the flexure failure thrusts.

Thus if $(\beta,\alpha) \in \Gamma_{ii}^F$, the flexure failure thrusts are interlaced with the barrelling failure thrusts regardless of aspect ratio l_2/l_1. The critical flexure failure thrust will, depending on the aspect ratio l_2/l_1, be either the $m = 1$ flexure failure or the $m = \infty$ wrinkling failure. The transition between the $m = 1$ flexure failure and the $m = \infty$ wrinkling failure occurs at the transition aspect ratio $l_2/l_1 = 2\eta_T/\pi$. At this transition aspect ratio $T_1^F = T_\infty^F$. Hence for a Γ_{ii}^F-plate which is sufficiently short in the direction of thrust (specifically $l_1 < l_2\pi/(2\eta_T)$), wrinkling is the critical flexure instability. However, for a Γ_{ii}^F-plate which is sufficiently long in the direction of thrust (specifically $l_1 > l_2\pi/(2\eta_T)$), the critical flexure instability is the $m = 1$ mode.

It is to be noted for $(\beta,\alpha) \in \Gamma_{ii}^F$, that there exist infinitely many aspect ratios at which a flexure failure thrust from $\mathfrak{S}_2$ will coincide with a flexure failure thrust from $\mathfrak{S}_3$. To see this choose λ in the interval $\lambda_\infty < \lambda < \Phi_F(\eta_{max},\beta,\alpha)$. There will exist two intersections of the horizontal line corresponding to this value of λ with the graph of $\Phi_F(\eta,\beta,\alpha)$. One intersection will occur in $\eta_T < \eta < \eta_{max}$ and the other will occur in $\eta > \eta_{max}$. Denote these intersection values of η by η_1 and η_2 respectively. The ratio η_2/η_1 can be made to take on any value greater than 1 by appropriately

choosing λ in this procedure. If this ratio is a rational number it then follows that $\eta_2/\eta_1 = r/s$ for infinitely many integer pairs r and s. Choose one such integer pair, for example the case where r and s are coprime. Then the aspect ratio $l_2/l_1 = 2\eta_1/(s\pi) = 2\eta_2/(r\pi)$ will yield $T_s^F = T_r^F$. Moreover this construction will hold for each rational number greater than 1. Note that there is no possibility that a single flexure failure thrust could correspond to three or more flexure failure modes m whenever $(\beta,\alpha) \in \Gamma_{ii}^F$.

The regions Γ_i^F and Γ_{ii}^F in the semi-infinite strip

$$\Pi = \{ (\beta,\alpha) \mid \beta \geq 0,\ 0 \leq \alpha \leq 1 \} , \tag{7.13}$$

of possible (β,α) parameter pairs have been determined by means of an exhaustive numerical sampling procedure and are displayed in Figure 7-5. This sampling was carried out as follows. First, for a given parameter pair (β,α), the corresponding region type was determined by examining the monotonicity of the λ-η flexure relation. This examination can be accomplished by means of the program FLEXURE3 in (III) of APPENDIX C. This program has then in turn been incorporated into the two separate programs FLEXURE4 and FLEXURE5 (in (IV) and (V) of APPENDIX C) which sample points (β,α) on specified horizontal line segments and vertical line segments of Π respectively. In this fashion, the boundaries between the various regions of Π were determined.

Points to the right (left) of the vertical line segment $\beta = 1$ correspond to cases in which the central ply is composed of a material which is more (less) stiff than the material comprising the outer plies. Points above (below) the horizontal line $\alpha = 1/2$ correspond to

cases in which the central ply comprises more (less) than half the construction. A conspicuous feature of Figure 7-5 is the presence of a region Γ_{iii}^{F} corresponding to pairs (β,α) which belong to neither Γ_{i}^{F} nor Γ_{ii}^{F}. The meaning of this region will be discussed below. In Figure 7-4 the points $(\beta,0) \in \Gamma_{i}^{F}$, $(\beta,1) \in \Gamma_{i}^{F}$ and $(1,\alpha) \in \Gamma_{i}^{F}$ by virtue of (4.55). However it is found that pairs (β,α) very close to these values may in fact not belong to Γ_{i}^{F}. For example one finds that $(0.5,0.99) \in \Gamma_{ii}^{F}$ and $(1.1,0.5) \in \Gamma_{ii}^{F}$. The "threading" of the segment $\beta = 1$ through the "pass" created by the regions Γ_{ii}^{F} and Γ_{iii}^{F} near $(\beta,\alpha) = (1.0,0.9)$ is displayed in Figure 7-6.

The presence of Γ_{ii}^{F} so near the boundary $\alpha = 1$ for $0 < \beta < 1$ indicates that if the aspect ratio l_2/l_1 is sufficiently large then the addition of relatively thin and stiff outer layers can suppress the low wavelength flexure modes enough to lead to the dominance of the $m = \infty$ wrinkling instability. Since each pair $(\beta,\alpha) \in \Gamma_{ii}^{F}$ gives rise to an aspect ratio dependence upon the critical flexural instability, we display the value of $\eta_T(\beta,\alpha)$, which determines the transition aspect ratio, for representative pairs $(\beta,\alpha) \in \Gamma_{ii}^{F}$ in table 7-1. This table was generated with the aid of PROJ1 in (XI) of APPENDIX C.

Now turn to consider the buckling behavior of composite constructions corresponding to parameter pairs $(\beta,\alpha) \in \Gamma_{iii}^{F}$. Each such pair (β,α) gives rise to a function $\Phi_F(\eta,\beta,\alpha)$ which contains both internal maxima and internal minima as η varies from 0 to ∞. The ordering of the flexure failure thrusts for composite configurations in which $(\beta,\alpha) \in \Gamma_{iii}^{F}$ may in fact be quite complicated. First of all it is to be noted that (7.3) might still hold. Specifically if the

number of internal maxima is finite and equal to the number of internal minima, then the asymptotic value λ_∞ will be approached from below and consequently (7.3) will continue to hold for sufficiently large aspect ratios l_2/l_1. However for each $(\beta,\alpha) \in \Gamma_{iii}^F$ it is also clear that there will exist certain aspect ratios such that (7.3) will not hold. In particular for each $(\beta,\alpha) \in \Gamma_{iii}^F$ there will exist infinitely many aspect ratios such that certain flexure failure thrusts will correspond to two distinct flexure mode m by the same argument used for $(\beta,\alpha) \in \Gamma_{ii}^F$. Finally the possibility of a single flexure failure thrust corresponding to three or more flexure mode m remains a possibility whenever $(\beta,\alpha) \in \Gamma_{iii}^F$.

The investigation shall now turn to consider the barrelling failure thrusts. The ordering (7.4) of barrelling failure thrusts will continue to hold if $\Phi_B(\eta,\beta,\alpha)$ is monotonically decreasing in η for all $\eta \geq 0$. Pairs (β,α) which give rise to $\Phi_B(\eta,\beta,\alpha)$ having this property will be said to belong to the set Γ_i^B. For example $(2,0.5) \in \Gamma_i^B$ (Figure 7-4).

On the other hand if $\Phi_B(\eta,\beta,\alpha)$ is found to be monotonically decreasing over an interval $0 \leq \eta < \eta_{min} = \eta_{min}(\beta,\alpha)$ and is subsequently monotonically increasing for $\eta > \eta_{min}(\beta,\alpha)$, then we shall say that $(\beta,\alpha) \in \Gamma_{ii}^B$. For example $(0.5,0.5) \in \Gamma_{ii}^B$ (Figure 7-3). Finally if (β,α) belong to neither Γ_i^B nor Γ_{ii}^B then it is said that $(\beta,\alpha) \in \Gamma_{iii}^B$. Clearly $(\beta,\alpha) \in \Gamma_{iii}^B$ implies that $\Phi_B(\eta,\beta,\alpha)$ has an internal maximum.

For $(\beta,\alpha) \in \Gamma_{ii}^B$, the relation (7.4) will no longer hold. Specifically, T_∞ can no longer be the critical barrelling failure thrust. In fact, the critical barrelling failure thrust can be made

to correspond to any mode number $m < \infty$ by, for example, taking an aspect ratio $l_2/l_1 = 2\eta_{min}(\beta,\alpha)/(m\pi)$. Coincidence of two failure barrelling thrusts is also a possibility whenever $(\beta,\alpha) \in \Gamma_{ii}^{B}$. In fact for consecutive integeres m and m+1, if $T_m^{B} = T_{m+1}^{B}$ then this common value of barrelling failure thrust must of necessity be the critical barrelling failure thrust. Moreover it can be shown that there exists a unique aspect ratio such that $T_m^{B} = T_{m+1}^{B}$ for any integer m. Finally, it is to be noted that interlacing of the flexural and barrelling buckling loads will occur regardless of aspect ratio l_2/l_1 if $(\beta,\alpha) \in \Gamma_{ii}^{B}$.

If $(\beta,\alpha) \in \Gamma_{iii}^{B}$, then the ordering of the barrelling failure thrusts is complicated by the precise placement of the internal maxima and minima of $\Phi_B(\eta,\beta,\alpha)$. In fact, phenomena paralleling the possibilities outlined previously for Γ_{iii}^{F} pertain also to Γ_{iii}^{B}.

The partitioning of Π into regions Γ_i^{B}, Γ_{ii}^{B} and Γ_{iii}^{B} is displayed in Figure 7-7. This was accomplished with the aid of BARRELLING3, BARRELLING4 and BARRELLING5 given in (VIII), (IX), (X) of APPENDIX C. These programs are the analogues of FLEXURE3, FLEXURE4 and FLEXURE5 respectively. Note from Figure 7-7 that the boundary of the region Γ_{ii}^{B} is at certain points quite close to the pairs (β,α) corresponding to the non-composite case (4.55). The presence of Γ_{ii}^{B} so near the boundary $\alpha = 1$ for $\beta > 1$ indicates that a plate which includes relatively thin and flexible outer layers can be "tuned" to any desired critical barrelling mode by appropriately selecting the aspect ratio l_2/l_1. For such a result to be of significant practical interest, however, it would seem that it would be necessary to devise a method to suppress the preceding flexure

modes.

Since the interlacing of the flexural and barrelling failure modes is an intriguing result, it would be useful to further characterize this behavior with respect to β, α and l_2/l_1. For a given pair (β,α) interlacing can be made to occur for at least one l_2/l_1 if for any value of η either $\Phi_F(\eta,\beta,\alpha) > \lambda_\infty$ or $\Phi_B(\eta,\beta,\alpha) < \lambda_\infty$. Furthermore interlacing is ensured for all l_2/l_1 if either $\Phi_F(\eta,\beta,\alpha)$ approaches λ_∞ from above as $\eta \to \infty$ or if $\Phi_B(\eta,\beta,\alpha)$ approaches λ_∞ from below as $\eta \to \infty$. One or the other such asymptotic behaviors giving rise to interlacing for all l_2/l_1 will occur if either $(\beta,\alpha) \in \Gamma_{ii}^{F}$ or $(\beta,\alpha) \in \Gamma_{ii}^{B}$. In addition, an asymptotic behavior that ensures interlacing could also occur if $(\beta,\alpha) \in \Gamma_{iii}^{F} \cup \Gamma_{iii}^{B}$, however for such points this asymptotic behavior may be extremely sensitive to small changes in (β,α) and hence difficult to determine. Even so, it is interesting to note from Figures 7-5 and 7-7 that points $(\beta,\alpha) \in \Gamma_{ii}^{F} \cup \Gamma_{ii}^{B}$ comprise the major portion of the strip II for both $\beta > 1$ and $\beta < 1$. Thus, from this point of view, interlacing is not at all unusual both when the stiffer material comprises the outer layers ($\beta < 1$, e.g. Figure 7-3), and when the stiffer material comprises the central ply ($\beta > 1$, e.g. Figure 7-4).

It is also interesting to classify the points (β,α) with respect to satisfaction of equations (7.3) and (7.4). There are three possibilities. First, it may be that both (7.3) and (7.4) --- and thus (7.1) --- hold for all aspect ratios l_2/l_1. In this case it will said that $(\beta,\alpha) \in \Xi_1$. For this to occur the pair (β,α) must belong to both Γ_i^{F} and Γ_i^{B}. Second, it may be that there is at least one aspect ratio l_2/l_1 that will result in both (7.3) and (7.4) being

violated. For this to occur the pair (β,α) must belong to neither Γ_i^F nor Γ_i^B. In this case it will said that $(\beta,\alpha) \in \Xi_2$. Finally it may be that for each aspect ratio l_2/l_1 either (7.3) or (7.4) holds, but that there is also at least one aspect ratio l_2/l_1 for which one of these relations is violated. This will occur for the remaining case in which (β,α) belong to either Γ_i^F or Γ_i^B, but not both. In this case it will said that $(\beta,\alpha) \in \Xi_3$. Summarizing then these definitions,

$$\begin{aligned} \Xi_1 &= \Gamma_i^F \cap \Gamma_i^B \ , \\ \Xi_2 &= (\Gamma_{ii}^F \cup \Gamma_{iii}^F) \cap (\Gamma_{ii}^B \cup \Gamma_{iii}^B) \ , \\ \Xi_3 &= (\Gamma_i^F \cap (\Gamma_{ii}^B \cup \Gamma_{iii}^B)) \cup (\Gamma_i^B \cap (\Gamma_{ii}^F \cup \Gamma_{iii}^F)) \ . \end{aligned} \tag{7.14}$$

One can determine these regions on the basis of Figures 7-5 and 7-7, the result of which is given in figure 7-8. This figure indicates that Ξ_1 is confined to a simply connected region containing pairs (β,α) corresponding to the non-composite case (4.54). Thus, in this sense, the composite constructions under consideration must be "close" to a non-composite construction if (7.1) is to hold. Figure 7-8 also indicates that the region Ξ_3 comprises the majority of the semi-infinite strip II. In particular the (β,α)-pairs (0.5,0.5) and (2.0,0.5), associated with Figures 7-3 and 7-4 respectively, are each a member of Ξ_3. The region Ξ_2, on the other hand, comprises the least area within the semi-infinite strip II. For pairs $(\beta,\alpha) \in \Xi_2$ both $\Phi_F(\eta,\beta,\alpha)$ and $\Phi_B(\eta,\beta,\alpha)$ display non-monotone behavior as for example shown in Figure 7-9 for the point $(\beta,\alpha) = (0.5,0.8)$. Finally it is to be noted from Figure 7-8 that the (β,α)-classification is far

more sensitive near $\alpha = 1$ than it is near $\alpha = 0$. This confirms one's intuition as to the effect that placement of thin "stiffeners" (or even "looseners") would have in a much thicker homogeneous plate; namely that the addition of thin plies on the external X_2-faces of the plate would have a more pronounced effect on the buckling behavior than would the insertion of a single double thickness ply on the plate's midplane. Thus it is found that burying a very thin ply at the center of a plate will mask its effect upon altering the order of the failure thrusts.

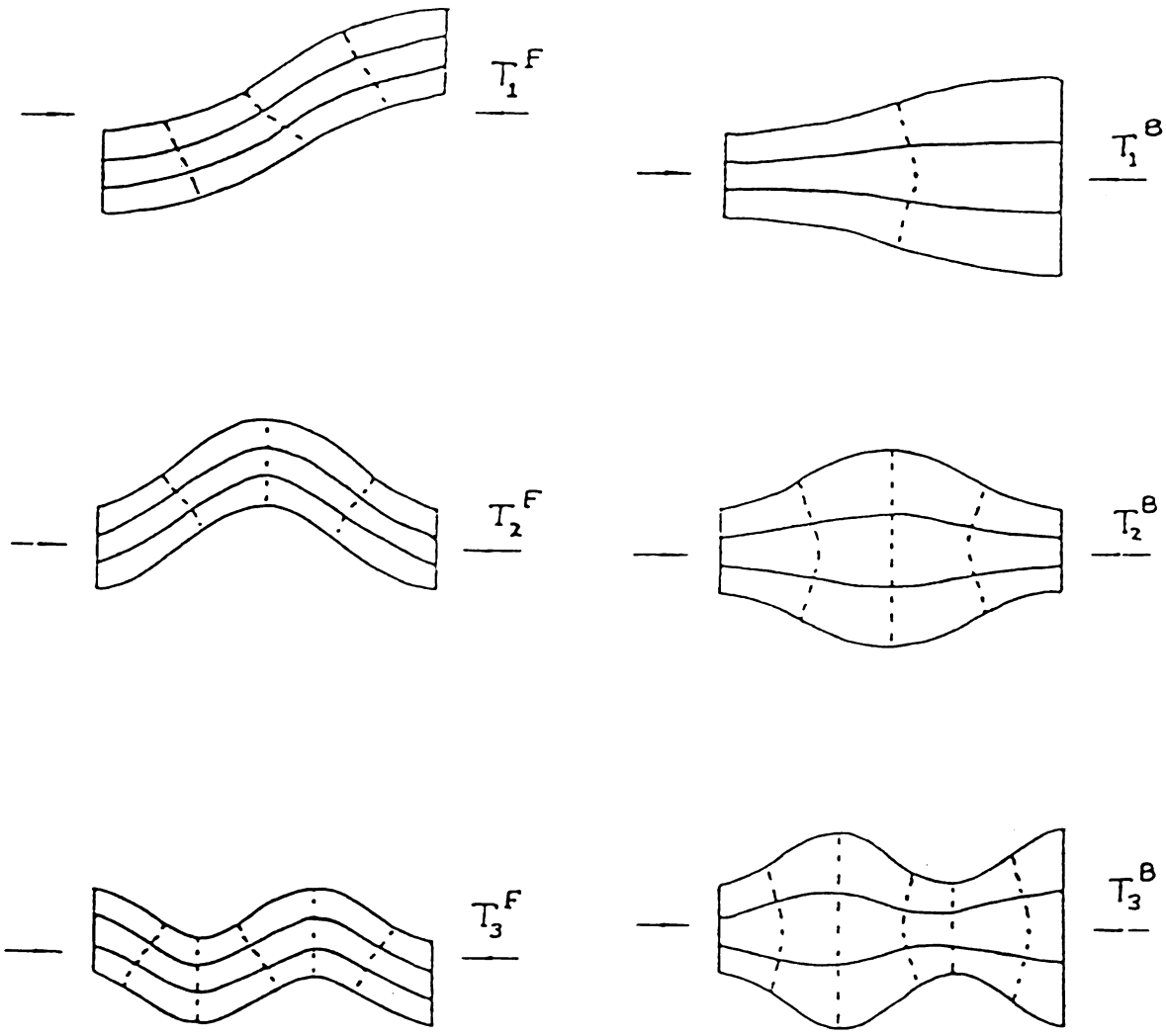

Figure 7-1:

Examples of the flexural and barrelling buckling modes, and failure thrusts, for m = 1,2 and 3. Higher order buckling modes involve additional repetition of the basic m = 1 half-wavelength mode shape.

Figure 7-2:

The functions $\Phi_F(\eta,\beta,\alpha)$ and $\Phi_B(\eta,\beta,\alpha)$ for all (β,α)-pairs corresponding to the non-composite case given in (4.38). Here $\lambda_\infty \approx 3.383$.

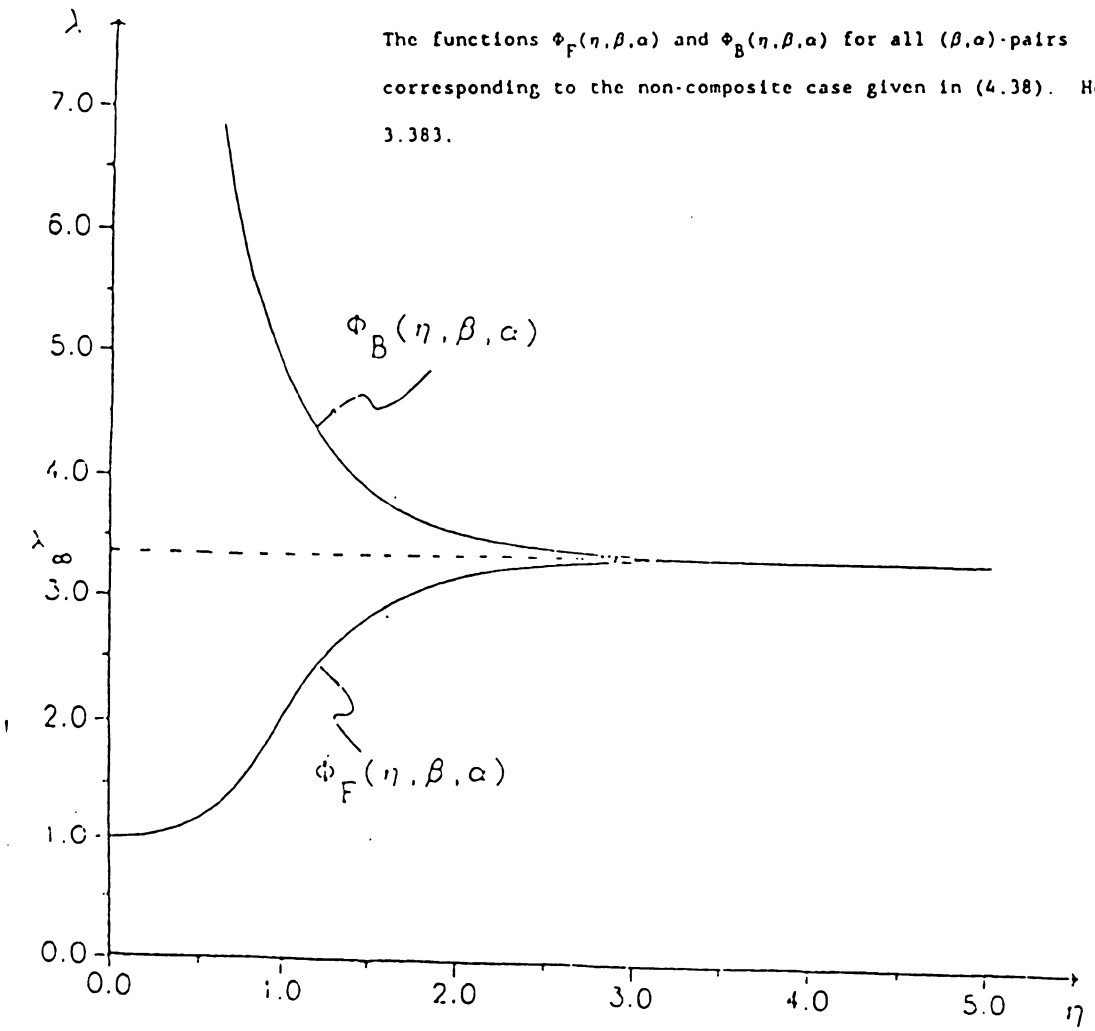

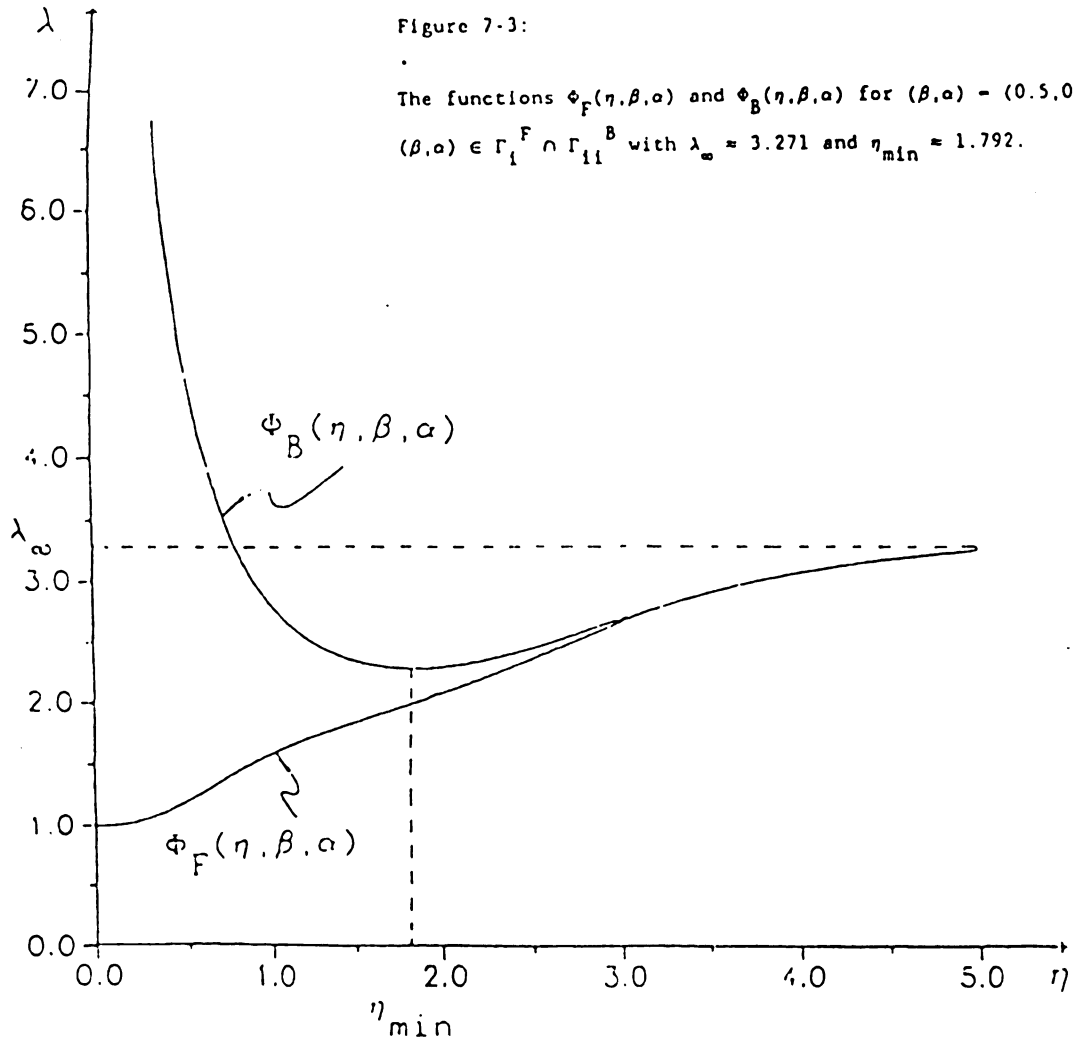

Figure 7-3:

The functions $\Phi_F(\eta,\beta,\alpha)$ and $\Phi_B(\eta,\beta,\alpha)$ for $(\beta,\alpha) = (0.5,0.5)$. $(\beta,\alpha) \in \Gamma_i^F \cap \Gamma_{ii}^B$ with $\lambda_\infty \approx 3.271$ and $\eta_{min} \approx 1.792$.

Figure 7-4:

The functions $\Phi_F(\eta,\beta,\alpha)$ and $\Phi_B(\eta,\beta,\alpha)$ for $(\beta,\alpha) = (2,0.5)$. Here $(\beta,\alpha) \in \Gamma_{11}^F \cap \Gamma_1^B$ with $\lambda_\infty \approx 3.439$, $\eta_{max} \approx 1.977$ and $\eta_T \approx 1.392$.

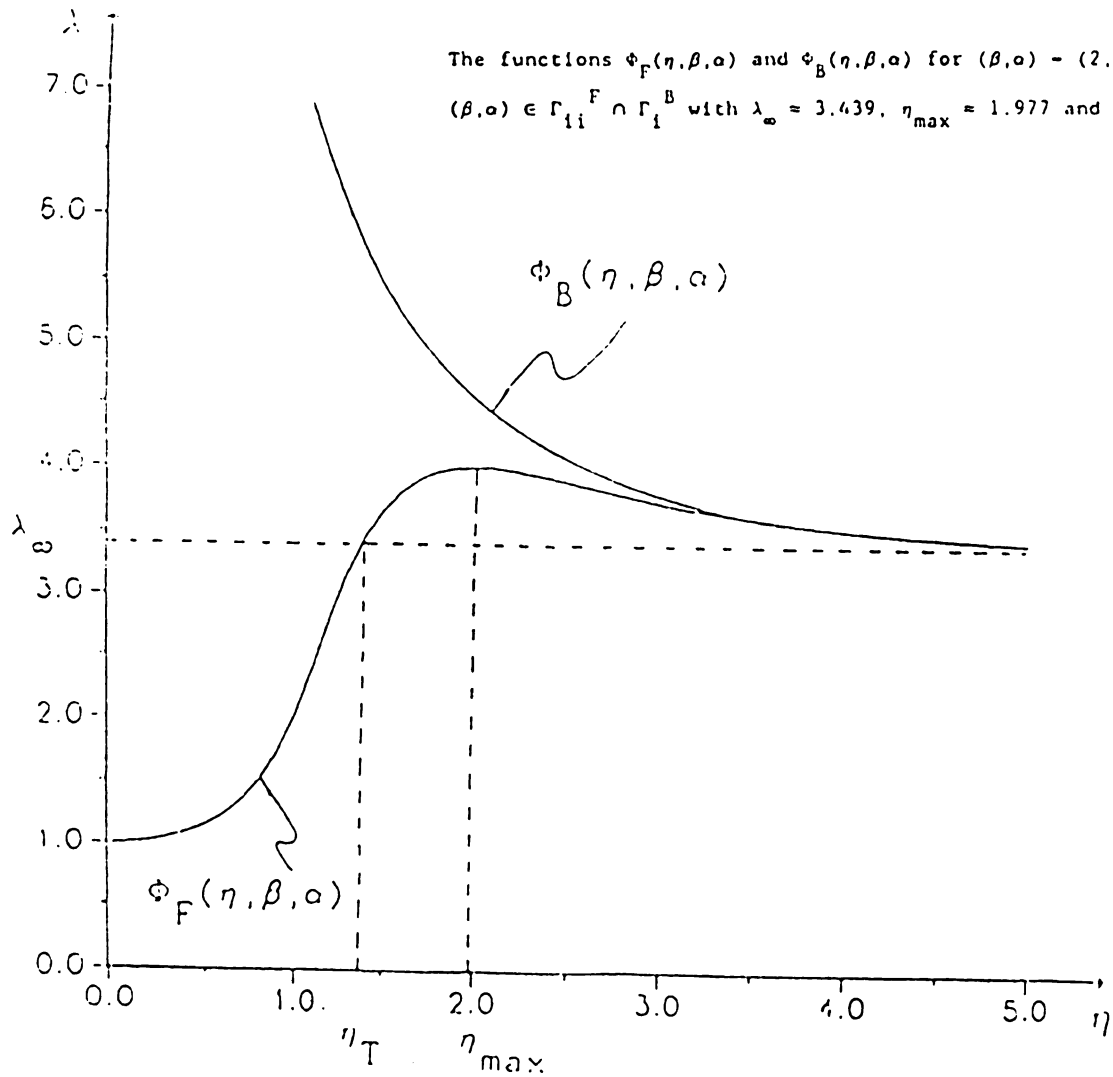

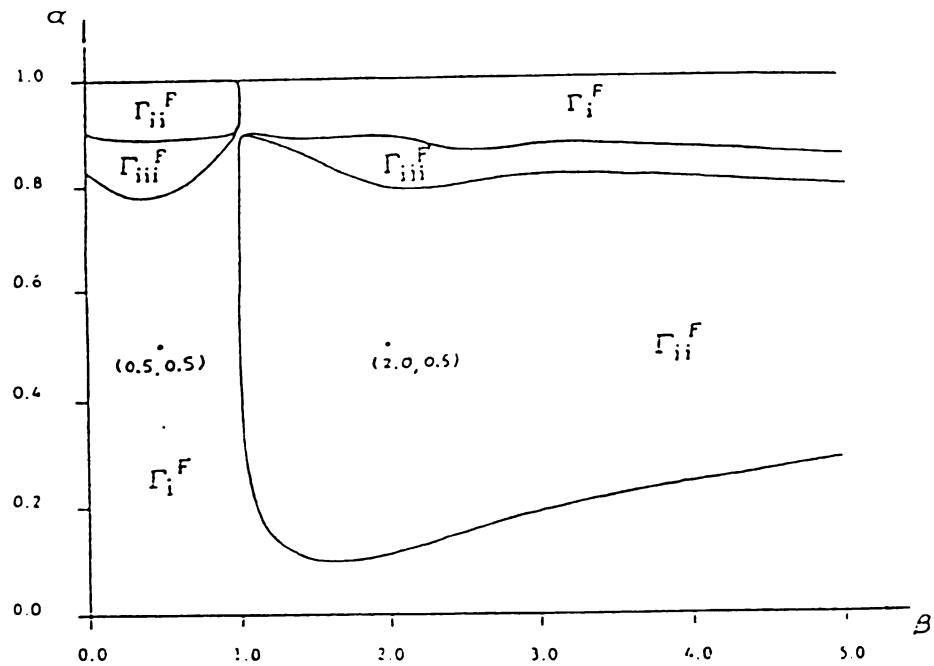

Figure 7-5:

Flexure failure behavior as represented in the semi-infinite strip . $0 < \alpha = R/l_2 < 1$, $0 < \beta = \mu^{(II)}/\mu^{(I)}$. The region type for each shade are as displayed. The two points shown correspond to the parameter pairs associated with Figures 7-3 and 7-4. Although it is not always obvious from this diagram, the parameter pairs obeying (4.55) are in the region Γ_i^F.

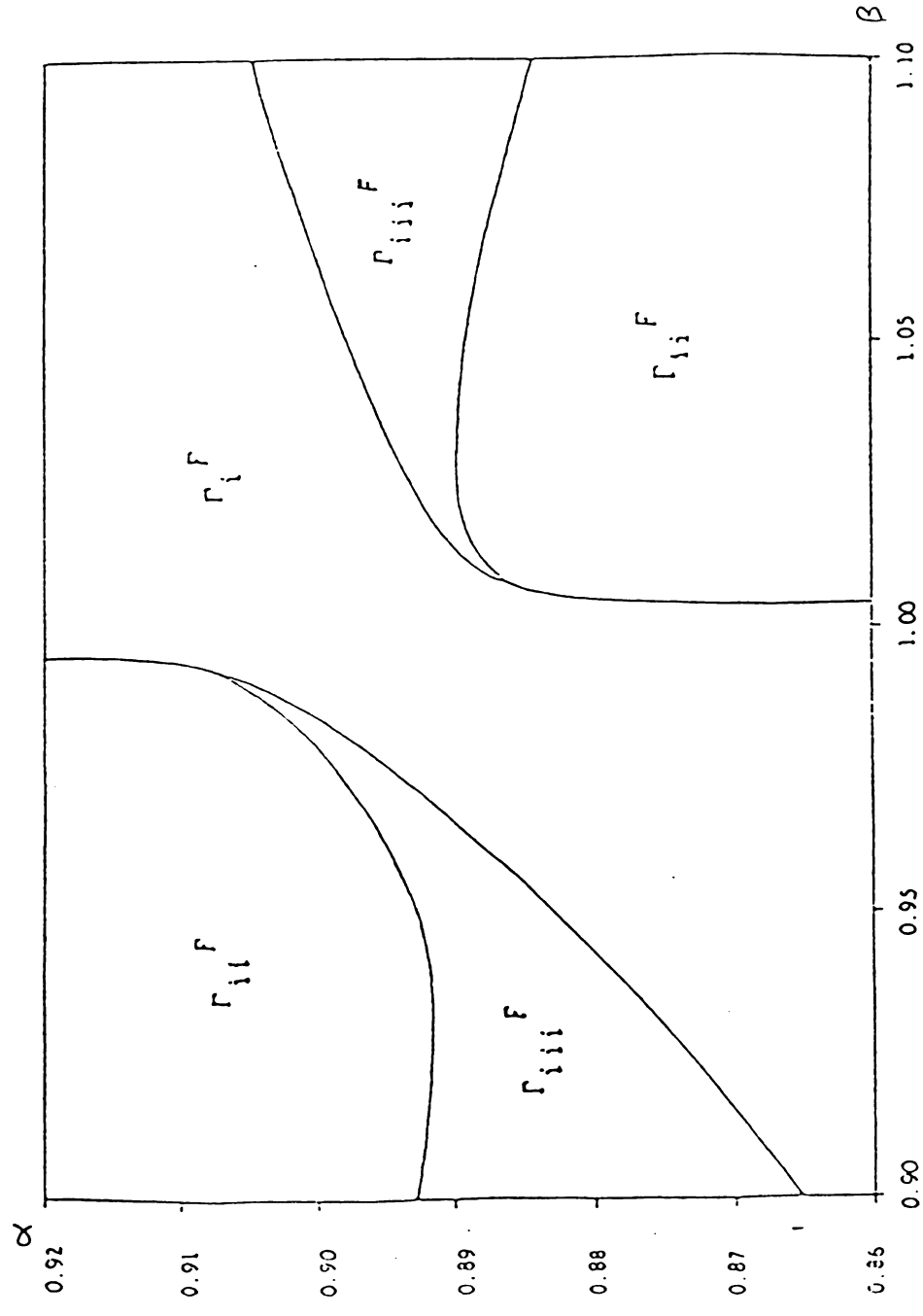

Figure 7-6: Magnified view of Figure 7-5 near $(\beta,\alpha) = (1.0,0.9)$. The points on β - 1 are ensured to lie on Γ_1^F by virtue of (4.55).

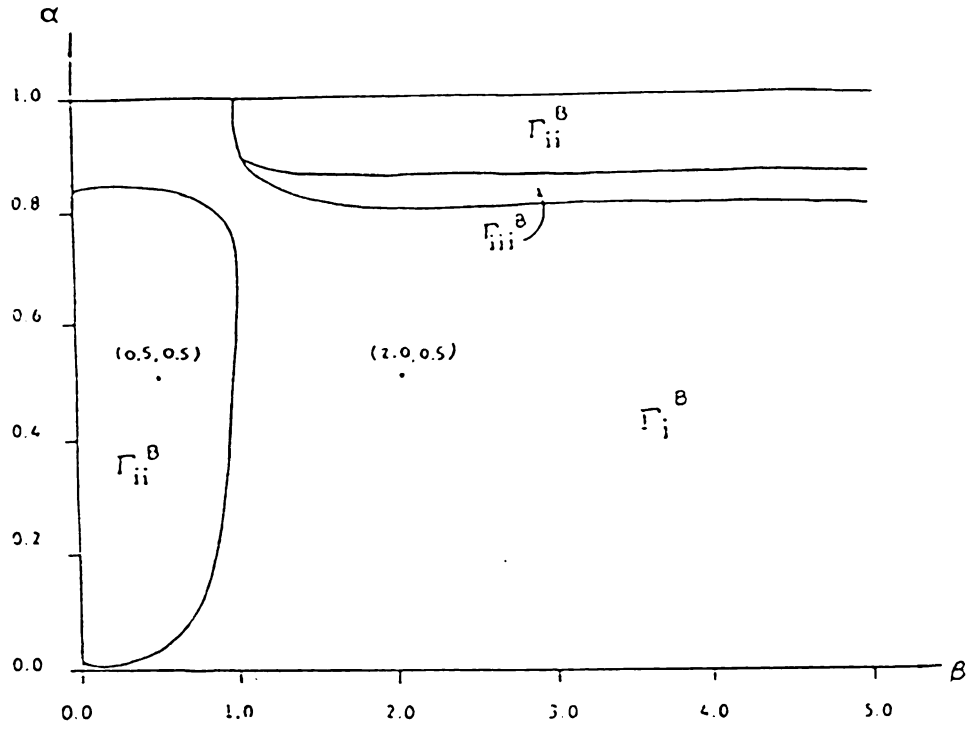

Figure 7-7:

Barrelling failure behavior as represented in the semi-infinite strip $0 < \alpha = R/l_2 < 1$, $0 < \beta = \mu^{(II)}/\mu^{(I)}$. The region type for each shade are as displayed. The two points shown correspond to the parameter pairs associated with Figures 7-3 and 7-4. Although it is not always obvious from this diagram, the parameter pairs obeying (4.35) are in the region Γ_i^B.

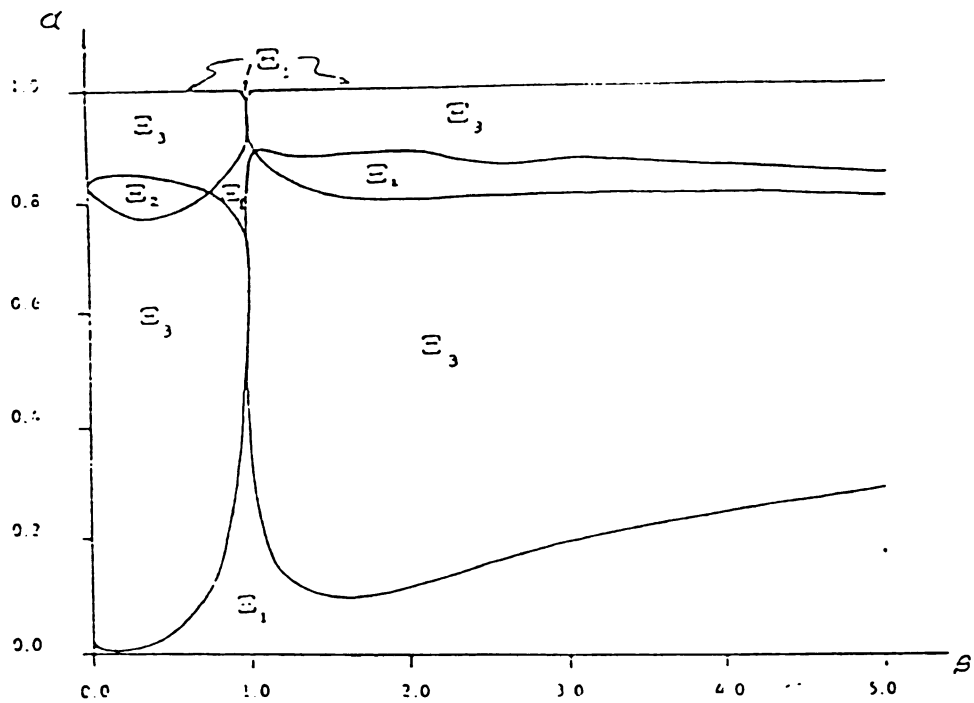

Figure 7-8:

The partitioning of the semi-infinite strip $0 < \alpha = R/l_2 < 1$, $0 < \beta = \mu^{(II)}/\mu^{(I)}$ into the regions Ξ_1, Ξ_2 and Ξ_3. The ordering (7.1) is ensured only for $(\beta,\alpha) \in \Xi_1$. . For $(\beta,\alpha) \in \Xi_2 \cup \Xi_3$ the ordering which replaces (7.1) is dependent on the aspect ratio l_2/l_1. Although it is not always obvious from this diagram, the parameter pairs obeying (4.55) are in the region Ξ_1.

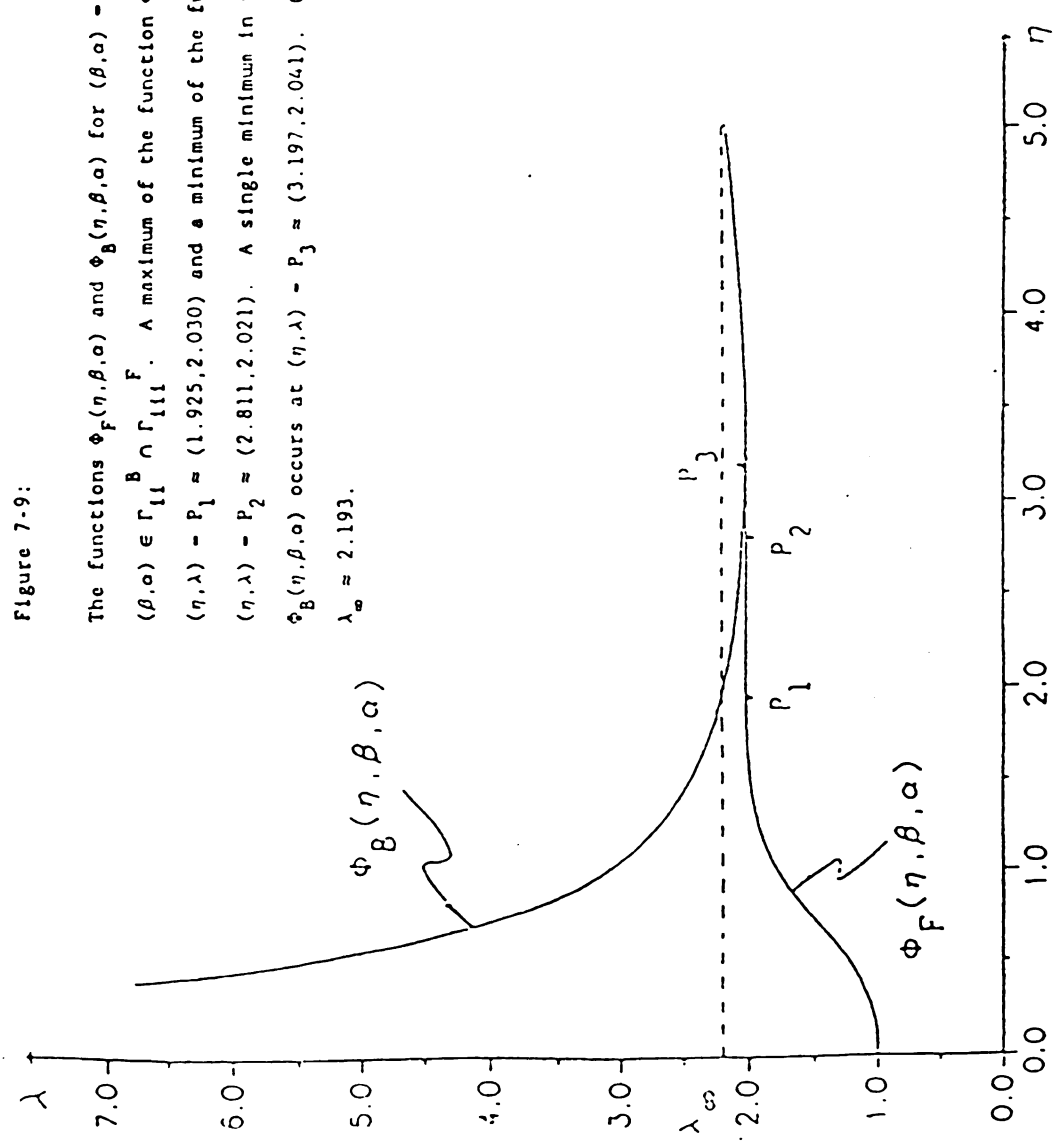

Figure 7-9:

The functions $\Phi_F(\eta,\beta,\alpha)$ and $\Phi_B(\eta,\beta,\alpha)$ for $(\beta,\alpha) = (0.5,0.8)$. Here $(\beta,\alpha) \in \Gamma_{11}^B \cap \Gamma_{111}^F$. A maximum of the function $\Phi^F(\eta,\beta,\alpha)$ occurs at $(\eta,\lambda) = P_1 \approx (1.925,2.030)$ and a minimum of the function occurs at $(\eta,\lambda) = P_2 \approx (2.811,2.021)$. A single minimum in the function $\Phi_B(\eta,\beta,\alpha)$ occurs at $(\eta,\lambda) = P_3 \approx (3.197,2.041)$. One also finds that $\lambda_\infty \approx 2.193$.

	β=0.1	0.2	0.5	0.8	0.9	1	1.1	1.5	2	2.5	3	4	5
α=1	/	/	/	/	/	/	/	/	/	/	/	/	/
.99	0.974	1.236	1.945	2.810	3.602	/	/	/	/	/	/	/	
.95	0.593	0.750	1.147	1.692	2.125	/	/	/	/	/	/	/	/
.9	0.555	0.711	1.070	1.653	2.166	/	/	/	/	/	/	/	/
.8	/	/	/	/	/	/	2.264	1.841	1.858	2.102	2.274	2.795	/
.7	/	/	/	/	/	/	1.862	1.383	1.410	1.439	1.599	1.726	1.912
.6	/	/	/	/	/	/	1.818	1.333	1.349	1.395	1.554	1.693	1.877
.5	/	/	/	/	/	/	1.951	1.347	1.392	1.497	1.675	1.965	2.147
.4	/	/	/	/	/	/	2.410	1.483	1.546	1.729	1.962	2.323	2.616
.3	/	/	/	/	/	/	3.186	1.764	1.889	2.196	2.536	3.060	3.365
.2	/	/	/	/	/	/	4.753	3.465	2.711	3.223	3.529	4.784	5.326
.1	/	/	/	/	/	/	/	4.857	5.065	5.903	6.398	/	/
α=0	/	/	/	/	/	/	/	/	/	/	/	/	/

Table 7-1:

Value of the transition aspect ratio $\eta_T(\beta,\alpha)$ for representative pairs $(\beta,\alpha) \in \Gamma_{ii}^F$. For $l_2/l_1 < \eta_T/\pi$, the critical instability is the m = 1 flexure mode, while for $l_2/l_1 > \eta_T/\pi$ the critical instability is m = ∞ wrinkling mode.

8. OPTIMAL DESIGN FOR COMPOSITE CONSTRUCTIONS

In this section the results obtained in section 7 shall be used to study a problem in optimal design. This problem is defined as follows.

It is desired to construct a plate occupying the region $-l_i \le X_i \le l_i$ $(i = 1,2,3)$ before the application of loads. To accomplish this purpose, fixed amounts of two neo-Hookean materials are available, material A with volume $V^{(A)}$ and shear modulus $\mu^{(A)}$, and material B with volume $V^{(B)}$ and shear modulus $\mu^{(B)}$. It is assumed that $V^{(A)} + V^{(B)} = 8l_1l_2l_3$ which is the total volume of the plate. These two materials shall be used to form a composite construction of the type (2.2).

There are thus only two competing configurations, namely

Configuration-1: in which material-A is used for the central ply and material-B is used for the outer plies, and

Configuration-2: in which material-B is used for the central ply and material-A is used for the outer plies. (8.1)

It shall be said that configuration-1 and configuration-2 as given above are conjugate to each other. The conjugate of a configuration is obtained by exchanging the roles of the two materials while maintaining fixed the values $V^{(A)}$ and $V^{(B)}$. Thus

$$R = \begin{cases} V^{(A)}/(8l_1l_3) & \text{for configuration-1,} \\ V^{(B)}/(8l_1l_3) & \text{for configuration-2.} \end{cases} \tag{8.2}$$

The relation between T and ρ corresponding to (6.10) is found to be given by

$$T = (\rho-\rho^{-3})[\mu^{(A)}V^{(A)}+\mu^{(B)}V^{(B)}]/(2l_1). \tag{8.3}$$

Thus, from the point of view of the thrust deflection properties of the plate undergoing a pure homogeneous deformation, there is no particular advantage to be gained by considering either configuration-1 or configuration-2.

Without loss of generality, let material A be the material with the lesser shear modulus,

$$\mu^{(A)} < \mu^{(B)} . \tag{8.4}$$

Let T_m^F and T_m^{F*} denote the flexure failure thrusts for configuration-1 and configuration-2 respectively. Similarly T_m^B and T_m^{B*} will denote the barrelling failure thrusts for configuration-1 and configuration-2. The lowest or *critical thrust* for each configuration is thus given by

$$T_{crit} = \min_{m=1,\infty} \{T_m^F, T_m^B\} \quad \text{and} \quad T_{crit}^* = \min_{m=1,\infty} \{T_m^{F*}, T_m^{B*}\}.$$

Now it was shown in section 7 that the critical thrust of a symmetric 3-ply sandwich always corresponds to flexure, thus

$$T_{crit} = \min_{m=1,\infty} \{T_m^F\},$$

$$T_{crit}^* = \min_{m=1,\infty} \{T_m^{F*}\}. \tag{8.5}$$

The configuration which yields the larger of the two critical thrusts will be said to be the **optimal design**. *Thus configuration-1 will be the optimal design if*

$$T_{crit} > T_{crit}^{*}, \tag{8.6}$$

while configuration-2 will be the optimal design if

$$T_{crit}^{*} > T_{crit}. \tag{8.7}$$

It shall be said that configuration-1 and configuration-2 are *equally optimal* if

$$T_{crit} = T_{crit}^{*}. \tag{8.8}$$

Recall at this juncture the definition of β and α as given in (4.49). For the purposes of this section these values shall be redefined as follows

$$\beta = \mu^{(A)}/\mu^{(B)}, \quad \alpha = V^{(A)}/(V^{(A)}+V^{(B)}). \tag{8.9}$$

Thus the results obtained in section 7 apply immediately to configuration-1. In particular, the critical thrust T_{crit} will, by virtue of (8.3) and $\rho = \lambda^{-1/2}$, be associated with the value

$$\lambda_{crit} = \min_{m=1,\infty} \{\lambda_m^F\}. \tag{8.10}$$

Furthermore,

$$\lambda_{crit} = \lambda_1^F, \quad T_{crit} = T_1^F, \quad \text{for } (\beta,\alpha) \in \Gamma_i^F, \tag{8.11}$$

and

$$\lambda_{crit} = \begin{cases} \lambda_1^F, \\ \lambda_\infty, \end{cases} \quad T_{crit} = \begin{cases} T_1^F, & \text{if } l_2/l_1 < 2\eta_T/\pi, \\ T_\infty, & \text{if } l_2/l_1 > 2\eta_T/\pi, \end{cases} \quad \text{for } (\beta,\alpha) \in \Gamma_{ii}^F. \tag{8.12}$$

Thus the parameter plane description exhibited in Figure 7-5 immediately provides useful information regarding the possibilities for the critical stretch ratio λ_{crit} and the critical thrust T_{crit} for the case of configuration-1. Recalling now the restriction (8.4), the definition of β given in (8.9) implies that

$$\beta < 1. \tag{8.13}$$

Displayed in Figure 7-5, however, are results found in section 7 that apply to values $\beta > 1$. This information is useful in determining the critical thrust T_{crit}^* for configuration-2. This is because (8.9) indicates that if (β,α) characterizes configuration-1, then (β^*,α^*) characterizes configuration-2 provided that

$$\beta^* = \beta^{-1}, \quad \alpha^* = 1 - \alpha. \tag{8.14}$$

It will be convenient for the purposes of this investigation to

introduce a conjugate function

$$\Phi_F^*(\eta,\beta,\alpha) = \Phi_F(\eta,\beta^*,\alpha^*) - \Phi_F(\eta,\beta^{-1},1-\alpha) \ , \tag{8.15}$$

and conjugate failure stretch ratios

$$\lambda_m^{F*} = \Phi_F^*(m\pi l_2/2l_1,\beta,\alpha), \quad m = 1,2,3... \ . \tag{8.16}$$

Also define $\lambda_\infty^*(\beta,\alpha)$ corresponding in the obvious fashion to (7.6) and, for $(\beta^*,\alpha^*) \in \Gamma_{ii}^F$, define the functions $\eta_T^*(\beta,\alpha)$ and $\eta_{max}^*(\beta,\alpha)$ obeying the counterpart to (7.10). Finally, recalling (8.10), let

$$\lambda_{crit}^* = \min_{m=1,\infty} \{\lambda_m^{F*}\} \ . \tag{8.17}$$

Then configuration-1 will be the optimal design if

$$\lambda_{crit} > \lambda_{crit}^* \ , \tag{8.18}$$

while configuration-2 will be the optimal design if

$$\lambda_{crit}^* > \lambda_{crit} \ . \tag{8.19}$$

The two configurations are *equally optimal* if

$$\lambda_{crit} = \lambda_{crit}^* \ . \tag{8.20}$$

Since $\Phi_F(\eta,\beta,\alpha)$ is initially monotonically increasing from the value 1 at $\eta = 0$ for all pairs (β,α) it follows that

$$\Phi_F(0,\beta,\alpha) = \Phi_F^*(0,\beta,\alpha) = 1. \tag{8.21}$$

It has been found by means of extensive numerical calculations, for fixed values of (β,α) obeying $0 < \alpha < 1$, $0 < \beta < 1$, that there exists a unique $\eta_{cross} > 0$ such that

$$\Phi_F(\eta_{cross},\beta,\alpha) = \Phi_F^*(\eta_{cross},\beta,\alpha) \ . \tag{8.22}$$

The program PROJ2 in (XII) of APPENDIX C can be used to find the value η_{cross}. It is found without exception that

$$\begin{aligned} &\Phi_F(\eta,\beta,\alpha) > \Phi_F^*(\eta,\beta,\alpha) \ , \qquad \text{for } 0 < \eta < \eta_{cross}, \\ &\Phi_F(\eta,\beta,\alpha) < \Phi_F^*(\eta,\beta,\alpha) \ , \qquad \text{for } \eta > \eta_{cross}. \end{aligned} \tag{8.23}$$

Note that $\eta_{cross} = \eta_{cross}(\beta,\alpha)$; this function shall be called the **crossover value function** between conjugate configurations (β,α) and (β^*,α^*). Table 8-1 gives this function for selected values of (β,α). From (8.23), (8.16) and $(7.2)_1$ it may be concluded that

$$\begin{aligned} &\lambda_1^F > \lambda_1^{F*} \ , \quad \text{if } \pi l_2/2l_1 < \eta_{cross}, \\ &\lambda_1^F < \lambda_1^{F*} \ , \quad \text{if } \pi l_2/2l_1 > \eta_{cross}. \end{aligned} \tag{8.24}$$

Thus the configuration with the stiffer material placed in the outer plies provides the greatest resistance to the m = 1 flexure mode for plates that are sufficiently long on the direction of thrust (specifically $l_1 > (\pi/2\eta_{cross})l_2$ *), while the configuration with the stiffer material placed in the central ply provides the greatest resistance to the m = 1 flexure mode for plates that are sufficiently short in the direction of thrust (specifically* $l_1 < (\pi/2\eta_{cross})l_2$ *).*

This result provides a prescription for the optimal design in cases in which the critical thrusts for both configuration-1 and configuration-2 are associated with m = 1 flexure. According to (8.10) this will occur if both $(\beta,\alpha) \in \Gamma_i^F$ and $(\beta^*,\alpha^*) \in \Gamma_i^F$. It follows that *if* $(\beta,\alpha) \in \Gamma_i^F$ *and* $(\beta^*,\alpha^*) \in \Gamma_i^F$ *then the optimal design is*

$$\textit{configuration-1} \quad \textit{if } l_2/l_1 < 2\eta_{cross}/\pi, \tag{8.25}$$

whereas the optimal design is

$$\textit{configuration-2} \quad \textit{if } l_2/l_1 > 2\eta_{cross}/\pi. \tag{8.26}$$

Note that in this case the special aspect ratio $l_2/l_1 = 2\eta_{cross}/\pi$ corresponds to the equally optimal configuration which serves as the switching point between the two competing configurations, both of which fail in m = 1 flexure. The representative case (β,α) = (0.5, 0.05) for the state of affairs described above is diagramed in Figure 8-1.

Whether or not $(\beta,\alpha) \in \Gamma_i^F$ can be determined immediately from Figure 7-5. To determine the corresponding information for the

conjugate pair (β^*,α^*) it is useful to map the region $\beta > 1$ of the semi-infinite strip $\beta \geq 0$, $0 \leq \alpha \leq 1$ of Figure 7-5 to the square $0 < \beta < 1$, $0 < \alpha < 1$ by means of the tranformation (8.14). The result of this mapping is given in Figure 8-2 where, in addition, the relevent portion of the original Figure 7-5 has also been included. Since Figure 7-5 was only determined to a value $\beta \approx 5$, the result of the mapping (8.14) is only given for the region $0.2 < \beta < 1$. Nevertheless the behavior of this mapping has been extrapolated by means of the dashed curves in Figure 8-2. The regions separated by the curves in Figure 8-2 are each associated with a different possibility as follows:

$$\left.\begin{array}{ll}
\text{region-a:} & (\beta,\alpha) \in \Gamma_i^F, \quad (\beta^*,\alpha^*) \in \Gamma_i^F \ ; \\
\text{region-b:} & (\beta,\alpha) \in \Gamma_i^F, \quad (\beta^*,\alpha^*) \in \Gamma_{ii}^F \ ; \\
\text{region-c:} & (\beta,\alpha) \in \Gamma_i^F, \quad (\beta^*,\alpha^*) \in \Gamma_{iii}^F \ ; \\
\text{region-d:} & (\beta,\alpha) \in \Gamma_{ii}^F, \quad (\beta^*,\alpha^*) \in \Gamma_i^F \ ; \\
\text{region-e:} & (\beta,\alpha) \in \Gamma_{ii}^F, \quad (\beta^*,\alpha^*) \in \Gamma_{ii}^F \ ; \\
\text{region-f:} & (\beta,\alpha) \in \Gamma_{iii}^F, \quad (\beta^*,\alpha^*) \in \Gamma_i^F \ ; \\
\text{region-g:} & (\beta,\alpha) \in \Gamma_{iii}^F, \quad (\beta^*,\alpha^*) \in \Gamma_{ii}^F \ .
\end{array}\right\} \qquad (8.27)$$

It is found that the following two cases do *not* occur:

$$\text{(i)} \quad (\beta,\alpha) \in \Gamma_{ii}^{F}, \quad (\beta^*,\alpha^*) \in \Gamma_{iii}^{F} ;$$

$$\text{(ii)} \quad (\beta,\alpha) \in \Gamma_{iii}^{F}, \quad (\beta^*,\alpha^*) \in \Gamma_{iii}^{F} . \tag{8.28}$$

For stiffness ratio β and volume fraction α correspoding to region-a, both configuration-1 and configuration-2 fail in m=1 flexure for all aspect ratios l_2/l_1. In this region of parameter pairs the optimal design is governed by (8.25) and (8.26). This region continues to the boundaries $\beta = 1$, $\alpha = 0$ and $\alpha = 1$ which according to (4.54) corresponds to the non-composite case in which the optimal design problem ceases to have meaning. It is to be noted that region-a comprises only a small part of the square $0 < \alpha < 1$, $0 < \beta < 1$, and that the complete extent of this region is dependent on the extrapolation of the curve in Figure 8-2.

If (β,α) is not in region-a of Figure 8-2, the possibility arises that either $T_{crit} \neq T_1^{F}$ or $T_{crit}^{*} \neq T_1^{F*}$. It is this possibility to which the investigation now turns. For points (β,α) not in region-a, the aspect ratio $l_2/l_1 = 2\eta_{cross}/\pi$ may, but need not, be associated with a switch in optimal designs. This can be demonstrated by considering pairs (β,α) belonging to region-d. Then (8.11) indicates that

$$\lambda_{crit}^{*} = \lambda_1^{F*} , \qquad ((\beta^*,\alpha^*) \in \Gamma_i^{F}), \tag{8.29}$$

whereas (8.12) gives

$$\lambda_{crit} = \begin{cases} \lambda_1^F & \text{if } \pi l_2/l_1 < 2\eta_T, \\ \lambda_\infty & \text{if } \pi l_2/l_1 > 2\eta_T, \end{cases} \quad ((\beta,\alpha) \in \Gamma_{ii}^F). \tag{8.30}$$

Thus even though (8.24) indicates that η_{cross} governs a change in the relative ordering of λ_1^F and λ_1^{F*}, it may or may not govern a change in the relative ordering of λ_{crit} and λ_{crit}^*. To make this clear, let it first be supposed that

$$\eta_T > \eta_{cross} . \tag{8.31}$$

An example of such a situation occurs if $(\beta,\alpha) = (0.9,0.9)$ since $(0.9,0.9) \in \Gamma_{ii}^F$, $(1/0.9,1-0.9) \approx (1.11,0.1) \in \Gamma_i^F$ (see the point p_2 in Figure 8-2) and $\eta_T(0.9,0.9) \approx 2.1660 > 0.9009 \approx \eta_{cross}(0.9,0.9)$. The curve $\Phi_F(\eta,\beta,\alpha)$ and $\Phi_F^*(\eta,\beta,\alpha)$ for $(\beta,\alpha) = (0.9,0.9)$ are given in Figure 8-3. According to (8.24), (8.29), (8.30) and (8.31) it follows that

$$\begin{aligned} &\lambda_{crit} - \lambda_1^F > \lambda_1^{F*} - \lambda_{crit}^* , \quad \text{if} \quad \pi l_2/2l_1 < \eta_{cross} , \\ &\lambda_{crit} - \lambda_1^F < \lambda_1^{F*} - \lambda_{crit}^* , \quad \text{if} \quad \eta_{cross} < \pi l_2/2l_1 < \eta_T , \\ &\lambda_{crit} - \lambda_\infty < \lambda_1^{F*} - \lambda_{crit}^* , \quad \text{if} \quad \pi l_2/2l_1 > \eta_T , \end{aligned} \tag{8.32}$$

whenever $(\beta,\alpha) \in \Gamma_{ii}^F$, $(\beta^*,\alpha^*) \in \Gamma_i^F$ provided that $\eta_T > \eta_{cross}$. In such a case the aspect ratio $l_2/l_1 = 2\eta_{cross}/\pi$ will once again give a change in the relative ordering of λ_{crit} and λ_{crit}^*, so that the optimal design is configuration-1 if $l_2/l_1 < 2\eta_{cross}/\pi$, and the

optimal design is configuration-2 if $l_2/l_1 > 2\eta_{cross}/\pi$. In all cases, the optimal design fails in m = 1 flexure. The change in λ_{crit} given by (8.30) plays no role in the determination of the optimal design. In the example $(\beta,\alpha) = (0.9,0.9)$ the equally optimal design case associated with a switch in optimal design occurs at the aspect ratio $l_2/l_1 = 2\eta_{cross}/\pi \approx 0.5736$.

In contrast, now suppose that $(\beta,\alpha) \in \Gamma_{ii}^{F}$, $(\beta^*,\alpha^*) \in \Gamma_{i}^{F}$ and

$$\eta_T < \eta_{cross}. \tag{8.33}$$

An example of such a situation occurs if $(\beta,\alpha) = (0.5,0.95)$ since $(0.5,0.95) \in \Gamma_{ii}^{F}$, $(1/0.5,1-0.95) = (2,0.05) \in \Gamma_{i}^{F}$ (see point p_3 in Figure 8-4) and $\eta_T(0.5,0.95) \approx 1.1505 < 1.2884 \approx \eta_{cross}(0.5,0.95)$. The associated curves $\Phi_F(\eta,\beta,\alpha)$ and $\Phi_F^*(\eta,\beta,\alpha)$ are given in Figure 8-4. According to (8.24), (8.29), (8.30) and (8.33) it follows that

$$\begin{aligned} &\lambda_{crit} = \lambda_1^{F} > \lambda_1^{F*} = \lambda_{crit}^{*}, \quad \text{if} \quad \pi l_2/2l_1 < \eta_T, \\ &\lambda_{crit} = \lambda_\infty < \lambda_1^{F*} = \lambda_{crit}^{*}, \quad \text{if} \quad \pi l_2/2l_1 > \eta_{cross}. \end{aligned} \tag{8.34}$$

Thus the optimal design is configuration-1 if $l_2/l_1 < 2\eta_T/\pi$ whereas the optimal design is configuration-2 if $l_2/l_1 > 2\eta_{cross}/\pi$.

A switch in the optimal design will thus occur for at least one aspect ratio l_2/l_1 in the interval $2\eta_T/\pi < l_2/l_1 < 2\eta_{cross}/\pi$. Since $\lambda_{crit} = \lambda_\infty$ and $\lambda_{crit}^{*} = \lambda_1^{F*}$ for all such aspect ratios, a switch in the optimal design can only occur at an aspect ratio l_2/l_1 which gives $\lambda_\infty = \lambda_1^{F*}$. Hence it is necessary to determine roots η to the equation

$$\Phi_F^*(\eta,\beta,\alpha) = \lambda_\infty(\beta,\alpha), \quad \eta_T < \eta < \eta_{cross}. \tag{8.35}$$

Since $(\beta^*,\alpha^*) \in \Gamma_i^F$ ensures that $\Phi_F^*(\eta,\beta,\alpha)$ is monotonically increasing in η, there will be a unique root $\bar{\eta}_{cross}$ to (8.35) obeying

$$\eta_T < \bar{\eta}_{cross} < \eta_{cross}. \tag{8.36}$$

For the example $(\beta,\alpha) = (0.5,0.95)$ it is found that $\eta_{cross}(0.5,0.95) \approx 1.1855$ (Figure 8-4). The significance of $\bar{\eta}_{cross}$ is that

$$\begin{aligned}
&\lambda_{crit} - \lambda_1^F > \lambda_1^{F*} - \lambda_{crit}^* , \quad \text{if} \quad \pi l_2/2l_1 < \eta_T , \\
&\lambda_{crit} - \lambda_\infty > \lambda_1^{F*} - \lambda_{crit}^* , \quad \text{if} \quad \eta_T < \pi l_2/2l_1 < \bar{\eta}_{cross} , \\
&\lambda_{crit} - \lambda_\infty < \lambda_1^{F*} - \lambda_{crit}^* , \quad \text{if} \quad \pi l_2/2l_1 > \bar{\eta}_{cross} .
\end{aligned} \tag{8.37}$$

Thus if $(\beta,\alpha) \in \Gamma_{ii}^F$, $(\beta^*,\alpha^*) \in \Gamma_i^F$ and $\eta_{cross} > \eta_T$, then there exists a unique value $\bar{\eta}_{cross}$ obeying (8.35) and the optimal design is configuration-1 if $l_2/l_1 < 2\bar{\eta}_{cross}/\pi$, whereas the optimal design is configuration-2 if $l_2/l_1 > 2\bar{\eta}_{cross}/\pi$. The failure mode of the optimal design is m = 1 flexure only if either $0 < l_2/l_1 < 2\eta_T/\pi$ or $l_2/l_1 > 2\bar{\eta}_{cross}/\pi$, whereas the failure mode of the optimal design is the $m = \infty$ wrinkling mode if $2\eta_T/\pi < l_2/l_1 < 2\bar{\eta}_{cross}/\pi$. Note that η_{cross} plays no role in either the determination of the optimal design or in the determination of the failure mode in this case.

In order to treat this and similar cases in a systematic fashion,

note that $\lambda_1^F = \Phi_F(\pi l_2/2l_1,\beta,\alpha)$ and $\lambda_1^{F*} = \Phi_F^*(\pi l_2/2l_1,\beta,\alpha)$ provide upper bounds for λ_{crit} and λ_{crit}^* respectively. In order to obtain lower bounds one may introduce the modified functions $\bar{\Phi}_F$ and $\bar{\Phi}_F^*$ as follows

$$\bar{\Phi}_F(\eta,\beta,\alpha) = \max_{\eta}\{\, F(\eta) \mid F \text{ non-decreasing, } F(\eta) \le \Phi_F(\eta,\beta,\alpha)\},$$

$$\bar{\Phi}_F^*(\eta,\beta,\alpha) = \max_{\eta}\{\, F(\eta) \mid F \text{ non-decreasing, } F(\eta) \le \Phi_F^*(\eta,\beta,\alpha)\}. \tag{8.38}$$

These definitions ensure that $\bar{\Phi}_F(\cdot,\beta,\alpha)$ is the *lower monotone envelope* of $\Phi_F(\cdot,\beta,\alpha)$ and that $\bar{\Phi}_F^*(\cdot,\beta,\alpha)$ is the *lower monotone envelope* of $\Phi_F^*(\cdot,\beta,\alpha)$. The value $\bar{\Phi}_F(\pi l_2/2l_1,\beta,\alpha)$ and $\bar{\Phi}_F^*(\pi l_2/2l_1,\beta,\alpha)$ are ensured to be lower bounds for λ_{crit} and λ_{crit}^* by virtue of $(7.2)_1$, (8.10),(8.16), (8.17).

The definition of Φ_F simplifies in the event that $(\beta,\alpha) \in \Gamma_i^F \cup \Gamma_{ii}^F$. Namely

$$\bar{\Phi}_F(\eta,\beta,\alpha) = \Phi_F(\eta,\beta,\alpha), \qquad \text{if } (\beta,\alpha) \in \Gamma_i^F, \tag{8.39}$$

and

$$\bar{\Phi}_F(\eta,\beta,\alpha) = \begin{cases} \Phi_F(\eta,\beta,\alpha), & 0 < \eta \le \eta_T, \\ \lambda_\infty(\beta,\alpha). & \eta \ge \eta_T, \end{cases} \quad \text{if } (\beta,\alpha) \in \Gamma_{ii}^F. \tag{8.40}$$

Thus one obtains from (8.11) and (8.12) that

$$\lambda_{crit} = \bar{\Phi}_F(\pi l_2/2l_1,\beta,\alpha) \ , \quad \text{if } (\beta,\alpha) \in \Gamma_i^F \cup \Gamma_{ii}^F. \tag{8.41}$$

However if $(\beta,\alpha) \in \Gamma_{iii}^F$ then λ_{crit} might correspond to a failure mode other than $m = 1$ or $m = \infty$ and thus its precise determination is complicated by the finite spacing of the λ_m^F. One may only conclude that

$$\bar{\Phi}_F(\pi l_2/2l_1,\beta,\alpha) \le \lambda_{crit} \le \Phi_F(\pi l_2/2l_1,\beta,\alpha) \ , \quad \text{if } (\beta,\alpha) \in \Gamma_{iii}^F. \tag{8.42}$$

Counterparts to (8.39)-(8.42) will of course also hold for the appropriate conjugate functions and variables:

$$\bar{\Phi}_F^*(\eta,\beta,\alpha) = \Phi_F^*(\eta,\beta,\alpha) \ , \quad \text{if } (\beta^*,\alpha^*) \in \Gamma_i^F, \tag{8.43}$$

$$\bar{\Phi}_F^*(\eta,\beta,\alpha) = \begin{cases} \Phi_F^*(\eta,\beta,\alpha), & 0 < \eta \le \eta_T^* \ , \\ \lambda_\infty^*, & \eta \ge \eta_T^* \ , \end{cases} \quad \text{if } (\beta^*,\alpha^*) \in \Gamma_{ii}^F, \tag{8.44}$$

$$\lambda_{crit}^{*} = \bar{\Phi}_F^{*}(\pi l_2/2l_1,\beta,\alpha) \ , \quad \text{if } (\beta^*,\alpha^*) \in \Gamma_i^F \cup \Gamma_{ii}^F \ , \tag{8.45}$$

and

$$\bar{\Phi}_F^{*}(\pi l_2/2l_1,\beta,\alpha) \le \lambda_{crit}^{*} \le \Phi_F^{*}(\pi l_2/2l_1,\beta,\alpha), \quad \text{if } (\beta^*,\alpha^*) \in \Gamma_{iii}^F. \tag{8.46}$$

It now follows from (8.22), (8.23), and (8.38) that for each (β,α) obeying $0 < \alpha < 1$, $0 < \beta < 1$, there exists a unique $\bar{\eta}_{cross} > 0$ such that

$$\bar{\Phi}_F(\bar{\eta}_{cross},\beta,\alpha) = \bar{\Phi}_F^{*}(\bar{\eta}_{cross},\beta,\alpha) \ , \tag{8.47}$$

and

$$\begin{aligned} &\bar{\Phi}_F(\eta,\beta,\alpha) > \bar{\Phi}_F^{*}(\eta,\beta,\alpha) \ , \qquad \text{for } 0 < \eta < \bar{\eta}_{cross}, \\ &\bar{\Phi}_F(\eta,\beta,\alpha) < \bar{\Phi}_F^{*}(\eta,\beta,\alpha) \ , \qquad \text{for } \eta > \bar{\eta}_{cross}. \end{aligned} \tag{8.48}$$

Note that $\bar{\eta}_{cross} = \bar{\eta}_{cross}(\beta,\alpha)$, and that this value may or may not coincide with η_{cross}. In particular it is seen from the examples previously under consideration that $\bar{\eta}_{cross} = \eta_{cross}$ for $(\beta,\alpha) = (0.5,0.05)$ and $(\beta,\alpha) = (0.9,0.9)$, but that $\bar{\eta}_{cross} < \eta_{cross}$ for $(\beta,\alpha) = (0.5,0.95)$.

According to (8.20), (8.41), (8.45) and (8.48), configuration-1 and configuration-2 are equally optimal at the aspect ratio

$$l_2/l_1 = 2\bar{\eta}_{cross}(\beta,\alpha)/\pi \ , \tag{8.49}$$

for all cases in which $(\beta,\alpha) \in \Gamma_i^F \cup \Gamma_{ii}^F$ and $(\beta^*,\alpha^*) \in \Gamma_i^F \cup \Gamma_{ii}^F$. In view of (8.27), such points correspond to the union of regions-a,b, d and e in Figure 8-2. Furthermore, in all such cases, the optimal design is:

$$\text{configuration-1 if } l_2/l_1 < 2\bar{\eta}_{cross}/\pi \tag{8.50}$$

while the optimal design is

$$\text{configuration-2 if } l_2/l_1 > 2\bar{\eta}_{cross}/\pi. \tag{8.51}$$

Consequently if $(\beta,\alpha) \in \Gamma_i^F \cup \Gamma_{ii}^F$ *and* $(\beta^*,\alpha^*) \in \Gamma_i^F \cup \Gamma_{ii}^F$ *(regions a,b,d,e) then the optimal design for a plate which is relatively long in the direction of thrust* ($l_1 > l_2\pi/2\bar{\eta}_{cross}$) *is given by a configuration with the stiff material in the outer plies, however the optimal design for a plate which is relatively short in the direction of thrust* ($l_1 < l_2\pi/2\bar{\eta}_{cross}$) *is given by the configuration with the stiff material in the central ply.* The critical failure mode in these cases will be either $m = 1$ or $m = \infty$ and, as shown for the case $(\beta,\alpha) = (0.5,0.95)$, a transition in the failure mode of the optimal design, but not the optimal design itself, may occur at an aspect ratio other than $l_2/l_1 = 2\bar{\eta}_{cross}/\pi$. Of course in region-a the failure mode of the optimal design will always correspond to $m = 1$ flexure.

The remaining regions-c, f and g are interesting because either (8.42) or (8.46) have potential ramifications regarding the validity

of (8.50)-(8.51) as a prescription for the optimal design. Consider a point (β,α) in region-g, since according to (8.27) this region would seem to offer the most potential for pathological behavior. An example corresponding to this case occurs if $(\beta,\alpha)=(0.5,0.8)$, and the associated curves $\Phi_F(\eta,\beta,\alpha)$, $\bar{\Phi}_F(\eta,\beta,\alpha)$, $\Phi_F^*(\eta,\beta,\alpha)$ and $\bar{\Phi}_F^*(\eta,\beta,\alpha)$ are given in Figure 8-5. For $(\beta,\alpha) = (0.5,0.8)$, $\bar{\Phi}_F^*(\eta,\beta,\alpha)$ ceases to coincide with $\Phi_F^*(\eta,\beta,\alpha)$ only on $\eta > \eta_T^* \approx 2.7110$ and $\bar{\Phi}_F(\eta,\beta,\alpha)$ ceases to coincide with $\Phi_F(\eta,\beta,\alpha)$ only on $\eta_1 < \eta < \eta_2$ where $\eta_1 \approx 1.6216$ and $\eta_2 \approx 2.7919$. Here η_2 is the abscissa of a local minimum for $\Phi_F(\eta,\beta,\alpha)$ and η_1 is the unique value of η obeying $\eta < \eta_2$ such that $\Phi_F(\eta,\beta,\alpha) = \Phi_F(\eta_2,\beta,\alpha)$. Since $\bar{\Phi}_F^*(\eta,\beta,\alpha) > \Phi_F(\eta,\beta,\alpha)$ for $\eta_1 < \eta < \eta_2$, the upper bound property of $\Phi_F(\eta,\beta,\alpha)$ embodied in (8.42) in conjunction with (8.46) ensures that configuration-2 is the optimal design for $\eta_1 < \pi l_2/2l_1 < \eta_2$. Since this is the only interval in η for which the optimal design was in doubt, it follows that (8.50)-(8.51) remains the correct prescription for the optimal design in the particular example $(\beta,\alpha) = (0.5, 0.8)$.

The prescription given in (8.50)-(8.51) can only fail for (β,α) in region-g if the function $\bar{\Phi}_F^*(\eta,\beta,\alpha)$ "cuts" the function $\bar{\Phi}_F(\eta,\beta,\alpha)$ at a value of η at which $\bar{\Phi}_F(\eta,\beta,\alpha)$ does not coincide with $\Phi_F(\eta,\beta,\alpha)$. The same conclusion holds for region-f. Analytically this gives

$$\Phi_F(\bar{\eta}_{cross},\beta,\alpha) \neq \bar{\Phi}_F(\bar{\eta}_{cross},\beta,\alpha) = \bar{\Phi}_F^*(\bar{\eta}_{cross},\beta,\alpha), \tag{8.52}$$

as the only condition which could lead to (8.50)-(8.51) becoming an incorrect prescription for the optimal design whenever (β,α) is in either region-f or region-g. Similarly if

$$\Phi_F^*(\bar{\eta}_{cross},\beta,\alpha) \neq \bar{\Phi}_F^*(\bar{\eta}_{cross},\beta,\alpha) = \bar{\Phi}_F(\bar{\eta}_{cross},\beta,\alpha), \qquad (8.53)$$

for (β,α) in region-c, then (8.50)-(8.51) could also be an incorrect prescription for the optimal design. If either (8.52) or (8.53) occurs, then the finite spacing of the failure thrusts λ_m^F and λ_m^{F*} must be taken into consideration and the failure mode may occur for a finite value of m other than m = 1. However, this investigation has yet to find an explicit example in which this state of affairs takes place.

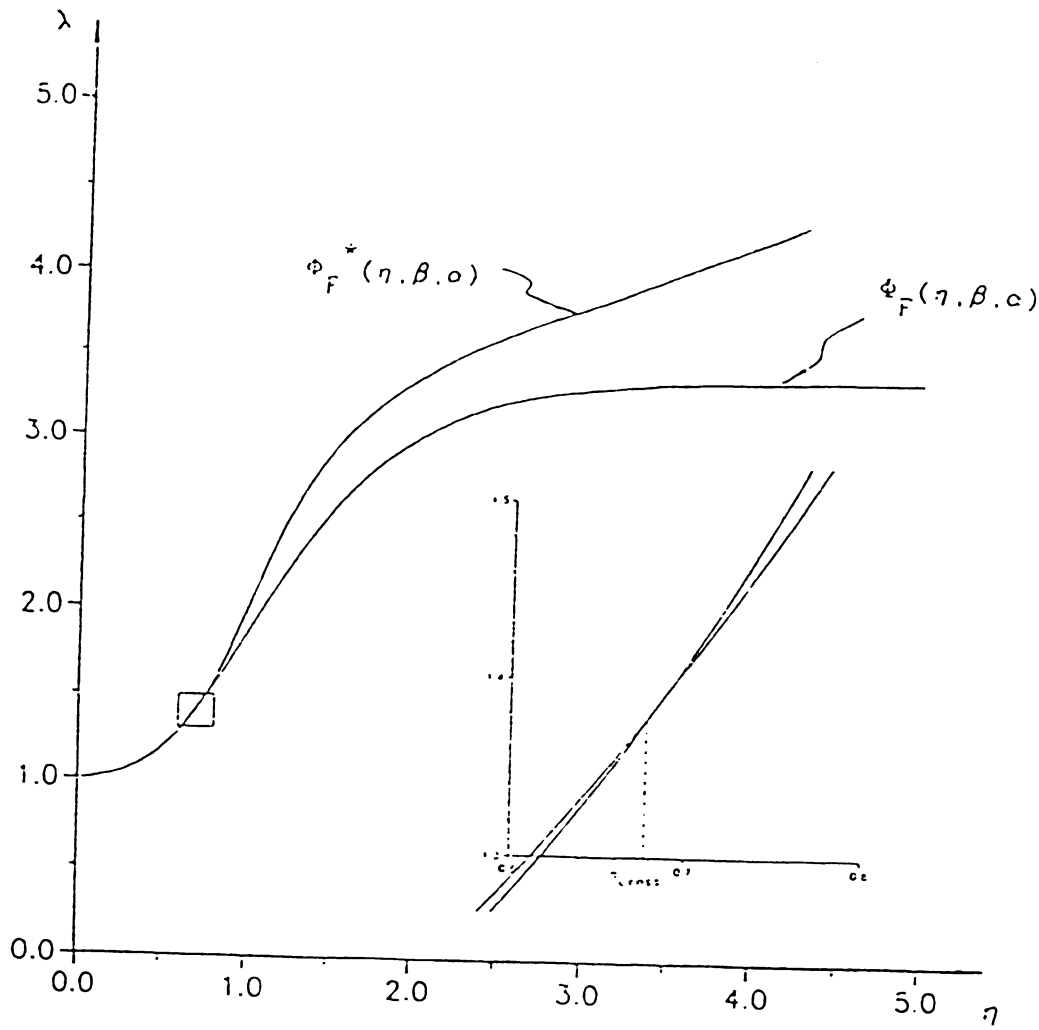

FIGURE 8-1

Figure 8-1:

The functions $\Phi_F(\eta,\beta,\alpha)$ and $\Phi_{F^*}(\eta,\beta,\alpha)$ for $(\beta,\alpha) = (0.5,0.05)$. Here $(\beta,\alpha) \in \Gamma_1^F$, $(\beta^*,\alpha^*) \in \Gamma_1^F$ and $\eta_{cross} = 0.6771$. The prescription for the optimal design is thus given by (8.25) and (8.26).

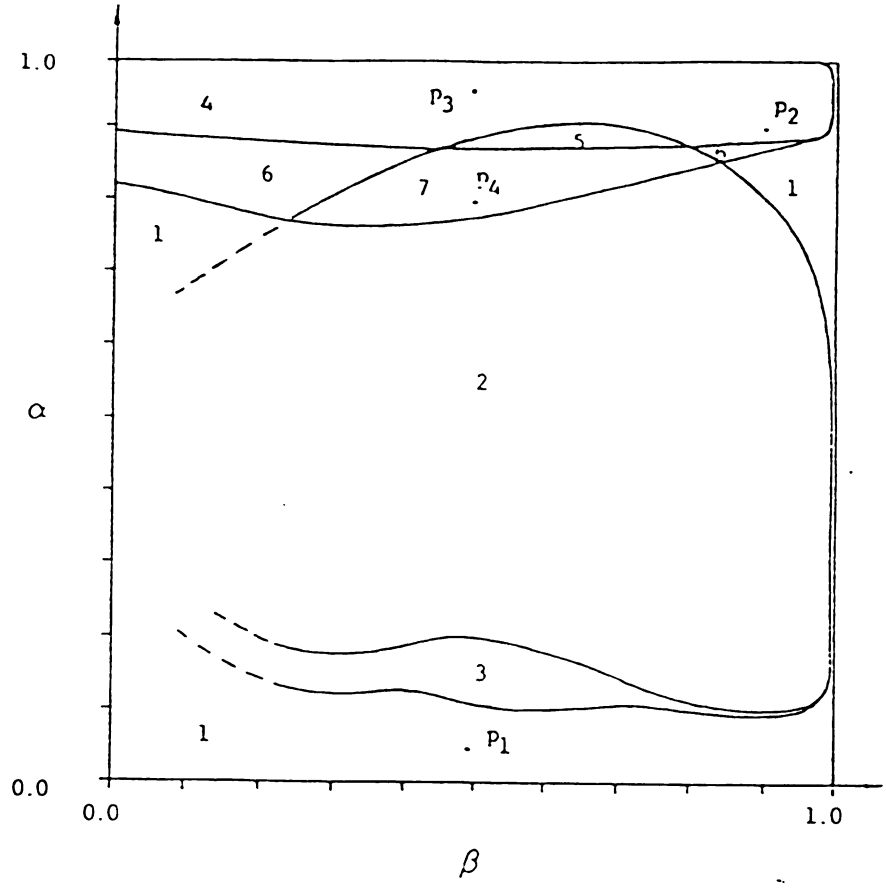

Figure 8-2:

The nature of the pairs (β,α) and (β^*,α^*) for $0 < \beta < 1$, $0 < \alpha < 1$ correspond to the region type as given in (8.27). The solids lines in this square are determined numerically, and the dashed lines are a possible extrapolation. The points P_1, P_2, P_3, P_4 correspond to Figure 8-1, 8-3, 8-4 and 8-5 respectively.

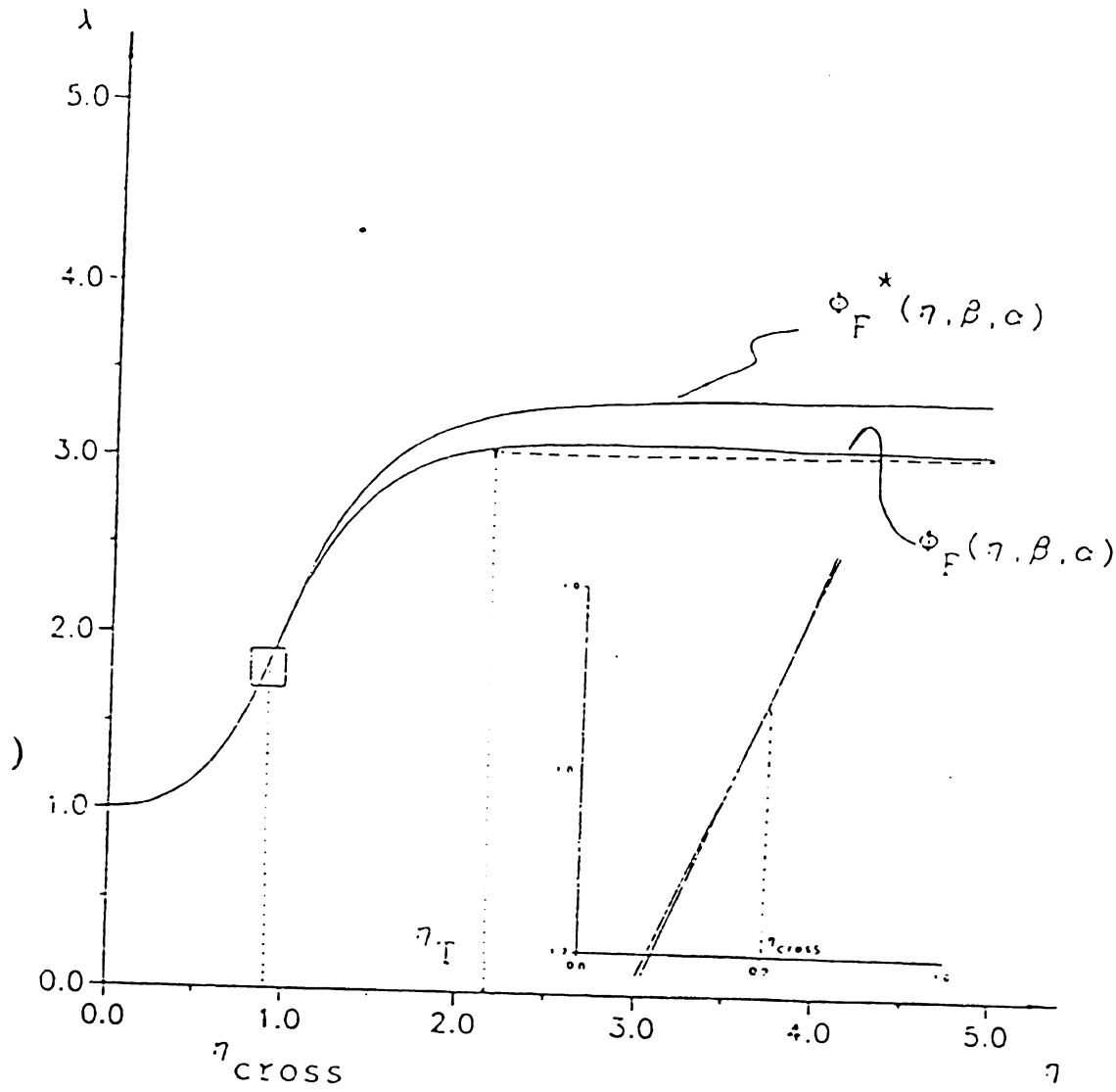

Figure 8-3:

The functions $\Phi_F(\eta,\beta,\alpha)$ and $\Phi_{F*}(\eta,\beta,\alpha)$ for $(\beta,\alpha) = (0.9,0.9)$. Here $(\beta,\alpha) \in \Gamma_{ii}^F$. $(\beta^*,\alpha^*) \in \Gamma_i^F$ and $\eta_T = 2.1660 > 0.9009 = \eta_{cross}$. The functions $\Phi_F(\eta,\beta,\alpha)$ where it differs from $\Phi_F(\eta,\beta,\alpha)$ is given by the dashed line.

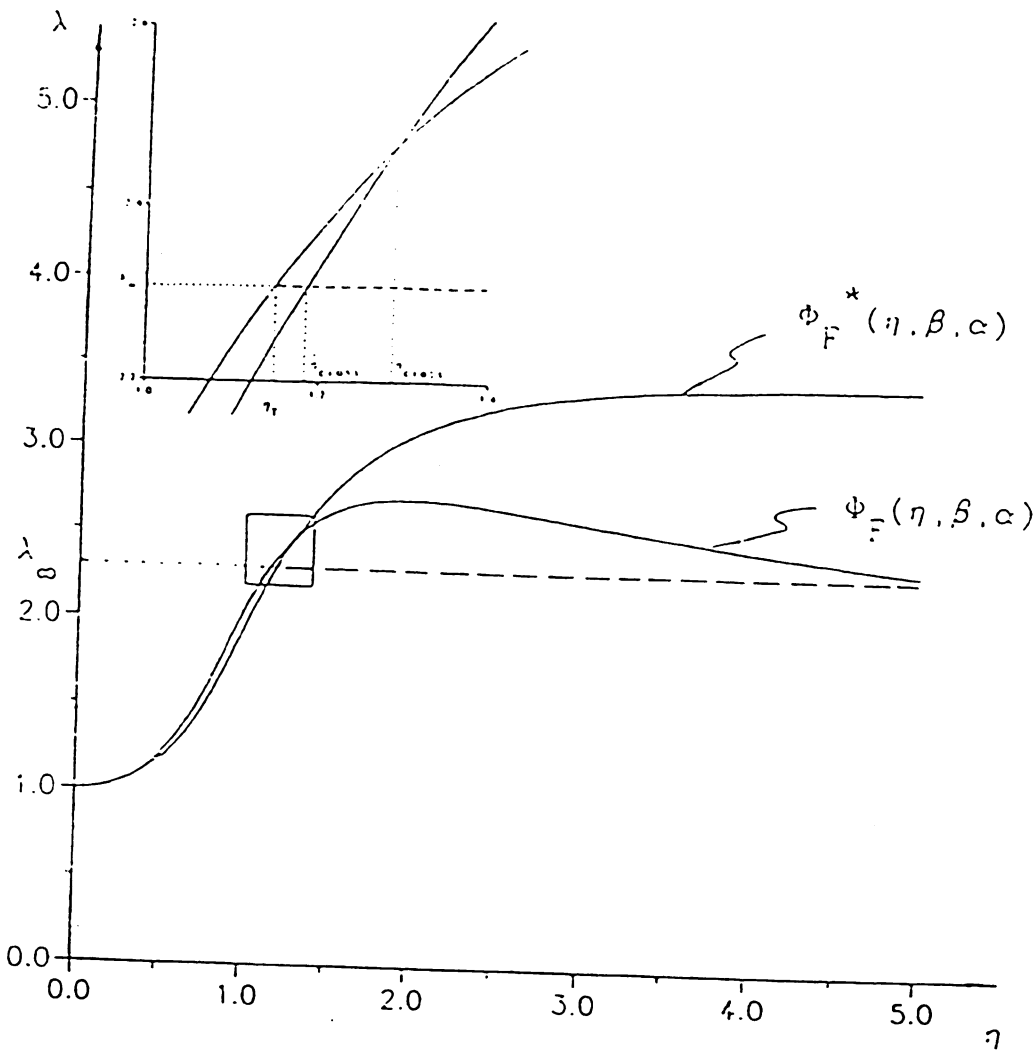

Figure 8-4:

The functions $\Phi_F(\eta,\beta,\alpha)$ and $\Phi_{F*}(\eta,\beta,\alpha)$ for $(\beta,\alpha) = (0.5,0.95)$. Here $(\beta,\alpha) \in \Gamma_{ii}^{F}$, $(\beta^*,\alpha^*) \in \Gamma_i^F$ and $\eta_{cross} \approx 1.2884 > 1.1505 \approx \eta_T$ and $\dot{\eta}_{cross} \approx 1.1855$. The functions $\dot{\Phi}_F(\eta,\beta,\alpha)$ where it differs from $\Phi_F(\eta,\beta,\alpha)$ is given by the dashed line.

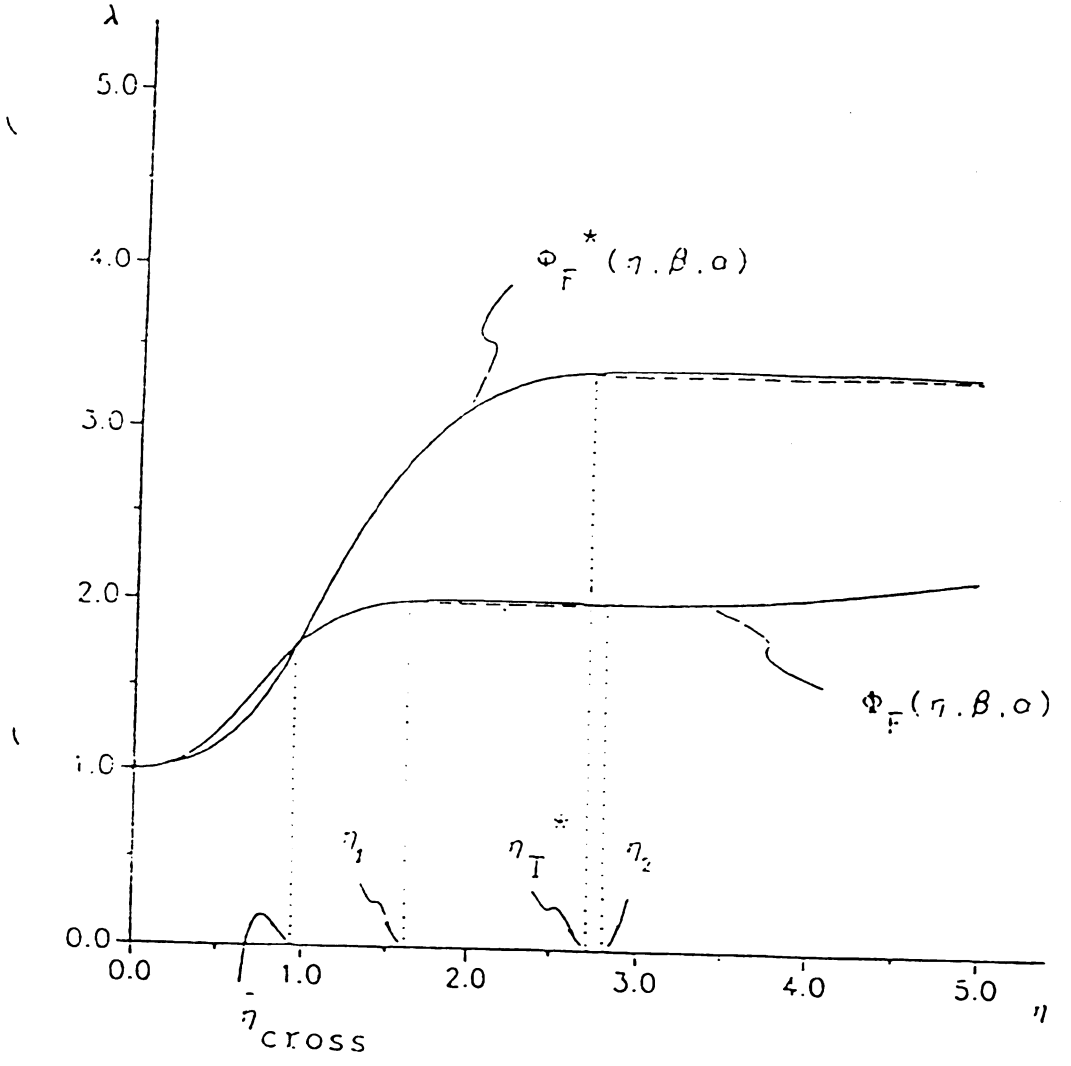

Figure 8-5:

The functions $\Phi_F(\eta,\beta,\alpha)$ and $\Phi_{F*}(\eta,\beta,\alpha)$ for $(\beta,\alpha) = (0.5,0.8)$. Here $(\beta,\alpha) \in \Gamma_{iii}^{F}$. $(\beta^*,\alpha^*) \in \Gamma_{ii}^{F}$. A local minimum of $\Phi_F(\eta,\beta,\alpha)$ occurs at $\eta_2 = 2.7919$ an $\dot{\Phi}_F(\eta,\beta,\alpha)$ differs from $\Phi_F(\eta,\beta,\alpha)$ only on $\eta_1 < \eta < \eta_2$ as shown by the dashed line segment. Similarly $\dot{\Phi}_F^{*}(\eta,\beta,\alpha)$ differs from $\Phi_F^{*}(\eta,\beta,\alpha)$ only on $\eta > \eta_T^{*} = 2.7110$ as shown by the dashed line. It is found that $\eta_{cross} - \dot{\eta}_{cross} = 0.9439$ and $\eta_1 = 1.6216$.

	β^*=-5.0	β^*=-4.5	β^*=-4.0	β^*=-3.5	β^*=-3.0	β^*=-2.5	β^*=-2.0	β^*=-1.5	β^*=-1.1	
α=0.9	1.5994	1.5417	1.4767	1.4016	1.3148	1.2153	1.1074	.9924	.8974	α^*=0.1
α=0.8	1.1821	1.1659	1.1400	1.1066	1.0623	.9900	.9439	.8774	.8238	α^*=0.2
α=0.7	.9682	.9635	.9564	.9422	.9253	.9018	.8604	.8210	.7960	α^*=0.3
α=0.6	.8354	.8392	.8414	.8409	.8368	.8275	.8132	.7941	.7667	α^*=0.4
α=0.5	.7400	.7500	.7612	.7699	.7750	.7787	.7758	.7655	.7556	α^*=0.5
α=0.4	.6667	.6808	.7077	.7129	.7261	.7373	.7471	.7534	.7588	α^*=0.6
α=0.3	.6039	.6186	.6357	.6585	.6833	.7099	.7277	.7500	.7714	α^*=0.7
α=0.2	.5357	.5560	.5857	.6117	.6342	.6719	.7123	.7513	8039	α^*=0.8
α=0.1	.4800	.5059	.5238	.5529	.6029	.6320	.6974	.7571	8400	α^*=0.9
	β=-.200	β=-.222	β=-.250	β=-.286	β=-.333	β=-.400	β=-.500	β=-.606	β=-.909	

Table 8-1:

Values of the crossover value function $\eta_{cross}(\beta,\alpha)$. The conjugate pairs (β^*,α^*) are also shown.

APPENDICES

APPENDIX A

APPENDIX A: VERIFICATION OF (4.45)

Throughout this appendix it is assumed that $\lambda > 0$, $\lambda \neq 1$, $\Omega > 0$. The goal is to prove that

$$\Omega_2^{(I)} < \Omega_2^{(II)} < \Omega_1^{(II)} < \Omega_1^{(I)}, \quad \text{if} \quad 0 < A_{II} < A_I .$$

Proof:

(i) $\Omega_2^{(II)} \leq \Omega_1^{(II)}$,

since

$$(\Omega_2^{(II)})^2 - (\Omega_1^{(II)})^2 =$$

$$= \Omega^2 \{[1+\lambda^2+(1-\lambda)^2 A_{II}] - [(1+\lambda^2+(1-\lambda)^2 A_{II})^2 - 4\lambda^2]^{1/2}\}/2 -$$

$$- \Omega^2 \{[1+\lambda^2+(1-\lambda)^2 A_{II}] + [(1+\lambda^2+(1-\lambda)^2 A_{II})^2 - 4\lambda^2]^{1/2}\}/2 =$$

$$= -\Omega^2 \{[(1+\lambda^2+(1-\lambda)^2 A_{II})^2 - 4\lambda^2]^{1/2}\}$$

$$= -\Omega^2 \{[(1-\lambda)^2 + 2(1+\lambda^2)(1-\lambda)^2 A_{II} + (1-\lambda)^4 A_{II}^2]^{1/2}\} < 0$$

(ii) $\Omega_1^{(II)} < \Omega_1^{(I)}$,

since

$$(\Omega_1^{(II)})^2 - (\Omega_1^{(I)})^2 = (\Omega^2/2) \{ (1-\lambda)^2 (A_{II} - A_I) +$$

$$+ [(1+\lambda^2+A_{II}(1-\lambda)^2)^2 - 4\lambda^2]^{1/2} - [(1+\lambda^2+A_I(1-\lambda)^2)^2 - 4\lambda^2]^{1/2} \} < 0 .$$

(iii) $\Omega_2^{(I)} < \Omega_2^{(II)}$,

Set

$$G(y) = \Omega^2\{[1+\lambda^2+(1-\lambda)^2y]-[(1+\lambda^2+(1-\lambda)^2y)^2-4\lambda^2]^{1/2}\}/2. \tag{A1}$$

Note that $G(A_k) = (\Omega_2^{(k)})^2$, k = I,II. It is found that G(y) is strictly decreasing in y by the following

$$G'(y) =$$

$$= \Omega^2\{(1-\lambda)^2-[(1+\lambda^2+(1-\lambda)^2y)^2-4\lambda^2]^{-1/2}(1+\lambda^2+(1-\lambda)^2y)(1-\lambda)^2\}/2$$

$$= \Omega^2(1-\lambda)^2\left[1 - \frac{(1+\lambda^2+(1-\lambda)^2y)}{(1+\lambda^2+(1-\lambda)^2y)^2-4\lambda^2]^{1/2}}\right]. \tag{A2}$$

Since the second part inside of the bracket on the right hand side in (A2) is strictly greater than one, it follows that

$$G'(y) < 0. \tag{A3}$$

This gives rise to

$$G(A_{II}) > G(A_I), \quad \text{if} \quad A_I > A_{II}. \tag{A4}$$

Therefore it is concluded that

$$\Omega_2^{(II)} > \Omega_2^{(I)} . \qquad \square$$

APPENDIX B

APPENDIX B: THE RELATION OF L_n AND M_n (n=1,2) FOR NON-COMPOSITE CASE

For the non-composite case $\mu^{(I)} = \mu^{(II)} = \mu$ and $A_I = A_{II} = A$. Note that in general the results in this appendix shall be developed for general value of A, not necessarily equal to zero. Therefore, from (4.35) and (4.47), it follows

$$(L_1^{(1)}, L_2^{(1)}, M_1^{(1)}, M_2^{(1)}) =$$

$$= (L_1^{(2)}, L_2^{(2)}, M_1^{(2)}, M_2^{(2)}) =$$

$$= (L_1^{(3)}, L_2^{(3)}, M_1^{(3)}, M_2^{(3)}) =$$

$$= (L_1, L_2, M_1, M_2) . \tag{B1}$$

Consider the flexural case so that $(6.11)_2$ gives $L_2 = M_2 = 0$. Now $(4.33)_1$ and (4.34) once again yields

$$\left.\begin{aligned} &(\Omega_1^2+\lambda^2\Omega^2)\cosh(\Omega_1 l_2)L_1 + (\Omega_2^2+\lambda^2\Omega^2)\cosh(\Omega_2 l_2)M_1 = 0, \\ &\Omega_1[(2+\lambda^{-2}+(1-\lambda^{-1})^2 A)\lambda^2\Omega^2-\Omega_1^2]\sinh(\Omega_1 l_2)L_1 + \\ &\quad + \Omega_2[(2+\lambda^{-2}+(1-\lambda^{-1})^2 A)\lambda^2\Omega^2-\Omega_2^2]\sinh(\Omega_2 l_2)M_1 = 0 . \end{aligned}\right\} \tag{B2}$$

Now using (4,36), it follows that

$$\Omega_1[(2+\lambda^{-2}+(1-\lambda^{-1})^2A)\lambda^2\Omega^2-\Omega_1^2] =$$

$$= \Omega_1\{ (2+\lambda^{-2}+(1-\lambda^{-1})^2A)\lambda^2\Omega^2 -$$

$$- (\Omega^2/2)[1+\lambda^2+(1-\lambda)^2A] - (\Omega^2/2)[(1+\lambda^2+(1-\lambda)^2A)^2-4\lambda^2]^{1/2} \} =$$

$$= \Omega_1\{ (\Omega^2/2)[4\lambda^2+2+2(1-\lambda)^2A-1-\lambda^2-(1-\lambda)^2A] -$$

$$- (\Omega^2/2)[(1+\lambda^2+(1-\lambda)^2A)^2-4\lambda^2]^{1/2} \} =$$

$$= \Omega_1\{ (\Omega^2/2)[3\lambda^2+1+(1-\lambda)^2A] - (\Omega^2/2)[(1+\lambda^2+(1-\lambda)^2A)^2-4\lambda^2]^{1/2} \} =$$

$$= \Omega_1\{ (\Omega^2/2)[1+\lambda^2+(1-\lambda)^2A]-(\Omega^2/2)[(1+\lambda^2+(1-\lambda)^2A)^2-4\lambda^2]^{1/2}+\lambda^2\Omega^2\}=$$

$$= \Omega_1 (\Omega_2^2 + \lambda^2\Omega^2) . \qquad \text{(B3)}$$

One obtains in a similar fashion using (4,36), that

$$\Omega_2[(2+\lambda^{-2}+(1-\lambda^{-1})^2A)\lambda^2\Omega^2-\Omega_2^2] =$$

$$= \Omega_2 (\Omega_1^2 + \lambda^2\Omega^2) . \qquad \text{(B4)}$$

Substituting from (B3), (B4) into $(B2)_2$ now yields

$$\Omega_1(\Omega_2^2+\lambda^2\Omega^2)\sinh(\Omega_1 l_2)L_1 + \Omega_2(\Omega_1^2+\lambda^2\Omega^2)\sinh(\Omega_2 l_2)M_1 = 0. \qquad \text{(B5)}$$

Note that (B5) is independent of the constant A. Equations $(B2)_1$ and (B5) therefore give

$$\left.\begin{aligned} \frac{\Omega_1^2 + \lambda^2\Omega^2}{\Omega_2^2 + \lambda^2\Omega^2} &= -\frac{\cosh(\Omega_2 l_2)\, M_1}{\cosh(\Omega_1 l_2)\, L_1} \\ \frac{\Omega_1^2 + \lambda^2\Omega^2}{\Omega_2^2 + \lambda^2\Omega^2} &= -\frac{\Omega_1 \sinh(\Omega_1 l_2)\, L_1}{\Omega_2 \sinh(\Omega_2 l_2)\, M_1} \end{aligned}\right\} , \tag{B6}$$

which, in turn, gives rise to

$$\frac{\tanh(\Omega_1 l_2)}{\tanh(\Omega_2 l_2)} = \left[\frac{\Omega_1^2 + \lambda^2\Omega^2}{\Omega_2^2 + \lambda^2\Omega^2} \right]^2 \frac{\Omega_2}{\Omega_1} , \tag{B7}$$

and the relation of unknown constants L_1 and M_1 is

$$\frac{L_1}{M_1} = -\frac{\Omega_2^2 + \lambda^2\Omega^2}{\Omega_1^2 + \lambda^2\Omega^2} \times \frac{\cosh(\Omega_2 l_2)}{\cosh(\Omega_1 l_2)} . \tag{B8}$$

Likewise, for the barrelling case ($L_1 = M_1 = 0$), one finds

$$\frac{\tanh(\Omega_2 l_2)}{\tanh(\Omega_1 l_2)} = \left[\frac{\Omega_1^2 + \lambda^2\Omega^2}{\Omega_2^2 + \lambda^2\Omega^2} \right]^2 \frac{\Omega_2}{\Omega_1} , \tag{B9}$$

and the relation of unknown constants L_2 and M_2 is

$$\frac{L_2}{M_2} = -\frac{\Omega_2^2 + \lambda^2\Omega^2}{\Omega_1^2 + \lambda^2\Omega^2} \times \frac{\sinh(\Omega_2 l_2)}{\sinh(\Omega_1 l_2)} . \tag{B10}$$

These are the same results obtained by Sawyers and Rivlin, that is equations (B7), (B8), (B9) and (B10) are the same as (4.21), (4.25), (4.20) and (4.24) of [10].

APPENDIX C

APPENDIX C: COMPUTER PROGRAMS

(I)

PROGRAM FLEXURE1

```
C
C     FOR A GIVEN COMPOSITE CONSTRUCTION CHARACTERIZED BY (BETA,ALPHA),
C     AND A CIVEN VALUE OF ETA, THIS PROGRAM DETERMINES THE VALUE OF
C     LAMBDA THAT LIES ON THE FLEXURE CURVE
C
      CHARACTER ANS*1
      REAL*8    M(6,6)
      REAL*8    LEMBDA, LMD1, LMD2, LMD
      INTEGER*2 IPVT(6), NOUT
      REAL*8    DET1, DET2, FAC(6,6)
      REAL*8    EPS, ETA, BETA, R, DET
C
      OPEN(6, FILE='DATAOUT', STATUS='NEW')
C     INPUT
10    PRINT*, 'INPUT THE RATIO OF MATERIAL PROPERTIES BETA:'
      READ(5,*) BETA
      PRINT*, 'INPUT THE RATIO OF DEMENSION ALPHA:'
      READ(5,*) R
      PRINT*, 'INPUT THE BUCKLING WAVE PARAMETER ETA:'
      READ(5,*) ETA
C
C     THE ROOT IS FOUND BY A SIMPLE BISECTOR ROUTINE AND MUST BE
C     BETWEEN PRESET INITIAL VALUES OF LMD1 AND LMD2.
C
C     INITIALIZE STEP
C
      LMD1=1.001
      LMD2=6.9
      EPS=0.000000001
C
C     LOOP THROUGH A SEQUENCE OF BISECTIONS
C
100   CONTINUE
      LMD=(LMD1+LMD2)*0.5
      LEMBDA=LMD
      CALL GETARRAY (LEMBDA, ETA, BETA, R, M)
      CALL DLFTRG (6, M, 6, FAC, 6, IPVT)
C
C     COMPUTE THE DETERMINANT USING THE SYSTEM SOFTWARE ROUTINE DLFDRG
C
      CALL DLFDRG (6, FAC, 6, IPVT, DET1, DET2)
      DET=-(DET1*10.0**DET2)
C
C     CHECK WHETHER WE INDEED HAVE A ROOT
```

```
C
      IF ( ABS(DET) .LE. EPS ) THEN
120      PRINT*, 'THE BUCKLING STRETCHING LEMBDA IS:'
         PRINT*, LMD
         WRITE(6,*) ETA, LMD
         PRINT*, 'DO YOU WANT TO GET ANOTHER LEMBDA BY ENTERING NEW',
     +           'SET OF ETA, BETA, ALPHA, ANSWER Y OR N.'
         READ(5,'(A1)') ANS
         IF (ANS .NE. 'N' .AND. ANS .NE. 'n') THEN
            GOTO 10
         ELSE
            GOTO 999
         END IF
      ELSE IF (DET .LT. 0.) THEN
         LMD1=LMD
         GOTO 100
      ELSE
C        (DET .GT. 0.)
         LMD2=LMD
         IF (LMD2-LMD1 .LT. EPS) THEN
            GOTO 120
         END IF
         GOTO 100
      END IF
      CLOSE(6)
999   STOP
      END
C
C
C
            SUBROUTINE GETARRAY (LEMBDA, ETA, BETA, R, M)
      REAL*8    M(6,6), INVLMD, LEMBDA, ETA, BETA, R
      REAL*8    T1, T2, T3, T4, C1, C2, C3, C4, S1, S2, S3, S4
      T1=ETA
      T2=LEMBDA*ETA
      T3=LEMBDA*ETA*R
      T4=ETA*R
      S1=SINH(T1)
      C1=COSH(T1)
      S1=SINH(T1)
      C1=COSH(T1)
      S2=SINH(T2)
      C2=COSH(T2)
      S3=SINH(T3)
      C3=COSH(T3)
      S4=SINH(T4)
      C4=COSH(T4)
      INVLMD=1.0/LEMBDA
      M(1,1)=2.0*LEMBDA*C2
      M(1,2)=-2.0*LEMBDA*S2
      M(1,3)=(INVLMD+LEMBDA)*C1
      M(1,4)=-(INVLMD+LEMBDA)*S1
      M(1,5)=0.0
      M(1,6)=0.0
```

```
      M(2,1)=-(INVLMD+LEMBDA)*S2
      M(2,2)=(INVLMD+LEMBDA)*C2
      M(2,3)=-2.0*S1
      M(2,4)=2.0*C1
      M(2,5)=0.0
      M(2,6)=0.0
      M(3,1)=-C3
      M(3,2)=S3
      M(3,3)=-C4
      M(3,4)=S4
      M(3,5)=C3
      M(3,6)=C4
      M(4,1)=LEMBDA*S3
      M(4,2)=-LEMBDA*C3
      M(4,3)=S4
      M(4,4)=-C4
      M(4,5)=-LEMBDA*S3
      M(4,6)=-S4
      M(5,1)=-4.0*LEMBDA*C3
      M(5,2)=4.0*LEMBDA*S3
      M(5,3)=-2.0*(INVLMD+LEMBDA)*C4
      M(5,4)=2.0*(INVLMD+LEMBDA)*S4
      M(5,5)=4.0*BETA*LEMBDA*C3
      M(5,6)=2.0*BETA*(INVLMD+LEMBDA)*C4
      M(6,1)=2.0*(INVLMD+LEMBDA)*S3
      M(6,2)=-2.0*(INVLMD+LEMBDA)*C3
      M(6,3)=4.0*S4
      M(6,4)=-4.0*C4
      M(6,5)=-2.0*BETA*(INVLMD+LEMBDA)*S3
      M(6,6)=-4.0*BETA*S4
      RETURN
      END
```

(II)

```
                    PROGRAM FLEXURE2


C
C     FOR A GIVEN COMPOSITE CONSTRUCTION CHARACTERIZED BY (BETA,ALPHA),
C     THIS PROGRAM DETERMINES A SET OF ORDERED PAIR (ETA,LAMBDA) THAT
C     LIES ON THE FLEXURE CURVE
C
      CHARACTER ANS*1
      REAL*8    M(6,6)
      REAL*8    LEMBDA, LMD1, LMD2, LMD
      INTEGER*2 IPVT(6), NOUT
      REAL*8    DET1, DET2, FAC(6,6)
      REAL*8    EPS, ETA, BETA, R, DET, ETAI, ETAF, ETASTP
C
```

```
      OPEN(6, FILE='DATAOUT', STATUS='NEW')
C     INPUT
      PRINT*, 'INPUT THE RATIO OF MATERIAL PROPERTIES BETA:'
      READ(5,*) BETA
      PRINT*, 'INPUT THE RATIO OF DEMENSION ALPHA:'
      READ(5,*) R
      PRINT*, 'WHAT IS THE INITIAL VALUE OF ETA:'
      READ(5,*) ETAI
      PRINT*, 'WHAT IS THE FINAL VALUE OF ETA:'
      READ(5,*) ETAF
      PRINT*, 'WHAT IS THE STEP SIZE FOR ETA:'
      READ(5,*) ETASTP
      ETA=ETAI-ETASTP
C
50    CONTINUE
      ETA=ETA+ETASTP
      IF (ETA.GT.ETAF) GOTO 900
C
C     THE ROOT IS FOUND BY A SIMPLE BISECTOR ROUTINE AND MUST BE
C     BETWEEN PRESET INITIAL VALUES OF LMD1 AND LMD2.
C
C     INITIALIZE STEP
C
      LMD1=1.001
      LMD2=6.9
      EPS=0.000000001
C
C     LOOP THROUGH A SEQUENCE OF BISECTIONS
C
100   CONTINUE
      LMD=(LMD1+LMD2)*0.5
      LEMBDA=LMD
      CALL GETARRAY (LEMBDA, ETA, BETA, R, M)
      CALL DLFTRG (6, M, 6, FAC, 6, IPVT)
C
C     COMPUTE THE DETERMINANT USING THE SYSTEM SOFTWARE ROUTINE DLFDRG
C
      CALL DLFDRG (6, FAC, 6, IPVT, DET1, DET2)
      DET=-(DET1*10.0**DET2)
      IF (ABS(DET) .LT. EPS) THEN
120      PRINT*,LMD
         WRITE(6,*) ETA, LMD
         GOTO 50
      ELSE IF (DET .LT. 0.) THEN
         LMD1=LMD
         GOTO 100
      ELSE
C        (DET .GT. 0.)
         LMD2=LMD
         IF (LMD2-LMD1 .LT. EPS) THEN
            GOTO 120
         END IF
         GOTO 100
      END IF
```

```
900   CONTINUE
      CLOSE(6)
999   STOP
      END
C
C
C
C           SUBROUTINE GETARRAY (LEMBDA, ETA, BETA, R, M)
C           (See (I))
```

(III)

PROGRAM FLEXURE3

```
C
C     FOR A GIVEN COMPOSITE CONSTRUCTION CHARACTERIZED BY (BETA,ALPHA),
C     THIS PROGRAM DETERMINES THE FLEXURE REGION TYPE
C
      REAL*8     X(50), Y(50)
      REAL*8     M(6,6)
      REAL*8     LEMBDA, LMD1, LMD2
      INTEGER*2 IPVT(6), NOUT
      REAL*8     DET1, DET2, FAC(6,6)
      REAL*8     EPS, ETA, BETA, R, DET, ETAI, ETASTP
C
      LOGICAL DECR, INCR
C
      DECR=.FALSE.
      INCR=.FALSE.
C     INPUT
      PRINT*, 'INPUT THE RATIO OF MATERIAL PROPERTIES BETA:'
      READ(5,*) BETA
      PRINT*, 'INPUT THE RATIO OF DEMENSION ALPHA:'
      READ(5,*) R
      PRINT*, 'WHAT IS THE INITIAL VALUE OF ETA:'
      READ(5,*) ETAI
      PRINT*, 'WHAT IS THE STEP SIZE FOR ETA:'
      READ(5,*) ETASTP
C
      DO 900  K=1,50
C
      X(K)=ETAI+(K-1)*ETASTP
C
C     THE ROOT IS FOUND BY A SIMPLE BISECTOR ROUTINE AND MUST BE
C     BETWEEN PRESET INITIAL VALUES OF LMD1 AND LMD2.
C
C     INITIALIZE STEP
C
      LMD1=1.001
```

```
      LMD2=6.9
      EPS=0.000000001
C
C     LOOP THROUGH A SEQUENCE OF BISECTIONS
C
100   CONTINUE
      Y(K)=(LMD1+LMD2)*0.5
      LEMBDA=Y(K)
      ETA=X(K)
      CALL GETARRAY (LEMBDA, ETA, BETA, R, M)
      CALL DLFTRG (6, M, 6, FAC, 6, IPVT)
C
C     COMPUTE THE DETERMINANT USING THE SYSTEM SOFTWARE ROUTINE DLFDRG
C
      CALL DLFDRG (6, FAC, 6, IPVT, DET1, DET2)
      DET=-(DET1*10.0**DET2)
C
      CHECK WHETHER WE INDEED HAVE A ROOT
C
      IF (ABS(DET) .LT. EPS) THEN
         GOTO 890
      ELSE IF (DET .LT. 0.) THEN
         LMD1=Y(K)
         GOTO 100
      ELSE
C        (DET .GT. 0.)
         LMD2=Y(K)
         IF (LMD2-LMD1 .LT. EPS) THEN
            GOTO 890
         END IF
         GOTO 100
      END IF
890   CONTINUE
      PRINT*, X(K), Y(K)
900   CONTINUE
C
      DO 920  J=2,50
C
C     WE NOW ASSUME THAT THERE IS NO FALSE DROP AT THE BEGINING
C
      IF (Y(J-1) .GT. Y(J)) DECR=.TRUE.
C
C     DECR IS SET EQUAL TO TRUE IF THE FLEXURE CURVE EXHIBITS A
C     DECREASE
C
C     ONCE DECR IS SET EQUAL TO TRUE, IT IS NEVER CHANGED
C
      IF (DECR .AND. Y(J-1) .LT. Y(J)) INCR=.TRUE.
C
C     INCR IS SET EQUAL TO TRUE IF THE FLEXURE CURVE EXHIBITS AN
C     INCREASE AFTER THE DECR, i.e. A SECOND INCREASE
C
920   CONTINUE
C
```

```
      IF (INCR) THEN
         PRINT*, 'GAMMA3F'
      ELSE IF (DECR) THEN
         PRINT*, 'GAMMA2F'
      ELSE
         PRINT*, 'GAMMA1F'
      END IF
999   STOP
      END
C
C
C
C           SUBROUTINE GETARRAY (LEMBDA, ETA, BETA, R, M)
C           (See (I))
```

(IV)

PROGRAM FLEXURE4

```
C
C     FOR A GIVEN VALUE ALPHA, THIS PROGRAM DETERMINES THE FLEXURE
C     REGION TYPE FOR A SEQUENCE OF BETA
C
      REAL*8     X(50), Y(50)
      REAL*8     M(6,6)
      REAL*8     LEMBDA, LMD1, LMD2
      INTEGER*2 IPVT(6), NOUT
      REAL*8     DET1, DET2, FAC(6,6)
      REAL*8     EPS, ETA, BETA, R, DET, BETAI, BETAF,BETASTP
C
      LOGICAL DECR, INCR
C
      OPEN (6, FILE='DATAOUT', STATUS='NEW')
C     INPUT
      PRINT*, 'INPUT THE RATIO OF DEMENSION ALPHA:'
      READ(5,*) R
      PRINT*, 'WHAT IS THE INITIAL VALUE OF BETA:'
      READ(5,*) BETAI
      PRINT*, 'WHAT IS THE FINAL VALUE OF BETA:'
      READ(5,*) BETAF
      PRINT*, 'WHAT IS THE STEP SIZE FOR BETA:'
      READ(5,*) BETASTP
C
      BETA=BETAI-BETASTP
50    CONTINUE
      BETA=BETA+BETASTP
      IF (BETA .GT. BETAF) GOTO 999
      DECR=.FALSE.
```

```
      INCR=.FALSE.
C
      DO 900  K=1,50
C
      X(K)=0.1+(K-1)*0.1
C
C     THE ROOT IS FOUND BY A SIMPLE BISECTOR ROUTINE AND MUST BE
C     BETWEEN PRESET INITIAL VALUES OF LMD1 AND LMD2.
C
C     INITIALIZE STEP
C
      LMD1=1.001
      LMD2=6.9
      EPS=0.000000001
C
C     LOOP THROUGH A SEQUENCE OF BISECTIONS
C
100   CONTINUE
      Y(K)=(LMD1+LMD2)*0.5
      LEMBDA=Y(K)
      ETA=X(K)
      CALL GETARRAY (LEMBDA, ETA, BETA, R, M)
      CALL DLFTRG (6, M, 6, FAC, 6, IPVT)
C
C     COMPUTE THE DETERMINANT USING THE SYSTEM SOFTWARE ROUTINE DLFDRG
C
      CALL DLFDRG (6, FAC, 6, IPVT, DET1, DET2)
      DET=-(DET1*10.0**DET2)
C
      CHECK WHETHER WE INDEED HAVE A ROOT
C
      IF (ABS(DET) .LT. EPS) THEN
         GOTO 890
      ELSE IF (DET .LT. 0.) THEN
         LMD1=Y(K)
         GOTO 100
      ELSE
C        (DET .GT. 0.)
         LMD2=Y(K)
         IF (LMD2-LMD1 .LT. EPS) THEN
            GOTO 890
         END IF
         GOTO 100
      END IF
890   CONTINUE
900   CONTINUE
C
      DO 920  J=2,50
C
C     WE NOW ASSUME THAT THERE IS NO FALSE DROP AT THE BEGINING
C
      IF (Y(J-1) .GT. Y(J)) DECR=.TRUE.
C
C     DECR IS SET EQUAL TO TRUE IF THE FLEXURE CURVE EXHIBITS A
```

```
C     DECREASE
C
C     ONCE DECR IS SET EQUAL TO TRUE, IT IS NEVER CHANGED
C
      IF (DECR .AND. Y(J-1) .LT. Y(J)) INCR=.TRUE.
C
C     INCR IS SET EQUAL TO TRUE IF THE FLEXURE CURVE EXHIBITS AN
C     INCREASE AFTER THE DECR, i.e. A SECOND INCREASE
C
920   CONTINUE
C
      IF (INCR) THEN
         PRINT*, BETA, R, 'GAMMA3F'
         WRITE*, 'BETA=', BETA, 'ALPHA=', R, 'GAMMA3F'
      ELSE IF (DECR) THEN
         PRINT*, BETA, R, 'GAMMA2F'
         WRITE*, 'BETA=', BETA, 'ALPHA=', R, 'GAMMA2F'
      ELSE
         PRINT*, BETA, R, 'GAMMA1F'
         WRITE*, 'BETA=', BETA, 'ALPHA=', R, 'GAMMA1F'
      END IF
      GOTO 50
999   CLOSE(6)
      STOP
      END
C
C
C
C           SUBROUTINE GETARRAY (LEMBDA, ETA, BETA, R, M)
C           (See (I))
```

(V)

PROGRAM FLEXURE5

```
C
C     FOR A GIVEN VALUE BETA, THIS PROGRAM DETERMINES THE FLEXURE
C     REGION TYPE FOR A SEQUENCE OF ALPHA
C
      REAL*8     X(50), Y(50)
      REAL*8     M(6,6)
      REAL*8     LEMBDA, LMD1, LMD2
      INTEGER*2 IPVT(6), NOUT
      REAL*8     DET1, DET2, FAC(6,6)
      REAL*8     EPS, ETA, BETA, R, DET, RI, RF, RSTP
C
      LOGICAL DECR, INCR
C
```

```
      OPEN (6, FILE='DATAOUT', STATUS='NEW')
C     INPUT
      PRINT*, 'INPUT THE RATIO OF DEMENSION BETA:'
      READ(5,*) BETA
      PRINT*, 'WHAT IS THE INITIAL VALUE OF ALPHA:'
      READ(5,*) RI
      PRINT*, 'WHAT IS THE FINAL VALUE OF ALPHA:'
      READ(5,*) RF
      PRINT*, 'WHAT IS THE STEP SIZE FOR ALPHA:'
      READ(5,*) RSTP
C
      R=RI-RSTP
50    CONTINUE
      R=R+RSTP
      IF (R .GT. RF) GOTO 999
      DECR=.FALSE.
      INCR=.FALSE.
C
      DO 900  K=1,50
C
      X(K)=0.1+(K-1)*0.1
C
C     THE ROOT IS FOUND BY A SIMPLE BISECTOR ROUTINE AND MUST BE
C     BETWEEN PRESET INITIAL VALUES OF LMD1 AND LMD2.
C
C     INITIALIZE STEP
C
      LMD1=1.001
      LMD2=6.9
      EPS=0.000000001
C
C     LOOP THROUGH A SEQUENCE OF BISECTIONS
C
100   CONTINUE
      Y(K)=(LMD1+LMD2)*0.5
      LEMBDA=Y(K)
      ETA=X(K)
      CALL GETARRAY (LEMBDA, ETA, BETA, R, M)
      CALL DLFTRG (6, M, 6, FAC, 6, IPVT)
C
C     COMPUTE THE DETERMINANT USING THE SYSTEM SOFTWARE ROUTINE DLFDRG
C
      CALL DLFDRG (6, FAC, 6, IPVT, DET1, DET2)
      DET=-(DET1*10.0**DET2)
C
      CHECK WHETHER WE INDEED HAVE A ROOT
C
      IF (ABS(DET) .LT. EPS) THEN
         GOTO 890
      ELSE IF (DET .LT. 0.) THEN
         LMD1=Y(K)
         GOTO 100
      ELSE
C        (DET .GT. 0.)
```

```
         LMD2=Y(K)
         IF (LMD2-LMD1 .LT. EPS) THEN
            GOTO 890
         END IF
         GOTO 100
      END IF
890   CONTINUE
900   CONTINUE
C
      DO 920  J=2,50
C
C     WE NOW ASSUME THAT THERE IS NO FALSE DROP AT THE BEGINING
C
      IF (Y(J-1) .GT. Y(J)) DECR=.TRUE.
C
C     DECR IS SET EQUAL TO TRUE IF THE FLEXURE CURVE EXHIBITS A
C     DECREASE
C
C     ONCE DECR IS SET EQUAL TO TRUE, IT IS NEVER CHANGED
C
      IF (DECR .AND. Y(J-1) .LT. Y(J)) INCR=.TRUE.
C
C     INCR IS SET EQUAL TO TRUE IF THE FLEXURE CURVE EXHIBITS AN
C     INCREASE AFTER THE DECR, i.e. A SECOND INCREASE
C
920   CONTINUE
C
      IF (INCR) THEN
         PRINT*, BETA, R, 'GAMMA3F'
         WRITE*, 'BETA=', BETA, 'ALPHA=', R, 'GAMMA3F'
      ELSE IF (DECR) THEN
         PRINT*, BETA, R, 'GAMMA2F'
         WRITE*, 'BETA=', BETA, 'ALPHA=', R, 'GAMMA2F'
      ELSE
         PRINT*, BETA, R, 'GAMMA1F'
         WRITE*, 'BETA=', BETA, 'ALPHA=', R, 'GAMMA1F'
      END IF
      GOTO 50
999   CLOSE(6)
      STOP
      END
C
C
C
C           SUBROUTINE GETARRAY (LEMBDA, ETA, BETA, R, M)
C           (See (I))
```

(VI)

PROGRAM BARRELLING1

```
C
C     FOR A GIVEN COMPOSITE CONSTRUCTION CHARACTERIZED BY (BETA,ALPHA),
C     AND A CIVEN VALUE OF ETA, THIS PROGRAM DETERMINES THE VALUE OF
C     LAMBDA THAT LIES ON THE BARRELLING CURVE
C
      CHARACTER ANS*1
      REAL*8    M(6,6)
      REAL*8    LEMBDA, LMD1, LMD2, LMD
      INTEGER*2 IPVT(6), NOUT
      REAL*8    DET1, DET2, FAC(6,6)
      REAL*8    EPS, ETA, BETA, R, DET
C
      OPEN(6, FILE='DATAOUT', STATUS='NEW')
C     INPUT
10    PRINT*, 'INPUT THE RATIO OF MATERIAL PROPERTIES BETA:'
      READ(5,*) BETA
      PRINT*, 'INPUT THE RATIO OF DEMENSION ALPHA:'
      READ(5,*) R
      PRINT*, 'INPUT THE BUCKLING WAVE PARAMETER ETA:'
      READ(5,*) ETA
C
C     THE ROOT IS FOUND BY A SIMPLE BISECTOR ROUTINE AND MUST BE
C     BETWEEN PRESET INITIAL VALUES OF LMD1 AND LMD2.
C
C     INITIALIZE STEP
C
      LMD1=1.001
      LMD2=6.9
      EPS=0.000000001
C
C     LOOP THROUGH A SEQUENCE OF BISECTIONS
C
100   CONTINUE
      LMD=(LMD1+LMD2)*0.5
      LEMBDA=LMD
      CALL GETARRAY (LEMBDA, ETA, BETA, R, M)
      CALL DLFTRG (6, M, 6, FAC, 6, IPVT)
C
C     COMPUTE THE DETERMINANT USING THE SYSTEM SOFTWARE ROUTINE DLFDRG
C
      CALL DLFDRG (6, FAC, 6, IPVT, DET1, DET2)
      DET=-(DET1*10.0**DET2)
C
C     CHECK WHETHER WE INDEED HAVE A ROOT
C
      IF ( ABS(DET) .LE. EPS ) THEN
120      PRINT*, 'THE BUCKLING STRETCHING LEMBDA IS:'
         PRINT*, LMD
         WRITE(6,*) ETA, LMD
         PRINT*, 'DO YOU WANT TO GET ANOTHER LEMBDA BY ENTERING NEW',
     +           'SET OF ETA, BETA, ALPHA, ANSWER Y OR N.'
         READ(5,'(A1)') ANS
         IF (ANS .NE. 'N' .AND. ANS .NE. 'n') THEN
            GOTO 10
```

```
         ELSE
            GOTO 999
         END IF
      ELSE IF (DET .LT. 0.) THEN
         LMD1=LMD
         GOTO 100
      ELSE
C        (DET .GT. 0.)
         LMD2=LMD
         IF (LMD2-LMD1 .LT. EPS) THEN
            GOTO 120
         END IF
         GOTO 100
      END IF
      CLOSE(6)
999   STOP
      END
C
C
C
            SUBROUTINE GETARRAY (LEMBDA, ETA, BETA, R, M)
      REAL*8    M(6,6), INVLMD, LEMBDA, ETA, BETA, R
      REAL*8    T1, T2, T3, T4, C1, C2, C3, C4, S1, S2, S3, S4
      T1=ETA
      T2=LEMBDA*ETA
      T3=LEMBDA*ETA*R
      T4=ETA*R
      S1=SINH(T1)
      C1=COSH(T1)
      S1=SINH(T1)
      C1=COSH(T1)
      S2=SINH(T2)
      C2=COSH(T2)
      S3=SINH(T3)
      C3=COSH(T3)
      S4=SINH(T4)
      C4=COSH(T4)
      INVLMD=1.0/LEMBDA
      M(1,1)=2.0*LEMBDA*C2
      M(1,2)=-2.0*LEMBDA*S2
      M(1,3)=(INVLMD+LEMBDA)*C1
      M(1,4)=-(INVLMD+LEMBDA)*S1
      M(1,5)=0.0
      M(1,6)=0.0
      M(2,1)=-(INVLMD+LEMBDA)*S2
      M(2,2)=(INVLMD+LEMBDA)*C2
      M(2,3)=-2.0*S1
      M(2,4)=2.0*C1
      M(2,5)=0.0
      M(2,6)=0.0
      M(3,1)=-C3
      M(3,2)=S3
      M(3,3)=-C4
      M(3,4)=S4
```

```
      M(3,5)=-S3
      M(3,6)=-S4
      M(4,1)=LEMBDA*S3
      M(4,2)=-LEMBDA*C3
      M(4,3)=S4
      M(4,4)=-C4
      M(4,5)=LEMBDA*C3
      M(4,6)=C4
      M(5,1)=-4.0*LEMBDA*C3
      M(5,2)=4.0*LEMBDA*S3
      M(5,3)=-2.0*(INVLMD+LEMBDA)*C4
      M(5,4)=2.0*(INVLMD+LEMBDA)*S4
      M(5,5)=-4.0*BETA*LEMBDA*S3
      M(5,6)=-2.0*BETA*(INVLMD+LEMBDA)*S4
      M(6,1)=2.0*(INVLMD+LEMBDA)*S3
      M(6,2)=-2.0*(INVLMD+LEMBDA)*C3
      M(6,3)=4.0*S4
      M(6,4)=-4.0*C4
      M(6,5)=2.0*BETA*(INVLMD+LEMBDA)*C3
      M(6,6)=4.0*BETA*C4
      RETURN
      END
```

(VII)

PROGRAM BARRELLING2

```
C
C     FOR A GIVEN COMPOSITE CONSTRUCTION CHARACTERIZED BY (BETA,ALPHA),
C     THIS PROGRAM DETERMINES A SET OF ORDERED PAIR (ETA,LAMBDA) THAT
C     LIES ON THE BARRELLING CURVE
C
      CHARACTER ANS*1
      REAL*8    M(6,6)
      REAL*8    LEMBDA, LMD1, LMD2, LMD
      INTEGER*2 IPVT(6), NOUT
      REAL*8    DET1, DET2, FAC(6,6)
      REAL*8    EPS, ETA, BETA, R, DET, ETAI, ETAF, ETASTP
C
      OPEN(6, FILE='DATAOUT', STATUS='NEW')
C     INPUT
      PRINT*, 'INPUT THE RATIO OF MATERIAL PROPERTIES BETA:'
      READ(5,*) BETA
      PRINT*, 'INPUT THE RATIO OF DEMENSION ALPHA:'
      READ(5,*) R
      PRINT*, 'WHAT IS THE INITIAL VALUE OF ETA:'
      READ(5,*) ETAI
      PRINT*, 'WHAT IS THE FINAL VALUE OF ETA:'
      READ(5,*) ETAF
      PRINT*, 'WHAT IS THE STEP SIZE FOR ETA:'
```

```
      READ(5,*) ETASTP
      ETA=ETAI-ETASTP
C
50    CONTINUE
      ETA=ETA+ETASTP
      IF (ETA.GT.ETAF) GOTO 900
C
C     THE ROOT IS FOUND BY A SIMPLE BISECTOR ROUTINE AND MUST BE
C     BETWEEN PRESET INITIAL VALUES OF LMD1 AND LMD2.
C
C     INITIALIZE STEP
C
      LMD1=1.001
      LMD2=6.9
      EPS=0.000000001
C
C     LOOP THROUGH A SEQUENCE OF BISECTIONS
C
100   CONTINUE
      LMD=(LMD1+LMD2)*0.5
      LEMBDA=LMD
      CALL GETARRAY (LEMBDA, ETA, BETA, R, M)
      CALL DLFTRG (6, M, 6, FAC, 6, IPVT)
C
C     COMPUTE THE DETERMINANT USING THE SYSTEM SOFTWARE ROUTINE DLFDRG
C
      CALL DLFDRG (6, FAC, 6, IPVT, DET1, DET2)
      DET=-(DET1*10.0**DET2)
C
C     CHECK WHETHER WE INDEED HAVE A ROOT
C
      IF (ABS(DET) .LT. EPS) THEN
120      PRINT*,LMD
         WRITE(6,*) ETA, LMD
         GOTO 50
      ELSE IF (DET .LT. 0.) THEN
         LMD1=LMD
         GOTO 100
      ELSE
C        (DET .GT. 0.)
         LMD2=LMD
         IF (LMD2-LMD1 .LT. EPS) THEN
            GOTO 120
         END IF
         GOTO 100
      END IF
900   CONTINUE
      CLOSE(6)
999   STOP
      END
C
C
C
C           SUBROUTINE GETARRAY (LEMBDA, ETA, BETA, R, M)
```

```
C           (See (VI))
```

(VIII)

PROGRAM BARRELLING3

```
C
C     FOR A GIVEN COMPOSITE CONSTRUCTION CHARACTERIZED BY (BETA,ALPHA),
C     THIS PROGRAM DETERMINES THE BARRELLING REGION TYPE
C
      REAL*8     X(50), Y(50)
      REAL*8     M(6,6)
      REAL*8     LEMBDA, LMD1, LMD2, LMD
      INTEGER*2 IPVT(6), NOUT
      REAL*8     DET1, DET2, FAC(6,6)
      REAL*8     EPS, ETA, BETA, R, DET, ETAI, ETAF, ETASTP
C
      LOGICAL DECR, INCR
C
C     INPUT
      PRINT*, 'INPUT THE RATIO OF MATERIAL PROPERTIES BETA:'
      READ(5,*) BETA
      PRINT*, 'INPUT THE RATIO OF DEMENSION ALPHA:'
      READ(5,*) R
      PRINT*, 'WHAT IS THE FINAL VALUE OF ETA:'
      READ(5,*) ETAF
C
      DECR=.FALSE.
      INCR=.FALSE.
      ETA=ETAF+0.1
10    CONTINUE
      ETA=ETA-0.1
      LMD1=1.001
      LMD2=9.9
      EPS=0.000000001
C
C     THE FOLLOWING LOOP IS USED TO WORK BACK FROM THE FINAL VALUE
C     OF ETA TO DETERMINE AN APPROPRIATE INITIAL VALUE OF ETA.
C
20    CONTINUE
      LMD=(LMD1+LMD2)*0.5
      LEMBDA=LMD
      CALL GETARRAY (LEMBDA, ETA, BETA, R, M)
      CALL DLFTRG (6, M, 6, FAC, 6, IPVT)
C
C     COMPUTE THE DETERMINANT USING THE SYSTEM SOFTWARE ROUTINE DLFDRG
C
      CALL DLFDRG (6, FAC, 6, IPVT, DET1, DET2)
```

```
      DET=-(DET1*10.0**DET2)
C
C     CHECK WHETHER WE INDEED HAVE A ROOT
C
      IF (ABS(DET) .LT. EPS) THEN
         GOTO 30
      ELSE IF (DET .LT. 0.) THEN
         LMD1=LMD
         GOTO 20
      ELSE
C        (DET .GT. 0.)
         LMD2=LMD
         IF (LMD2-LMD1 .LT. EPS) THEN
            GOTO 30
         END IF
         GOTO 20
      END IF
C
30    IF (LMD .GT. 5.9) THEN
         ETAI=ETA-0.1
         PRINT*, 'ETAI=', ETAI, LMD
         ETASTP=(ETAF-ETA)/49.0
         PRINT*, 'ETASTP=', ETASTP
         GOTO 50
      ELSE
         PRINT*, LMD
         GOTO 10
      END IF
C
C     END OF FIRST LOOP
C
C     THIS SECOND LOOP NOW WORKS FORWARD FROM THE INITIAL VALUE OF
C     ETA TO THE FINAL VALUE OF ETA, DETERMINING LAMBDA FOR EACH
C     SUCH ETA
C
50    DO 900  K=1,50
C
      X(K)=ETAI+(K-1)*ETASTP
C
C     THE ROOT OF IS FOUND BY A SIMPLE BISECTOR ROUTINE AND MUST BE
C     BETWEEN PRESENT INITIAL VALUE OF LMD1 AND LMD2.
C
C     INITIALIZE STEP
      LMD1=1.001
      LMD2=8.9
      EPS=0.000000001
C
C     LOOP THROUGH A SEQUENCE OF BISECTIONS
C
100   CONTINUE
      Y(K)=(LMD1+LMD2)*0.5
      LEMBDA=Y(K)
      ETA=X(K)
      CALL GETARRAY (LEMBDA, ETA, BATA, R, M)
```

```
      CALL DLFTRG (6, M, 6, FAC, 6, IPVT)
      CALL DLFDRG (6, FAC, 6, IPVT, DET1, DET2)
      DET=-(DET1*10.0**DET2)
C
C     CHECK WHETHER WE INDEED HAVE A ROOT
C
      IF (ABS(DET) .LE. EPS) THEN
120      PRINT*, X(K), Y(K)
         GOTO 890
      ELSE IF (DET .LT. 0.) THEN
         LMD1=Y(K)
         GOTO 100
      ELSE
C        (DET .GT. 0.)
         LMD2=Y(K)
         IF (LMD2-LMD1 .LT. EPS) THEN
            GOTO 120
         END IF
         GOTO 100
      END IF
C
C     END OF SECOND LOOP
C
890   CONTINUE
900   CONTINUE
C
      DO 920  J=2,50
C
      IF (Y(J-1) .LT. Y(J)) INCR=.TRUE.
C
C     INCR IS SET EQUAL TO TRUE IF THE BARRELLING CURVE EXHIBITS AN
C     INCREASE
C
C     ONCE INCR IS SET EQUAL TO TRUE, IT IS NEVER CHANGED
C
      IF (INCR .AND. Y(J-1) .GT. Y(J)) DECR=.TRUE.
C
C     DECR IS SET EQUAL TO TRUE IF THE BARRELLING CURVE EXHIBITS A
C     DECREASE AFTER THE INCR, i.e. A SECOND DECREASE
C
920   CONTINUE
C
      IF (DECR) THEN
         PRINT*, 'GAMMA3B'
      ELSE IF (INCR) THEN
         PRINT*, 'GAMMA2B'
      ELSE
         PRINT*, 'GAMMA1B'
      END IF
999   STOP
      END
C
C
C
```

```
C           SUBROUTINE GETARRAY (LEMBDA, ETA, BETA, R, M)
C           (See (VI))
```

(IX)

PROGRAM BARRELLING4

```
C
C     FOR A GIVEN VALUE ALPHA, THIS PROGRAM DETERMINES THE BARRELLING
C     REGION TYPE FOR A SEQUENCE OF BETA
C
      REAL*8     X(50), Y(50)
      REAL*8     M(6,6)
      REAL*8     LEMBDA, LMD1, LMD2, LMD
      INTEGER*2 IPVT(6), NOUT
      REAL*8     DET1, DET2, FAC(6,6)
      REAL*8     EPS, ETA, BETA, R, DET, BETAI, BETAF,BETASTP
      REAL*8     ETAI, ETAF, ETASTP
C
      LOGICAL DECR, INCR
C
      OPEN (6, FILE='DATAOUT', STATUS='NEW')
C     INPUT
      PRINT*, 'INPUT THE RATIO OF DEMENSION ALPHA:'
      READ(5,*) R
      PRINT*, 'WHAT IS THE FINAL VALUE OF ETA:'
      READ(5,*) ETAF
      PRINT*, 'WHAT IS THE INITIAL VALUE OF BETA:'
      READ(5,*) BETAI
      PRINT*, 'WHAT IS THE FINAL VALUE OF BETA:'
      READ(5,*) BETAF
      PRINT*, 'WHAT IS THE STEP SIZE FOR BETA:'
      READ(5,*) BETASTP
C
      BETA=BETAI-BETASTP
5     CONTINUE
      BETA=BETA+BETASTP
      IF (BETA .GT. BETAF) GOTO 999
      DECR=.FALSE.
      INCR=.FALSE.
      ETA=ETAF+0.1
10    CONTINUE
      ETA=ETA-0.1
      LMD1=1.001
      LMD2=9.9
      EPS=0.000000001
C
C     THE FOLLOWING LOOP IS USED TO WORK BACK FROM THE FINAL VALUE
```

```
C     OF ETA TO DETERMINE AN APPROPRIATE INITIAL VALUE OF ETA
C
20    CONTINUE
      LMD=(LMD1+LMD2)*0.5
      LEMBDA=LMD
      CALL GETARRAY (LEMBDA, ETA, BETA, R, M)
      CALL DLFTRG (6, M, 6, FAC, 6, IPVT)
      CALL DLFDRG (6, FAC, 6, IPVT, DET1, DET2)
      DET=-(DET1*10.0**DET2)
C
      IF (ABS(DET) .LT. EPS) THEN
         GOTO 30
      ELSE IF (DET .LT. 0.) THEN
         LMD1=LMD
         GOTO 20
      ELSE
C        (DET .GT. 0.)
         LMD2=LMD
         IF (LMD2-LMD1 .LT. EPS) THEN
            GOTO 30
         END IF
         GOTO 20
      END IF
C
30    IF (LMD .GT. 5.9) THEN
         ETAI=ETA-0.1
         PRINT*, 'ETAI=', ETAI, LMD
         ETASTP=(ETAF-ETA)/49.0
         PRINT*, 'ETASTP=', ETASTP
         GOTO 50
      ELSE
         PRINT*, LMD
         GOTO 10
      END IF
C
C     END OF FIRST LOOP
C
C     THIS SECOND LOOP NOW WORKS FORWARD FROM THE INITIAL VALUE OF
C     ETA TO THE FINAL VALUE OF ETA, DETERMINING LAMBDA FOR EACH
C     SUCH ETA
C
50    DO 900  K=1,50
C
      X(K)=ETAI+(K-1)*ETASTP
C
C     THE ROOT IS FOUND BY A SIMPLE BISECTOR ROUTINE AND MUST BE
C     BETWEEN PRESET INITIAL VALUES OF LMD1 AND LMD2.
C
C     INITIALIZE STEP
C
      LMD1=1.001
      LMD2=8.9
      EPS=0.000000001
C
```

```
C     LOOP THROUGH A SEQUENCE OF BISECTIONS
C
100   CONTINUE
      Y(K)=(LMD1+LMD2)*0.5
      LEMBDA=Y(K)
      ETA=X(K)
      CALL GETARRAY (LEMBDA, ETA, BETA, R, M)
      CALL DLFTRG (6, M, 6, FAC, 6, IPVT)
C
C     COMPUTE THE DETERMINANT USING THE SYSTEM SOFTWARE ROUTINE DLFDRG
C
      CALL DLFDRG (6, FAC, 6, IPVT, DET1, DET2)
      DET=-(DET1*10.0**DET2)
C
      CHECK WHETHER WE INDEED HAVE A ROOT
C
      IF (ABS(DET) .LT. EPS) THEN
120      PRINT*, X(K), Y(K)
         GOTO 890
      ELSE IF (DET .LT. 0.) THEN
         LMD1=Y(K)
         GOTO 100
      ELSE
C        (DET .GT. 0.)
         LMD2=Y(K)
         IF (LMD2-LMD1 .LT. EPS) THEN
            GOTO 120
         END IF
         GOTO 100
      END IF
C
C     END OF SECOND LOOP
C
890   CONTINUE
900   CONTINUE
C
      DO 920  J=2,50
C
      IF (Y(J-1) .LT. Y(J)) INCR=.TRUE.
C
C     INCR IS SET EQUAL TO TRUE IF THE BARRELLING CURVE EXHIBITS AN
C     INCREASE
C
C     ONCE INCR IS SET EQUAL TO TRUE, IT IS NEVER CHANGED
C
      IF (INCR .AND. Y(J-1) .GT. Y(J)) DECR=.TRUE.
C
C     DECR IS SET EQUAL TO TRUE IF THE BARRELLING CURVE EXHIBITS A
C     DECREASE AFTER THE INCR, i.e. A SECOND DECREASE
C
920   CONTINUE
C
      IF (DECR) THEN
         PRINT*, BETA, R, 'GAMMA3B'
```

```
      WRITE*, 'BETA=', BETA, 'ALPHA=', R, 'GAMMA3B'
    ELSE IF (INCR) THEN
      PRINT*, BETA, R, 'GAMMA2B'
      WRITE*, 'BETA=', BETA, 'ALPHA=', R, 'GAMMA2B'
    ELSE
      PRINT*, BETA, R, 'GAMMA1B'
      WRITE*, 'BETA=', BETA, 'ALPHA=', R, 'GAMMA1B'
    END IF
    GOTO 5
999 CLOSE(6)
    STOP
    END
C
C
C
C           SUBROUTINE GETARRAY (LEMBDA, ETA, BETA, R, M)
C           (See (VI))
```

(X)

PROGRAM BARRELLING5

```
C
C    FOR A GIVEN VALUE BETA, THIS PROGRAM DETERMINES THE BARRELLING
C    REGION TYPE FOR A SEQUENCE OF ALPHA
C
     REAL*8    X(50), Y(50)
     REAL*8    M(6,6)
     REAL*8    LEMBDA, LMD1, LMD2, LMD
     INTEGER*2 IPVT(6), NOUT
     REAL*8    DET1, DET2, FAC(6,6)
     REAL*8    EPS, ETA, BETA, R, DET, RI, RF,RSTP
     REAL*8    ETAI, ETAF, ETASTP
C
     LOGICAL DECR, INCR
C
     OPEN (6, FILE='DATAOUT', STATUS='NEW')
C    INPUT
     PRINT*, 'INPUT THE RATIO OF DEMENSION BETA:'
     READ(5,*) BETA
     PRINT*, 'WHAT IS THE FINAL VALUE OF ETA:'
     READ(5,*) ETAF
     PRINT*, 'WHAT IS THE INITIAL VALUE OF ALPHA:'
     READ(5,*) RI
     PRINT*, 'WHAT IS THE FINAL VALUE OF ALPHA:'
     READ(5,*) RF
     PRINT*, 'WHAT IS THE STEP SIZE FOR ALPHA:'
     READ(5,*) RSTP
```

```
C
      R=RI-RSTP
5     CONTINUE
      R=R+RSTP
      IF (R .GT. RF) GOTO 999
      DECR=.FALSE.
      INCR=.FALSE.
      ETA=ETAF+0.1
10    CONTINUE
      ETA=ETA-0.1
      LMD1=1.001
      LMD2=9.9
      EPS=0.000000001
C
C     THE FOLLOWING LOOP IS USED TO WORK BACK FROM THE FINAL VALUE
C     OF ETA TO DETERMINE AN APPROPRIATE INITIAL VALUE OF ETA
C
20    CONTINUE
      LMD=(LMD1+LMD2)*0.5
      LEMBDA=LMD
      CALL GETARRAY (LEMBDA, ETA, BETA, R, M)
      CALL DLFTRG (6, M, 6, FAC, 6, IPVT)
      CALL DLFDRG (6, FAC, 6, IPVT, DET1, DET2)
      DET=-(DET1*10.0**DET2)
C
      IF (ABS(DET) .LT. EPS) THEN
         GOTO 30
      ELSE IF (DET .LT. 0.) THEN
         LMD1=LMD
         GOTO 20
      ELSE
C        (DET .GT. 0.)
         LMD2=LMD
         IF (LMD2-LMD1 .LT. EPS) THEN
            GOTO 30
         END IF
         GOTO 20
      END IF
C
30    IF (LMD .GT. 5.9) THEN
         ETAI=ETA-0.1
         PRINT*, 'ETAI=', ETAI, LMD
         ETASTP=(ETAF-ETA)/49.0
         PRINT*, 'ETASTP=', ETASTP
         GOTO 50
      ELSE
         PRINT*, LMD
         GOTO 10
      END IF
C
C     END OF FIRST LOOP
C
C     THIS SECOND LOOP NOW WORKS FORWARD FROM THE INITIAL VALUE OF
C     ETA TO THE FINAL VALUE OF ETA, DETERMINING LAMBDA FOR EACH
```

```
C     SUCH ETA
C
50    DO 900  K=1,50
C
      X(K)=ETAI+(K-1)*ETASTP
C
C     THE ROOT IS FOUND BY A SIMPLE BISECTOR ROUTINE AND MUST BE
C     BETWEEN PRESET INITIAL VALUES OF LMD1 AND LMD2.
C
C     INITIALIZE STEP
C
      LMD1=1.001
      LMD2=8.9
      EPS=0.000000001
C
C     LOOP THROUGH A SEQUENCE OF BISECTIONS
C
100   CONTINUE
      Y(K)=(LMD1+LMD2)*0.5
      LEMBDA=Y(K)
      ETA=X(K)
      CALL GETARRAY (LEMBDA, ETA, BETA, R, M)
      CALL DLFTRG (6, M, 6, FAC, 6, IPVT)
C
C     COMPUTE THE DETERMINANT USING THE SYSTEM SOFTWARE ROUTINE DLFDRG
C
      CALL DLFDRG (6, FAC, 6, IPVT, DET1, DET2)
      DET=-(DET1*10.0**DET2)
C
      CHECK WHETHER WE INDEED HAVE A ROOT
C
      IF (ABS(DET) .LT. EPS) THEN
120      PRINT*, X(K), Y(K)
         GOTO 890
      ELSE IF (DET .LT. 0.) THEN
         LMD1=Y(K)
         GOTO 100
      ELSE
C        (DET .GT. 0.)
         LMD2=Y(K)
         IF (LMD2-LMD1 .LT. EPS) THEN
            GOTO 120
         END IF
         GOTO 100
      END IF
C
C     END OF SECOND LOOP
C
890   CONTINUE
900   CONTINUE
C
      DO 920  J=2,50
C
      IF (Y(J-1) .LT. Y(J)) INCR=.TRUE.
```

```
C
C     INCR IS SET EQUAL TO TRUE IF THE BARRELLING CURVE EXHIBITS AN
C     INCREASE
C
C     ONCE INCR IS SET EQUAL TO TRUE, IT IS NEVER CHANGED
C
      IF (INCR .AND. Y(J-1) .GT. Y(J)) DECR=.TRUE.
C
C     DECR IS SET EQUAL TO TRUE IF THE BARRELLING CURVE EXHIBITS A
C     DECREASE AFTER THE INCR, i.e. A SECOND DECREASE
C
920   CONTINUE
C
      IF (DECR) THEN
         PRINT*, BETA, R, 'GAMMA3B'
         WRITE*, 'BETA=', BETA, 'ALPHA=', R, 'GAMMA3B'
      ELSE IF (INCR) THEN
         PRINT*, BETA, R, 'GAMMA2B'
         WRITE*, 'BETA=', BETA, 'ALPHA=', R, 'GAMMA2B'
      ELSE
         PRINT*, BETA, R, 'GAMMA1B'
         WRITE*, 'BETA=', BETA, 'ALPHA=', R, 'GAMMA1B'
      END IF
      GOTO 5
999   CLOSE(6)
      STOP
      END
C
C
C
C           SUBROUTINE GETARRAY (LEMBDA, ETA, BETA, R, M)
C           (See (VI))
```

(XI)

```
                    PROGRAM PROJ1
C     THIS PROGRAM CALCULATES THE TRANSITION VALUE FOR ETA FROM DATA
C     FILE CORRESPODING TO (BETA,ALPHA) IN GAMMA2F
C
      INTEGER IMAX, IMIN
      REAL X(50), Y(50), D, YMAX, DMIN
      CHARACTER*20 NAME
      DO 70  I=1, 1000
      PRINT*, 'ENTER FILE NAME OR TYPE END -->'
      READ(*,*) NAME
C
      IF (NAME(:3) .EQ. 'END') THEN
         CLOSE (5)
         STOP
      END IF
      OPEN (5, FILE=NAME, STATUS='OLD')
C
```

```
      YMAX=0.0
      DO 20  J=1, 50
      READ(5,*) X(J), Y(J)
C
C     FIND THE INTERNAL MAXIMUM
C
      IF (YMAX .LT. Y(J)) THEN
         YMAX=Y(J)
         IMAX=J
      END IF
20    CONTINUE
      PRINT*, 'THE MAXIMUM VALUE OF LAMBDA OCCURS NEAR THE PAIR',
     +         '(ETA,LAMBDA)=', X(IMAX), Y(IMAX)
C
      DMIN=1000.0
C
C     FIND THE TRANSITION VALUE OF ETA
C
      DO 50  L=1,IMAX
      D=ABS(Y(L)-Y(50))
C
      IF (DMIN .GT. D) THEN
         DMIN=D
         IMIN=L
      END IF
50    CONTINUE
      PRINT*, 'THE TRANSITION ETA IS NEAR', X(IMIN)
         CLOSE(5)
70    CONTINUE
C
      STOP
      END
```

(XII)

```
                    PROGRAM PROJ2
C
C     THIS PROGRAM FINDS THE VALUE OF ETA SWITCH FOR OPTIMUM DESIGN
C     BETWEEN (BETA,ALPHA) AND ITS CONJUGATE CONFIGURATION.  THIS
C     PROGRAM NEEDS THE DATA FILE OF (ETA,LAMBDA)-PAIRS FOR BOTH
C     (BETA,ALPHA) AND ITS CONJUGATE.
C
      CHARACTER*20 NAME1, NAME2
      REAL X1(50), X2(50), Y1(50), Y2(50), D(50), CHECK, ETASWITCH
      LOGICAL SIG1, SIG2
C
      DO 30  I=1, 1000
      PRINT*, 'ENTER FILE NAMES OR END -->'
      READ(*,*) NAME1, NAME2
      IF (NAME1(:3) .EQ. 'END') THEN
         CLOSE(10)
```

```
      CLOSE(20)
      STOP
   END IF
   OPEN (10, FILE=NAME1, STATUS='OLD')
   OPEN (20, FILE=NAME2, STATUS='OLD')
C
   SIG1=.FALSE.
   SIG2=.FALSE.
C
   DO 40  J=1, 50
   READ (10,*) X1(J), Y1(J)
   READ (20,*) X2(J), Y2(J)
C
   CHECK=Y1(1)-Y2(1)
   IF (CHECK .GT. 0.) GOTO 200
   DO 159  K=1, 50
   D(K)=Y1(K)-Y2(K)
   IF (D(K) .GT. 0.) THEN
      IF (SIG1 .AND. D(K) .GT. 0.) THEN
         GOTO 150
      ELSE
         SIG=.TRUE.
         ETASWITCH=(X1(K)+X1(K-1))/2
      END IF
   END IF
150  CONTINUE
C
200  CONTINUE
   DO 250  L=2, 50
   D(L)=Y1(L)-Y2(L)
   IF (D(L) .LT. 0.) THEN
      IF (SIG2 .AND. D(L) .LT. 0.) THEN
         GOTO 250
      ELSE
         SIG2=.TRUE.
         ETASWITCH=(X1(L)+X1(L-1))/2
      END IF
   END IF
250  CONTINUE
40   CONTINUE
   PRINT*, 'THE CROSS POINT IS', ETASWITCH
30   CONTINUE
C
   STOP
   END
```

LIST OF REFERENCES

REFERENCES:

[1] Abeyaratne, R. and Knowles, J.K. (1987). Non-elliptic elastic materials and the modeling of dissipative mechanical behavior: an example. *J. Elasticity* **18**, 227-278.

[2] Burgess, I.W. and Levinson, M. (1972). The instability of slightly compressible rectangular rubberlike solids under biaxial loadings. *Int. J. Solids Struct.* **8**, 133-148.

[3] Davies, P.J. (1989). Buckling and barrelling instabilites in finite elasticity. *J. Elasticity* **21**, 147-192.

[4] Green, A.E. and Spencer, A.J.M. (1959). The stability of a circular cylinder under finite extension and torsion. *J. Math. Phys.* **37**, 316-338.

[5] Horgan, C.O. and Pence, T.J. (1989). Void nucleation in tensile deadloading of a composite incompressible nonlinearly elastic sphere. *J. Elasticity* **21**, 61-82.

[6] Horgan, C.O. and Pence, T.J. (1989). Cavity formation at the center of a composite nonlinearly elastic sphere. *J. Appl. Mech.* **111**, 302-308.

[7] Knowles, J.K. (1977). The finite anti-plane shear field near the tip of a crack for a class of incompressible elastic solids. *Int. J. Fracture.* **13**, 611-639.

[8] Leissa, A.W. (1987). A review of laminated composite plate buckling. *Appl. Mech. Rev.* **40**, 575-591.

[9] Ogden, R.W. (1984). Nonlinear elastic deformations. *Halsted Press, New York.*

[10] Sawyers, K.N. and Rivlin, R.S. (1974). Bifurcation conditions for a thick elastic plate under thrust. *Int. J. Solid Structure* 10, 483-501.

[11] Sawyers, K.N. and Rivlin, R.S. (1982). Stability of a thick elastic plate under thrust. *J. Elasticity* 12, 101-124.

[12] Simpson, H.C. and Spector, S.J. (1984). On barrelling for a special material in finite elasticity. *Q. Appl. Math.* 42, 99-111.

[13] Wilkes, E.W. (1955). On the stability of a circular tube under end thrust. *Q. J. Mech. Appl. Math.* 8, 88-100.